«ELECTRICAL ENGINEERING & ELECTROMECHANICS»

SCIENTIFIC & PRACTICAL JOURNAL

Journal was founded in 2002 by

National Technical University «Kharkiv Polytechnic Institute»

Co-Founder – State Institution «Institute of Technical Problems of Magnetism of the NAS of Ukraine»

Адреса редакції / Editorial office address:
Кафедра "Електричні апарати", НТУ "ХПІ", вул. Фрунзе, 21, м. Харків, 61002, Україна
Dept. of Electrical Apparatus, NTU "KhPI", Frunze Str., 21, Kharkiv, 61002, Ukraine
тел. / phone: +38 057 7076281, +38 067 359 46 96, e-mail: a.m.grechko@mail.ru (**Гречко Олександр Михайлович / Grechko O.M.)**

ISSN (print) 2074-272X
ISSN (online) 2309-3404

Printed 26.02.2016. Format 60 x 90 ⅛. Paper – offset. Laser printing.
Edition 200 copies. Order no.66/172-01-2016.
Design of cover by Vyrovets L.P. e-mail: vsv_2007@ukr.net
Printed by Printing house «Madrid Ltd» (11, Olminskogo Str., Kharkiv, 61024, Ukraine)

ELECTRICAL ENGINEERING & ELECTROMECHANICS

Scientific and practical journal

2016/1

TABLE OF CONTENTS

Electrical Engineering. Great Events. Famous Names

Electrical Machines and Apparatus

Theoretical Electrical Engineering and Electrophysics

High Electric and Magnetic Field Engineering. Cable Engineering

Power Stations, Grids and Systems

UDC 621.3:537.311:910.4 **doi: 10.20998/2074-272X.2016.1.01**

M.I. Baranov

AN ANTOLOGY OF THE DISTINGUISHED ACHIEVEMENTS IN SCIENCE AND TECHNIQUE. PART 30: PORTRAIT OF THE KHARKOV MATHEMATICIAN, MECHANICAL ENGINEER AND CYBERNETICIST VLADIMIR LOGVINOVICH RVACHEV

Purpose. *Description of basic scientific achievements, features of personality and way of life of the known Kharkov mathematician, mechanical engineer and cyberneticist, academician of NAS of Ukraine Rvachev V.L .in the short form is presented.* ***Methodology.*** *Existent scientific approaches for treatment and systematization of mathematical knowledges, modern achievements in area of methods of direct solution of linear (nonlinear) boundary problems of mechanics and mathematical physics with the scope terms of different types for the physical bodies of difficult geometrical form. Methods of historical method at research of development in society of analytical geometry, applied mathematics, classical mechanics and mathematical physics.* ***Results.*** *Short information is resulted about the basic creative and vital stages, and also fundamental scientific achievements of the indicated scientist-mathematician the scientific legacy of which entered in the treasure-house of world mathematical science. Are some personal qualities of this prominent soviet Ukrainian mathematician of the 20-th century, forming scientific school on the mathematical method of R−functions and leaving about itself kind memory for thankful students and descendants.* ***Originality.*** *First taught in 1970-th at the known mathematician of contemporaneity of Rvachev V.L. to bases of the applied mathematics and theory of R−functions by a scientist-electrophysicist from the Kharkov polytechnic institute presented for the wide circle of readers a short scientifically-historical essay about this large scientist-teacher, being based on his scientific labours, published biobibliographic materials and flashbacks of his devoted students-followers about him.* ***Practical value.*** *Scientific popularization of the special physical and mathematical knowledges and distinguished scientific achievements of the known Kharkov scientist-mathematician Rvachev V.L. in area of the applied mathematics, classical mechanics of continuous media, mathematical physics and technical cybernetics.* References 43, figures 13.

Key words: **history, mathematics, mechanics, cybernetics, Kharkov region, distinguished scientific achievements.**

Приведен краткий научно-исторический очерк об известном ученом-математике Харьковщины − академике АН УССР (НАН Украины) Рвачеве В.Л. и о его выдающемся вкладе в мировую математическую науку. Библ. 43, рис. 13.

Ключевые слова: **история, математика, механика, кибернетика, Харьковская область, выдающиеся научные достижения.**

90th anniversary of Vladimir Logvinovich Rvacheva – famous Ukrainian mathematician, mechanical engineer and cybernetics dedicated.

Introduction. Papers [1, 2] have previously been described by the author of a number of portraits of the outstanding mathematicians of Kharkiv – Ukrainian Soviet and Russian academics Pogorelov A.V., Marchenko V.A and Sadovnichy V.A., as well as a correspondent member of the Ukrainian Academy of Sciences Akhiezer N.I., which became in the second half of the 20th and early 21st century, the personification of intellectual image of Kharkiv, and close to many of us Slobozhanshina region. The continuation of this academic «mathematical» a number of prominent Russian scientists, mathematicians for such leading scientific and educational centers of Ukraine as Kharkiv, certainly is and our illustrious compatriot – Doctor of Physical and Mathematical Sciences, Prof., Academician of the Ukrainian Academy of Sciences (NASU) Vladimir Logvinovich Rvachev [3].

His basic mature creative, scientific and educational life he spent in the «walls» of the Institute of Mechanical Engineering Problems (IPMach) named after Academician NASU A.N. Podgorny and Kharkiv Polytechnic Institute (KhPI). Author in 1976 while studying at postgraduate KhPI was fortunate to attend a course of lectures on applied mathematics and foundations of the so-called R-functions performed by this well-known mathematician and an excellent teacher. Remembering with a share of nostalgia that «golden» period of scientific research, the requirements of the many manifestations of extremism in their youth, creative hobbies and education, I can say that the empty seats in the classroom in the classroom scientist-maitre V.L. Rvachev usually not. These sessions aim to proactively attend professional development of young professionals and other leading universities of Kharkiv. It is time to his many disciples and who knew this remarkable Kharkiv mathematics experts from other fields of scientific activities to acquaint the general reader with this significant for the domestic and international public research and the human figure. So try in the form of short scientific and historical essay on the basis of scientific papers by Rvachev V.L. known literary sources, materials Museum KhPI, photographs from the family archive of our illustrious scientist and information from the Internet to «draw» a portrait of this extraordinary personality with a description of its major outstanding scientific results in the field of applied mathematics, mechanical engineer and mathematical physics.

1. The main stages of the life and career of the Kharkiv academic mathematician. Born Rvachev V.L. (Fig. 1) October 21, 1926 in Chigirin (Cherkasy region) in a family of teachers [3, 4]. After graduating from high school in the difficult years of the Second World War, he worked as an apprentice turner at the «Tashselmash» (Tashkent). In 1944 he was called to serve in the Navy of the USSR. After demobilization in 1947 he entered the Physics and Mathematics of Lviv University named after Franko. In 1952 Rvachev V.L. graduated from a higher educational institution of the USSR (Fig. 2).

Fig. 1. Outstanding Soviet Ukrainian mathematics, mechanical engineer and cybernetics, Doctor of Physical and Mathematical Sciences, Prof., Academician of the Ukrainian Academy of Sciences (NASU), laureate of the State Prize of the USSR in the field of Science and Technology, Honored Worker of Science and Technology, an honorary doctor of NTU «KhPI» and other universities Vladimir Logvinovich Rvachev (1926-2005) [4]

By the way, in the 4th year of the above university, he was a scholar of Stalin [4]. After graduating from the University of Lviv named after Franko and being already married to his classmate Irina Konstantinova Semiray full of creative plans Rvachev V.L. again in the ranks of the Soviet Navy, working as a lieutenant of the Soviet Navy senior lecturer at the Naval Academy (Pushkino, Leningrad region) [3, 4]. Despite these harsh circumstances of life, in 1955, he successfully defended his thesis on «*The calculation of the infinite beam lying on an elastic foundation*» (supervisor Prof. M.J. Leonov) and becomes Candidate of Physical and Mathematical Sciences [3, 4]. For family reasons (because of the urgent need to change the climate for the wife) Rvachev V.L. and Rvacheva I.K. in 1955 moved to the warm Sea of Azov, and both are teachers of the department of higher mathematics in Berdyansk Pedagogical Institute [3, 4].

It is believed that in the initial period of the life and scientific formation of Rvachev V.L. Berdyansk is a period (1955-1963), his life and scientific activity proved to be a most vivid and fruitful [5-10]. In 1960, he successfully defended at the Institute of Mechanics of the USSR Academy of Sciences doctoral thesis on «*The spatial contact problem of elasticity theory and some of its applications*» [3, 4]. It is believed that in the final moment of preparation for the defense of the scientific work on mechanics, he «*went to the main result of his future mathematical discoveries*» [4]. Opening concerned special R-functions («***Rvachev functions***»), solves the problem of taking into account a complex geometric configuration (information) for any technical object during analysis. Basic scientific work at it for a fundamentally new direction in mathematics – the theory R-functions became his short article [11].

Fig. 2. Purposeful mathematician Rvachev V.L. after the Physics and Mathematics Faculty of the Lviv University named after Franko (1952, Lviv) [4]

In 1963, Doctor of Physical and Mathematical Sciences, Prof. Rvachev V.L. was invited to work at the Kharkiv Institute of Mining Engineering, Automation and Computer Engineering (in the near future, the Kharkiv Institute of Radio Electronics – KhIRE) to head the Department of Computational Mathematics [3, 4]. Beginning of Kharkiv period (1963-2005) work for Rvachev V.L. (Fig. 3) coincided with a period of rapid development in the Soviet Union cybernetics and

computer science. In this regard, Rvachev V.L. boundary value problems of mechanics began to consider since the common position of the theory of science. That is why his attention was drawn to the problem of geometrical information specific to a broad class of optimization problems and mathematical physics solved with the help of computers – computers [3]. It is believed that the mathematical theory R-functions proposed Rvachev V.L., originated at the crossroads of the classical methods of applied mathematics, cybernetics and methods of mathematical logic [3, 4].

Fig. 3. Head of the Department of Computational Mathematics KhIRE, Doctor of Physical and Mathematical Sciences, Prof. Rvachev V.L. (third from right) before flying out of the airport of Paris home after successful participation in the International Conference on Computational Mathematics and Cybernetics (1966) [4]

Heading 1967 Department of Applied Mathematics and Computational Methods in IPMach of the Ukrainian Academy of Sciences, Doctor of Physical and Mathematical Sciences, Prof. Rvachev V.L. (Fig. 4), together with colleagues in the period 1960 – 1980 is developing the mathematical apparatus of the theory of R-functions [12-19].

Developing the theory R- functions Rvachev V.L. drew particular attention to the constructive means of its implementation. It is the lack of such structural funds so long restrained use of classical variational methods for constructing explicitly coordinate functions exactly satisfy the given boundary conditions for the areas of complex geometrical shape [3, 4]. Rvachev V.L. together with their students through constructive theory of R-functions of functions we have developed a common approach to the problem of constructing coordinate sequences known for the main variation and projection methods [20]. At the same time it was the decision of problems of mechanics, electrodynamics, thermal physics and mathematical physics with boundary conditions of various types for almost any form fields [20]. Mathematical ***R-functions method*** in the future was a universally recognized abbreviation *RFM* [4].

Fig. 4. Meeting of the Academic Council of IPMach of the Ukrainian Academy of Sciences, chaired by its director, correspondent member of the Ukrainian Academy of Sciences Anatoly N. Podgorny, discuss the achievements of the USSR Academician V.L. Rvachev (far right) and his students in the development and practical application of a mathematical apparatus of R-functions in mechanics cybernetics, thermal physics, electrodynamics, radio physics and other technical applications (1985, Kharkiv) [4]

In 1969, Doctor of Physical and Mathematical Sciences, Prof. Rvachev V.L. was invited by the rector of KhPI Prof. Semko M.F. to head the department on the theoretical and mathematical physics at the permanent place of his work in IPMach of the Ukrainian Academy of Sciences [4]. During this time period, the search for effective organization of the numerical solution of boundary value problems of mathematical physics led Rvachev V.L. to understand the need to create ***a new programming technology*** [3]. In 1970, under his supervision in the department of applied mathematics and computational methods IPMach of the Ukrainian Academy of Sciences started work on the creation of the first version of automated programming systems family «Field» [3, 4]. In the future, by these institutions in the system «field» become instrumental base for numerical experiments and solve many practical problems, freeing mathematicians and engineers in various fields from the programming process [3].

1972, Doctor of Physical and Mathematical Sciences, Prof. Rvachev V.L. was elected as Corresponding Member of the Ukrainian Academy of Sciences, and in 1978 – full member of the Ukrainian Academy of Sciences [3, 4]. In 1980, for the development, creation and implementation of the national economy of the theory functions R-functions group of authors of employees IPMach of the Ukrainian Academy of Sciences as part Rvachev V.L. (head of investigations) and his disciples Stoyan Y.G., Protsenko V.S., Manko G.P., Slesarenko A.P., Shejko T.I. and Sinekop N.S. was awarded the State Prize of Ukraine in the field of science and technology [3, 4]. We point out that the results of studies by Rvachev V.L. On the supply side, and he adjusted his students to use in practice, the mathematical method R-functions (RFM) for the period of his active work are reflected in more than 350 [3]. The author also

because of the limited scope of this essay is only referred to their score. These must include at least another two monographs by the Academician of the NASU V.L. Rvachev defining certain stages and development perspectives in science «***Rvachev functions***». It is published in Ukraine following books: in 1967 «*Geometric applications of algebra of logic*» [21] and in 1974, «*Methods of the algebra of logic in mathematical physics*» [22].

In my opinion, one of the main factors that led it our hero scientist in mathematical discovery of special R-functions features is the fact that this man had an encyclopedic knowledge. He was the highest expert not only in terms of pure mathematics, and engineering cybernetics (the science of the laws governing the management processes and information transfer machines [23]), as well as classical mechanics, mathematical physics and mathematical logic (Boolean algebra, based on logical operations Similar actions on sets [23]). It is a synthesis of these unique abilities and knowledge, focusing it, and brought Rvachev V.L. to consider opening. Needs practice in solving complex scientific and technical problems in these areas of knowledge and skill of Rvachev V.L. in a complex cover such problems, and brought him to the scientific insight – creation ***theory of R-functions***.

October 21, 1986 the academic community of Kharkov and the whole of our country celebrated the 60th anniversary of the outstanding scientist of our time, academician of the USSR Vladimir Logvinovich Rvachev, held at his place of work in the long at his native IPMach of the Ukrainian Academy of Sciences (Fig. 5).

Fig. 5. Director of IPMach of the Ukrainian Academy of Sciences, Corresponding Member of the Ukrainian Academy of Sciences A.N. Podgorny (left) warmly congratulates the 60th anniversary of his dear colleague, jubilee – Ukrainian Academy of Sciences Academician V.L. Rvachev (right) (1986 ,IPMach of the Ukrainian Academy of Sciences, Kharkiv) [4]

Subsequent decades of fruitful scientific and pedagogical activity in IPMach of the Ukrainian Academy of Sciences (NASU) and NTU «KhPI» (since 1971 as a professor of the department of the above University, called since 1981 the Department of Applied Mathematics, part-time) our domestic scientist Maitre Rvachev V.L. dedicated individual topical areas of application in the field of mechanics (contact problems of elasticity theory and nonlinear problems of the theory of plates of complex shape), thermal physics, magnetohydrodynamics, physics, cybernetics (automation software tasks in solving boundary value problems) and mathematics (problems in the theory approximation and atomic functions), to develop him and his numerous students on the basis of the data created by the world-renowned creator of the mathematical theory of R-functions [24-38].

Academician of the National Academy of Sciences of Ukraine V.L. Rvachev (Fig. 6) at the beginning of the 21st century he has continued the best of their moral standing and physical strength to work in his areas of educational and scientific spheres as an academic consultant IPMach NASU, «his» chair of applied mathematics at the NTU «KhPI», KhIRE and aerospace University «Kharkiv Aviation Institute» until his death, the ensuing 26 April 2005 [4, 39-42].

Fig. 6. The members of the organizing committee of the international conference on nonlinear dynamics «*Nonlinear Dynamics*» (from left to right: Prof. Tovazhnyansky L.L., academician of the NAS Rvachev V.L.,Prof. Morachkovsky O.K., Prof. Kurpa L.V., Prof. Kravets V.A., 2004, NTU «KhPI», Kharkiv) [4]

October 23, 2006 in NTU «KPI» in honor of the outstanding scientist of the XX century in the field of mathematics and mechanics, the author of scientific ideas for the ***theory of R-functions***, academician of the NASU Rvachev V.L. it was discovered a marble plaque (Fig. 7).

2. Main scientific achievements of the Kharkiv academic mathematician. Scientifically known Prof. V.L. Rvachev brought the original results of his work on a solution based on a new mathematical approach of boundary value problems in classical mechanics, mathematical physics, thermal physics, electrodynamics, radio physics and magnetohydrodynamics. We will try to lower it on the basis of a number of scientific papers [3, 5-22, 24-38] to formulate the basic fundamental scientific results obtained by famous mathematician, academician of the Ukrainian Academy of Sciences (NASU) V.L. Rvachev in these areas of physical and mathematical knowledge:

• Formulated at the present mathematical level of knowledge of ***the centuries-old scientific problem*** that goes back to the founder of analytical geometry – the great French mathematician and physicist René Descartes (1596-1650) And consisting of the construction of the equation of a geometric object of any shape he was initially given a graphic outline or drawing (1960th years);

Fig. 7. General view of the marble memorial plaque in honor of outstanding Soviet Ukrainian Mathematics and Cybernetics, Academician of NAS of Ukraine, honorary doctor of NTU «KhPI» Vladimir Logvinovich Rvachev (1926-2005), Opened in NTU «KPI» in 2006 and mounted on a brick wall of Mathematical Building of the University

• Developed in relation to the solution of boundary value problems of classical mechanics, thermal physics, mathematical physics, electrodynamics, radio physics and magnetohydrodynamics new mathematical method for constructing complete systems of basis (coordinate) functions for geometric objects of arbitrary configuration with boundary conditions of various types and an arbitrary functional form of the recording, use the original special ***R-function (Rvachev functions***) (1960th years);

• Developed a framework of a new ***mathematical theory of R-functions*** with its numerous technical applications, one of the main results of which is the inverse problem of analytical geometry, which consists in establishing a mathematical equation for a given geometric object of arbitrary shape, which describes its geometry and the coordinates of its external borders for different areas in two- and three-dimensional Euclidean space (1960th years);

• Submitted the required ***equation for the inverse problem of analytic geometry*** and the coordinates of external borders (coordinate functions of the boundary conditions for the boundary value problems in technical applications) for geometric objects of complex shapes in a single analytic expression that contains elementary functions (1970th years);

• Detail developed and brought to practical application in solving various boundary value problems of classical mechanics, thermal physics, mathematical physics, electrodynamics, the theory of radio physics and magnetohydrodynamics R-functions is the opinion of authoritative scholars one of the great scientific discoveries in the field of applied mathematics of the second half 20 century (1970th years) [40-42];

• On the basis of the constructive universal theory R-function creates ***a new programming technology***, implemented under his supervision in the department of applied mathematics and computational methods IPMach of the Ukrainian Academy of Sciences in relation to direct methods for solving boundary value problems in mechanics and mathematical physics described by partial differential equations, in the form automated programming systems family «Field» (1970th – 1980th years);

• Solved large complex application of linear and nonlinear two-and three-dimensional boundary-value problems in the theory of elastic plates, rods, hollow cylinders and other metal complex form, transient heat conduction of solid bodies of finite size, and the theory of electromagnetism in relation to radio and antenna systems with MHD generators R-method involving mathematical functions (*RFM*) (1970th – 2000th years);

• With the aid of his theory of generalized R-functions and constructively implemented in functional spaces are widely used in practice the formula of Taylor-Lagrange-Hermite that will open a new class of finite infinitely often differentiable functions (atomic functions) that are of great practical importance for the further development approximation theory, methods of digital processing of electrical signals and methods for solving diverse boundary value problems of mathematical physics (1980th years);

• He has made a significant contribution to the development of ***non-Archimedean calculus***, which is algebraically isomorphic to the classical calculus of Archimedes, and adapt it to the fundamental problems of modern astrophysics outer space (1990th years);

• Established an internationally recognized ***scientific school of Kharkiv*** for mathematical method of R-functions (1970th – 2000th years).

Here is the incomplete list of significant for the world of physics and mathematics community of scientific results academician of Ukrainian Academy of Sciences (NAS) Rvachev V.L. for many years of his active and fruitful work in the field of applied mathematics, classical mechanics, thermal physics, mathematical physics, cybernetics and electricity. Moreover, the results that can be proud of a real mathematician and who entered the treasury of the world of mathematics [3, 4, 39-43].

These results of research and teaching Rvachev V.L. We received recognition in the community and were awarded the following high state awards and marks of distinction [4, 39]:

• Order of the Red Banner of Labor (1961);

• election corresponding member of the Ukrainian Academy of Sciences (1972) and full member of the Ukrainian Academy of Sciences (1978);

• Order «Badge of Honor» (1976);

• award of the Prize of Academician A.N Dinnik of

the Ukrainian Academy of Sciences (for outstanding contribution to the development of mathematical physics, 1976);

- awarding of the State Prize of Ukraine in Science and Technology (for the creation, development and practical application of the theory of R-functions, 1980);
- Order of Friendship of Peoples (1986)

• rank of «Honored Worker of Science and Technology of Ukraine» (1997);

- Order of Prince Yaroslav the Wise V degree (2001);
- award of the title «Honorary Doctor» of the National Technical University «KhPI», Kharkiv National University of Radio Electronics and the University of Wisconsin (USA).

3. The scientific school of Kharkiv academic mathematician. The data presented in Section 2, it follows that the main scientific development scientist and mathematician Rvachev V.L. he created a mathematical theory R-functions with its numerous technical applications [3, 4, 42]. Due to the complex work carried out under the supervision of Academician V.L. Rvachev for a number of decades in IPMach of the Ukrainian Academy of Sciences (NASU), NTU «KhPI», KhIRE, KHAI and towards the development and practical application of the method of R-functions (RFM), it was formed by a recognized scientific school in the world [3, 4]. Below in Fig. 8-12 shows some of the scientists who formed the «backbone» of the scientific school. At the beginning of the 21st century, this scientific school has 22 doctors of technical and physical and mathematical sciences and 70 candidates of physical and mathematical sciences [4, 42]. Among the talented scientists and students of Academician of the NASU V.L. Rvachev. There are two corresspondent members of the NASU – E. Alexander Evgenievich Bozhko and Yuri Grigorievich Stoyan working now in IPMach NASU [4, 41].

Fig. 8. Corresponding member of the UkrSSR Academy of Sciences Rvachev V.L. on vacation with his disciples IPMach of the Ukrainian Academy of Sciences and the future D.Sc. and the winners of the State Prize of Ukraine in the field of science and technology for 1980: Shejko T.I. (first left) and Slesarenko A.P. (center) (1972, a suburb of Kharkiv) [4]

Fig. 9. Academician of the Ukrainian Academy of Sciences V.L. Rvachev (center) with his students, followers from IPMach of the Ukrainian Academy of Sciences: D.Sc. Goncharyuk I.V. (left) and future corresponding member of the NASU and the winner of the State Prize of Ukraine in the field of science and technology for 1980, D.Sc. Stoyan Yu.G. (right) (1978, IPMach of the Ukrainian Academy of Sciences, Kharkiv) [4]

Fig. 10. Academician of the Ukrainian Academy of Sciences V.L. Rvachev (left) with his student D.Sc. winner of the State Prize of Ukraine in the field of science and technology for 1980 Protsenko V.S. (right) (1986, IPMach of the Ukrainian Academy of Sciences, Kharkiv) [4]

Fig. 11. Academician of the National Academy of Sciences of Ukraine Rvachev V.L. with his talented student, D. Sc. Prof. Kurpa Lydia Vasilievna – Head of the Department of Applied Mathematics at NTU «KhPI» (1999, NTU «KhPI», Kharkiv) [4]

Fig. 12. Academician of the National Academy of Sciences of Ukraine V.L. Rvachev (right) and his student, D.Sc. Kravchenko V.F. (left) (1999, Kharkiv) [4]

One of his students, Prof. D.Sc. Lytvyn Oleg Nikolaevich won the prestigious awards named after Academician V.M. Glushkov and Academician M.V. Ostrogradskii of the NASU [41, 42]. Another of his disciple, D.Sc. Viktor Filippovich Kravchenko became honored worker of science and technology of the Russian Federation [43]. Section 1 has been given the names of six scientists and students from IPMach of the Ukrainian Academy of Sciences, which became in 1980 the winners of the State Prize of Ukraine in science and technology. Many of the students Rvachev V.L. or head of the department was headed by education in high schools of Kharkov and other cities of Ukraine (for example, B.N. Borisenko, V.P. Buzko, V.N. Verzhikovsky, I.V. Goncharyuk, V.D. Kozhukhov, L.V. Kurpa, L.N. Kutsenko, O.N. Litvin, V.S. Protsenko, N.S. Sinekop, I.B. Sirodzha, V.P. Fedko, Yu.P. Shabanov-Kushnarenko, T.I. Shejko, L.I. Shklyarov, A.V. Shmatko et al.) [4, 43].

4. Features of the personality and lifestyle of the Kharkiv academic mathematician. What was Vladimir Logvinovich outside his research interests and work? From the memoirs of his students to be their teacher, «*was the epitome of Kindness and Love to the people*» [42]. This smart, educated and talented man, a mathematician who became a world scale, organically embodied and connected scruples, compassion and the ability to assist the other person, the ability to enjoy other people's success and ability in science mentoring [4, 42]. They, has seen a lot in his life and in his youth passed through many sufferings and deprivations during the 1930s (because of the contrived political reasons for the arrest, conviction and subsequent to the end of his rehabilitation courageous parents), brought up a whole generation of scientists and mathematicians who called themselves «r*vachevites*» and proud of this title [4]. While on vacation, or at home, it is as a «workaholic», firmly adhered to the rules worked out over the years, «*least one hour to devote scientific work at least one page a day to write about the results of the research*» [4]. Mathematics was, as they say in «blood» family of Rvachev: his parents Logwin Fedorovich and Ksenia Alekseevna were school teacher of mathematics, Sister Catherine Logvinovna, having a hard way of life, it has become a well-known scientist-mathematician (one of the first in the USSR women-coder and corresponding member of the NASU) and wife Irina Konstantinova (Fig. 13), which became a 1952 teacher of mathematics in the higher school of the USSR and reliable support in the life of Vladimir Logvinovich [4, 41]. Together with her and her children – a son Valery and a daughter Irina they deserve «*passed through life, enduring all the joys and sorrows*» [4, 42].

In [4, 42] worthy and faithful disciple of Academician of the NASU V.L. Rvachev, Doctor of Technical Sciences, Prof., Head of the department of applied mathematics NTU «KhPI» Lidia Vasilievna Kurpa wrote about his teacher the following remarkable words: *«… members of the Polytechnic University will always keep the memory of this talented Scientist, great Teachers and outstanding Person*».

Fig. 13. Beloved wife and vital support of academician of the NASU Rvachev V.L., Math teacher at the Kharkiv Tank School (since March 2003 this institution was included as part of the faculty KhPI) Irina Konstantinova Rvacheva (Semiray) (1965, Kharkiv) [4]

REFERENCES

1. Baranov M.I. an anthology of the distinguished achievements in science and technique. Part 26: Three portraits of worldwide known mathematicians of Kharkov region *Elektro-*

tekhnika i elektromekhanika − Electrical engineering & electromechanics, 2015, no.3, pp. 3-13. (Rus).

2. Baranov M.I. An anthology of the distinguished achievements in science and technique. Part 27: Portrait of the Kharkov mathematician Naum Il'ich Akhiezer. *Elektrotekhnika i elektromekhanika − Electrical engineering & electromechanics*, 2015, no.4, pp. 3-6. (Rus).

3. Gopko L.M., Kravchenko L.K., Shidlovskij A.K. *Vladimir Logvinovich Rvachev. AN USSR (Biobibliografija uchenyh Ukr. SSR).* [Vladimir Logvinovich Rvachev. Ukrainian Academy of Sciences (Biobibliography scientists Ukr. SSR)]. Kiev, Naukova dumka Publ., 1988. 52 p. (Rus).

4. Kurpa L.V., Shmatko T.V., Shmatko A.V. *Rvachev Vladimir Logvinovich. Se chelovek. Mnogo zvanyh − Malo izbrannyh* [Rvachev Vladimir Logvinovich. It homo. Many are called − Not selected]. Kharkov, Novoe slovo Publ., 2006. 80 p. (Rus).

5. Rvachev V.L. The pressure on the elastic half-space stamp, in terms of having a band shape. *Prikladnaja matematika i mekhanika − Applied Mathematics and Mechani*cs, 1956, vol.20, no.2, pp. 248-254. (Rus).

6. Mossakovskiy V.I., Rvachev V.L. On the problem of horizontal hydrodynamic shock sphere. *Prikladnaja matematika i mekhanika − Applied Mathematics and Mechani*cs, 1958, vol.22, no.6, pp. 847-849. (Rus).

7. Rvachev V.L. The character of the pressure distribution under the stamp, outlined in the plan two contiguous circles. *Izvestija AN SSSR. Mekhanika i mashinostroenie – Proceedings of Academy of sciences of the USSR. Mechanics and machine construction*, 1959, no.2, pp. 147-158. (Rus).

8. Rakov A.Kh., Rvachev V.L. Contact task theories of resiliency for half-space the module of resiliency of which is the sedate function of depth. *Dopovidi AN Ukrainskoj SSR − Reports of Academy of sciences of the Ukrainian SSR*, 1961, no.3, pp.286-290. (Ukr).

9. Bilik G.I., Rvachev V.L. About main integral equalization of contact task theories of resiliency for half-space the module of resiliency of which is the sedate function of depth. *Dopovidi AN Ukrainskoj SSR − Reports of Academy of sciences of the Ukrainian SSR*, 1962, no.8, pp. 1041-1044. (Ukr).

10. Rvachev V.L. An analytical description of some geometric objects. *Doklady AN SSSR − Reports of Academy of sciences of the USSR*, 1963, vol.153, no.4, pp. 765-768. (Rus).

11. Rvachev V.L. To the decision of one task of theory of potential. *Dopovidi AN Ukrainskoj SSR − Reports of Academy of sciences of the Ukrainian SSR*, 1958, no.2, pp. 144-146. (Ukr).

12. Rvachev V.L., Yushchenko E.L. *Nekotorye voprosy analiticheskogo opisaniia geometricheskikh ob»ektov slozhnoi logicheskoi struktury* [Some questions the analytical description of geometric objects with complex logic structure]. Kiev, Znanie USSR Publ., 1965. 53 p. (Rus).

13. Rvachev V.L., Stoyan Yu.G. On the optimal cutting material. *Voprosy teoreticheskoj kibernetiki − Questions of theoretical cybernetics*, 1965, pp. 189-199. (Rus).

14. Volkov A.P., Kravchenko V.F., Man'ko G.P., Rvachev V.L. On the solution of boundary task method by R- functions. *Differencial'nye uravnenija − Differential equations*, 1967, vol.3, no.9, pp. 1602-1605. (Rus).

15. Rvachev V.L., Shklyarov L.I. R_x− functions. *Dopovidi AN Ukrainskoj SSR. Ser. A − Reports of Academy of sciences of the Ukrainian SSR. Ser. A*, 1968, no.5, pp. 415-417. (Ukr).

16. Rvachev V.L., Uchishvili L.O. Calculation freely being plates by a method R− functions. *Dopovidi AN Ukrainskoj SSR. Ser. A − Reports of Academy of sciences of the Ukrainian SSR. Ser. A*, 1968, no.10, pp. 935-937. (Ukr).

17. Rvachev V.L., Rakova L.V. Use of method for the decision of task on determination of frequencies and forms of vibrations of plates of difficult form. *Dopovidi AN Ukrainskoj SSR. Ser. A − Reports of Academy of sciences of the Ukrainian SSR. Ser. A*, 1969, no.10, pp. 902-905. (Ukr).

18. Kravchenko V.F., Polyakov V.F., Rvachev V.L. Solution of the task of diffraction of a plane wave by a system of two metal strips by a method R− functions. *Radiotekhnika − Radio engineering*, 1970, no.13, pp. 168-176. (Rus).

19. Rvachev V.L., Yarmolyuk V.K. About the use method R− functions for the decision of stationary tasks of heat conductivity and electrodynamics. *Dopovidi AN Ukrainskoj SSR. Ser. A − Reports of Academy of sciences of the Ukrainian SSR. Ser. A*, 1971, no.11, pp. 1003-1005. (Ukr).

20. Rvachev V.L. *Teorija R− funkcij i nekotorye ee prilozhenija* [Theory R- functions and some its applications]. Kiev, Naukova dumka Publ., 1982. 552 p. (Rus).

21. Rvachev V.L. *Geometricheskie prilozhenija algebry logiki* [Geometric algebra application logic]. Kiev, Naukova dumka Publ., 1967. 212 p. (Rus).

22. Rvachev V.L. *Metody algebry logiki v matematicheskoj fizike* [Methods of algebra of logic in mathematical physics]. Kiev, Naukova dumka Publ., 1974. 259 p. (Rus).

23. *Bol'shoj illjustrirovannyj slovar' inostrannyh slov* [Large illustrated dictionary of foreign words]. Moscow, Russkie slovari Publ., 2004. 957 p. (Rus).

24. Rvachev V.L., Slesarenko A.P. On a modification of the structural method for solving mixed boundary tasks of heat conduction for areas of complex shape. *Matematicheskaja fizika − Mathematical physics*, 1974, no.15, pp. 137-140. (Rus).

25. Kravchenko V.F., Polevoy V.I., Rvachev V.L. The calculation of the basic parameters of antennas complex shapes by R− functions. *Metrologicheskie voprosy radiofiziki − Metrological questions of radiophysics*, 1974. pp.87-106. (Rus).

26. Rvachev V.L., Sheyko T.I. On the question of the distribution of the electric potential in the course of conducting liquid in a nonuniform magnetic field. *Matematicheskaja fizika − Mathematical physics*, 1975, no.18, pp. 135-139. (Rus).

27. Rvachev V.L., Slesarenko A.P. *Algebra logiki i integral'nye preobrazovanija v kraevyh zadachah* [The algebra of logic and integral transformations in the boundary tasks]. Kiev, Naukova dumka Publ., 1976. 287 p. (Rus).

28. Rvachev V.L., Procenko V.S. *Kontaktnye zadachi teorii uprugosti dlja neklassicheskih oblastej* [The contact tasks theories of resiliency for non-classical areas]. Kiev, Naukova dumka Publ., 1977. 235 p. (Rus).

29. Rvachev V.L., Slesarenko A.P. *Algebro-logicheskie i proekcionnye metody v zadachah teploobmena* [Algebraic, logical and projection methods in tasks of thermal exchange]. Kiev, Naukova dumka Publ., 1978. 140 p. (Rus).

30. Rvachev V.L., Rvachev V.A. *Teorija priblizhenij i atomarnye funkcii* [Approximation theory and atomic functions]. Moscow, Znanie Publ., 1978. 64 p. (Rus).

31. Rvachev V.L., Rvachev V.A. *Neklassicheskie metody teorii priblizhenij v kraevyh zadachah* [Non-classical methods of approximation theory to boundary tasks]. Kiev, Naukova dumka Publ., 1979. 196 p. (Rus).

32. Rvachev V.L., Sinekop N.S. Formula convolution method R- functions and their application to the construction of struc-

tures of solutions of boundary tasks. *Doklady AN SSSR − Reports of Academy of sciences of the USSR*, 1980, vol.255, no.1, pp. 80-83. (Rus).
33. Rvachev V.L., Sinekop N.S. An approximate solution of the plane task theories of resiliency for orthotropic body R- functions method. *Dopovidi AN Ukrainskoj SSR. Ser. A − Reports of Academy of sciences of the Ukrainian SSR. Ser. A*, 1981, no.10, pp. 61-64. (Rus).
34. Rvachev V.L., Man'ko G.P. *Avtomatizacija programmirovanija v kraevyh zadachah* [Automation programming in of boundary tasks]. Kiev, Naukova dumka Publ., 1983. 230 p. (Rus).
35. Rvachev V.L., Kurpa L.V., Shevchenko A.N. R− functions method in tasks of non-stationary vibrations of plates. *Problemy prochnosti − Problems durability*, 1984, no.6, pp. 22-25. (Rus).
36. Rvachev V.L., Kurpa L.V. Method R− functions in tasks of bending of anisotropic plates. *Doklady AN SSSR − Reports of Academy of sciences of the USSR*, 1985, vol.280, no.2, pp. 314-317. (Rus).
37. Rvachev V.L., Kurpa L.V. *R− funkcii v zadachah teorii plastin* [R− functions in of tasks theory of plates]. Kiev, Naukova dumka Publ., 1987. 175 p. (Rus).
38. Rvachev V.L., Man'ko G.P. Theory R− functions in the mathematical modeling of physical fields. *Elektronnoe modelirovanie – Electronic modeling*, 1987, vol.9, no.2, pp. 3-6. (Rus).
39. Rvachev Vladimir Logvinovich (Rvachev Vladimir Logvinovich) Available at: https://ru.wikipedia.org/wiki/Рвачёв, Владимир Логвинович (accessed 28 February 2013). (Rus).
40. Available at: http://rvachev.narod.ru (accessed 08 October 2013). (Rus).
41. Available at: http://www.impach.kharkov.ua/ PersonPages/Rvachev.htm (accessed 20 August 2012). (Rus).
42. Available at: http://polytechnic.kpi.kharkov.ua/ ViewArticle.asp?id=1171 (accessed 12 March 2014). (Rus).
43. Available at: http://dic.academic.ru/dic.nsf/ruwiki/1289464 (accessed 11 May 2014). (Rus).

Received 03.07.2015

M.I. Baranov, Doctor of Technical Science, Chief Researcher,
Scientific-&-Research Planning-&-Design Institute «Molniya»
National Technical University «Kharkiv Polytechnic Institute»,
47, Shevchenko Str., Kharkiv, 61013, Ukraine,
phone +38 057 7076841, e-mail: eft@kpi.kharkov.ua

How to cite this article:
Baranov M.I. An antology of the distinguished achievements in science and technique. Part 30: Portrait of the Kharkov mathematician, mechanical engineer and cyberneticist Vladimir Logvinovich Rvachev. *Electrical engineering & electromechanics*, 2016, no.1, pp. 3-11. doi: 10.20998/2074-272X.2016.1.01.

UDC 621.316.53 **doi: 10.20998/2074-272X.2016.1.02**

O.G. Volkova, L.B. Zhornyak

INVESTIGATION OF HIGH-CURRENT INTERRUPTING CONTACTS WORKING SURFACES MECHANICAL INTERACTION NATURE

Introduction. The nature of the interaction of high-working surfaces of the electrical contact uniquely affects their performance. By the failure of the contacts in the main drive processes resulting from complex destructive factors affecting their performance. However, not all processes are studied in detail and give in modeling. The purpose of the paper is to show the possibility of using the method of holographic interferometry to estimate the plastic deformation in the zone of contact interaction. One of the significant factors affecting the work of the contact pair is the compressive force of the contact surfaces. Compression discontinuous contact is directly connected with the processes of elastic and plastic deformation of the contact material, which is particularly evident in the contact details of the powder or composite materials. The paper focuses on the plastic deformation of the surface layers of discontinuous contact in circuit, it is believed that it is directly related to the mechanism of conductivity of contacts. As shown, a significant effect on the deformation of the contact surfaces and renders the working environment, in particular transformer oil. Methodology. Assessing the impact of compression forces on the deformation of the contact surface was conducted experimentally using the method of holographic interferometry. Results. Experimental studies, which indicated that the compact and powder materials plastic deformation in and around the area microcontacts simplistically stated that requires experimental verification. A method for evaluating the state of stress, which affects the formation and destruction of the local contact spots. Practical value. Using the experimental method of determining the movement of the contact region allows you to optimize discontinuous contacts from composite and powder materials. References 7, tables 2, figures 4.
Key words: **electrical contacts, contact surfaces, deformation of contact materials, method of holographic interferometry.**

Характер взаимодействие рабочих поверхностей сильноточных электрических контактов однозначно влияют на их работоспособность. К отказу в работе контактов в основном приводят процессы, возникающие в результате комплекса факторов деструктивно влияющих на их работоспособность. При этом не все процессы подробно изучены и поддаются моделированию. Одним из существенных факторов, влияющим на работу контактной пары, служит усилие сжатия контактных поверхностей. Сжатие разрывных контактов напрямую связано с процессами упругой и пластической деформации контактных материалов, что особенно наглядно проявляются на контакт-деталях из порошковых или композиционных материалов. В статье основное внимание уделяется пластической деформации поверхностных слоев разрывных контактов в процессе замыкания, поскольку считается, что она напрямую связана с механизмом проводимостью контактов. Как показано, существенное влияние на деформацию контактных поверхностей оказывает и рабочая среда, в частности трансформаторное масло. Оценка влияния усилия сжатия на деформацию контактной поверхности проводилась экспериментально с использованием метода голографической интерферометрии. Приведены результаты исследования, в которых указывалось, что для компактных и порошковых материалов пластическая деформация внутри и вокруг зоны микроконтактов указывается упрощенно, что требует экспериментального уточнения. Библ. 7, табл. 2, рис. 4.
Ключевые слова: **электрические контакты, контактные поверхности, деформация контактных материалов, метод голографической интерферометрии.**

Introduction. The mechanism of the conduction of current through the contact is determined by the state of the contact surfaces and contacting conditions. It is known that the compressive force is one of the main factors shaping the nature of the contact interaction. Without sufficient compressive force the contact resistance increases, or conductivity of contacts is completely broken. The conductivity is proportional to the compression force, leading to the first elastic and then plastic deformation of the contact surfaces. Naturally, together with the change of compression force, the internal mechanical stress in the contact material changes. Distribution of plastic deformation of powder and composite materials is more complicated than for compact (cast) materials and assessment of the behavior of the surfaces contact-details made from these materials should be based on experimental observations, rather than simplified models.

The goal of the paper is to demonstrate the possibility of using the method of holographic interferometry to estimate the plastic deformation in the zone of contact interaction.

Modeling of contact surfaces interaction. Experimentally proved that a decrease in compression force in 2 times, transition resistance of contact-pieces depending on their size can be increased in 4 times or more. For high-current contacts there is an empirical relationship [1] showing that the contact resistance R_c is mainly a function of the compression force, and the role of other factors, such as surface films is secondary and is taken into account by correction factors:

$$R_{\text{c}} = \frac{k \cdot (1 + \frac{2}{3} \cdot \alpha \cdot T)}{(0{,}1 \cdot P_c)^m}.$$

where α is the resistance temperature coefficient, 1/°C; T is the temperature of the contact's heating, °C; P_c is the contacts compression force, N; k, m are the coefficients taking into account contact materials and contacting nature.

The desire to find the general laws of the transition resistance of the compression force leads to the modeling of contact problems in the simplified model. For example, at the contact interaction simulation as a compression of two elastic spherical surfaces. According to the Hertz formula, the radius of the contact area of this model will be:

$$r = 0{,}9 \cdot \sqrt[3]{\frac{P_c r_{eff}}{E}},$$

where P_c is the contacts compression force; r_{eff} is the effective radius of curvature of the contact surfaces; E is the contact materials modulus of elasticity [2].

In this case, the contact resistance can be expressed by the formula

$$R_c = \frac{\varepsilon}{P_c^{1/3}}.$$

In the range of compression force from 20 to 500 N, which is typical for most of the switching devices, the value of the empirical coefficient ε can be taken as follows: for copper $47 \cdot 10^{-6}$ Ω·kg$^{1/3}$; for brass $200 \cdot 10^{-6}$ Ω·kg$^{1/3}$.

At the plastic nature of the contact interaction, when the radius of the area of collapse is given by equation

$$r = \sqrt{\frac{P_c}{\pi \sigma_c}},$$

where σ_c is the collapse resistance of contact materials, the contact resistance of contact is assessed as [2]

$$R_c = \frac{k}{P_c^{1/2}},$$

where the coefficient коэффициент k for some contact materials are presented in Table 1.

Table 1

Contact materials properties

Contact materials	Coefficient k for high-current contacts, Ω·kg$^{1/2}$
Copper	$1.0 \cdot 10^{-4}$
Silver	$0.5 \cdot 10^{-4}$
Brass	$6.7 \cdot 10^{-4}$
Steel	$7.6 \cdot 10^{-4}$

The ratio between the applied load and the actual contact area can be represented as

$$P_{c1} = \zeta \cdot H \cdot A_i,$$

where $1/3 \le \zeta \le 1$ is the coefficient taking into account the elastic component of the deformation of the contact surfaces; H is the hardness of the contact material taking into account the temperature; A_i is the actual contact area.

Guided by similar models, contact problem is solved by using computer by numerical methods simultaneously with evaluation zones of contact interaction with the elastic and plastic deformation.

There are software packages that allow to simulate these processes and to ensure their control. These requirements largely correspond to software packages for finite element analysis (e.g. ANSYS), which have recently been widely used in the calculations of various mechanical structures.

A common approach to solving the problems of contact interaction of solid surfaces is reduced to a phased implementation of the following basic steps of calculation [3]:

1. Creation of solid objects that represent the geometry of the switching contacts, and their meshing.
2. The determination of a contact pair.
3. Appointment of the target and contact surfaces, elements of which are interconnected by physical constants and allow to take into account the kinematics of the deformation of the contact.
4. Determination of the key features of elements and actual constants of contact surfaces.
5. Determination of motion of a rigid contact surface.
6. Specification of the necessary boundary conditions.
7. Setting options of force loading and the problem solution.
8. The solution of the contact problem.
9. Analysis of the results.

As an example a 2D picture of the contact interaction of the main contacts of the contactor of the on-load tap-changing transformer KHOA 110/1000 may be considered. Fig. 1 shows elements of the contact pair in the form of closed elastic-plastic bodies covered with the finite element (FE) mesh.

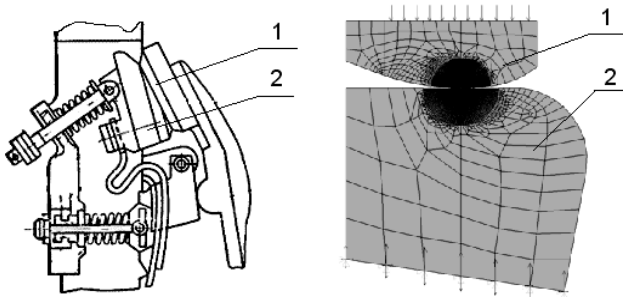

Fig. 1. An example of the use of the finite element analysis to study the interaction of pairs of contact:
1 – movable contact; 2 – fixed contact

The introduction of such techniques, provided the stability of the mechanical properties of the contact surfaces, allows to solve contact problems quickly and with greater accuracy. However, when assessing the effect of the compression force it is necessary to take into account the mechanical properties of contact materials (at operating temperatures), configuration and microgeometry of contacting surfaces, as well as the mechanical and adhesive properties of surface films and others. Such a number of factors suggests that analytically

it is impossible to establish a general pattern for the compression forces ensuring optimal operation of the contacts [4].

Experimental determination of the contact surface deformation. Simulation methods do not allow to adequately take into account the real nature of the interaction of the contact details for long term of use, due to the development of destructive processes on their surfaces. It is not only the shielding effect of surface films, the effect of which is well known [5], and the plastic deformation of the contact surfaces. The cause of this is the high value for the compressive force of the contact surfaces, electrothermal processes, and plasticizing effect of the environment, such as transformer oil.

In general, the deformation of the surface layer has a complex mechanism, because the plastic material of the contact can not only spread but also to penetrate into the body contact. Under the influence of the compressive force varies and the internal mechanical stress in the contact material. The force of compression is set to the maximum possible for a particular contact pair not only improves the conductivity, but also leads to deformation and destruction of the contact surfaces during operation, and hence reduces their efficiency.

Particularly, these processes are shown in the contact pairs of powder and composite materials. The widespread use of multi-component powder materials for discontinuous contacts in high-switching devices is a common practice. The work of these materials is of interest because of their specific behavior that requires more detailed study.

Multicomponent powders and composite materials generally have a sufficiently high strength, due to the presence of the frame structure. Consider this as an example of a contact material КМК-Б20, used for high-current contacts in the contactors of the on-load tap-changing transformer (Fig. 2).

Frame consisting of solid compounds based on W, Ni or Ti, Cr, Zr receives mechanical stress from the main compression force and displacement, which stabilizes the amount of strain in the material and contact surface. To improve the antifriction and ensure the hardness value of the contact pair in the material composition is administered as a solid lubricant of molybdenum disulfide, graphite and others. Plastic conductive base (copper) of powder material largely relieved by the application of compression force and the biasing force, and it is only the volume adjacent to the area of direct contact, experiencing stress.

Furthermore dissipation of mechanical energy due to the compression and friction of the contact surfaces when switching occurs and accumulation of residual stress at the sites of actual contact [6]. Because of the random shape and dimensions of irregularities, as well as their locations on the friction surface, the residual stresses are randomly distributed over the surface and over time. An important role is played and by the porosity of the structure. If in some areas in a given time is an accumulation of internal energy (elastic deformation), the other process may be reaching a maximum decay with the release of heat or the formation of fracture nucleus. The area of increased ductility generally coincides with the area of greatest stress, i.e. the central region touch pad. After multiple cycles of closure-opening contacts are prerequisites for the emergence of cracks, leading to the destruction of the working surfaces of the contact pair. Presence of stochastically arranged in the powder material porosity evident as fracture cracks and ductility in the contacting zone.

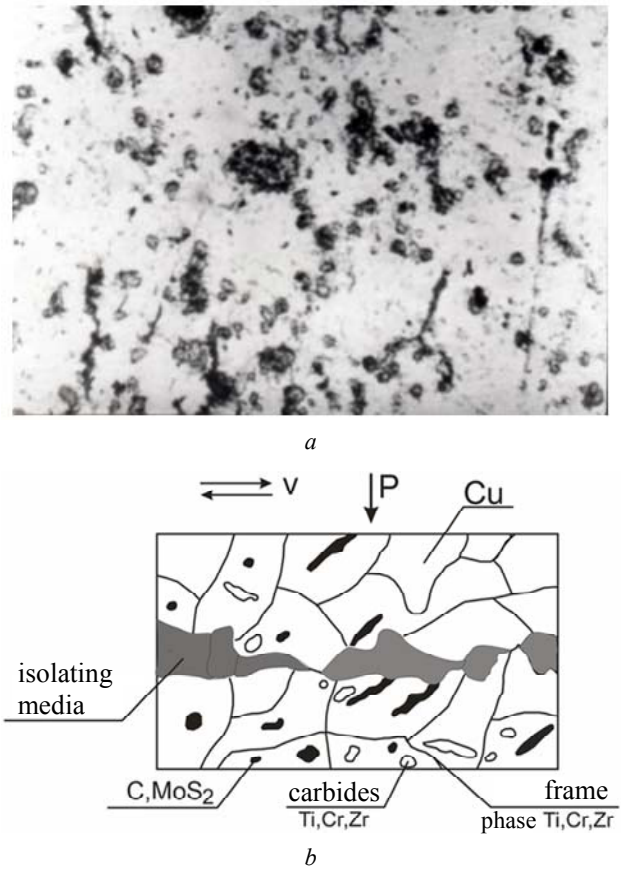

Fig. 2. The structure of the multi-component powder material (*a*) and model of the contact surface (*b*)

Behavioral fluctuations of contact surfaces of the compact and powder materials, can be seen on the model of the contact pairs in the design of the on-load tap-changing transformer РНТА 35/320. For comparison, the moving contacts materials were chosen copper М1 and powder material КМК-Б20. The material of the fixed contact in both cases was brass ЛС 59-1.

In the experiment the method of investigation of contact interaction of solid bodies using holographic interferometry, which allows to record the displacement vector of points of the contact area by a double exposure of the subject of observation under a light source of coherent radiation is used.

During the experiment, the contacts were fixed in the support prism with loading device and were the subject in a holographic pattern as shown in Fig. 3. The original survey was carried out on the contact plate in the unloaded condition. Subsequently a repeated exposure of contacts loaded compression forces P, Q_1, Q_2 on the same photographic plate.

If the thus obtained double-exposed hologram illuminate by a copy of the reference wave, then there is a holographic image of the contact pairs with superimposed grid of fringes. The strips are located on the subject, and on the adjoining area. Photocopies of such holograms are shown in Fig. 4.

Quantitative estimation of the deformation of the contact surface was carried out by monitoring the deflection of the interference fringes of the so-called zero-order band. In this case, the zero-order interference fringe is defined as a single, it does not change its position when the double exposure. Visually, this is defined as the maximum bright band on the interferogram [7].

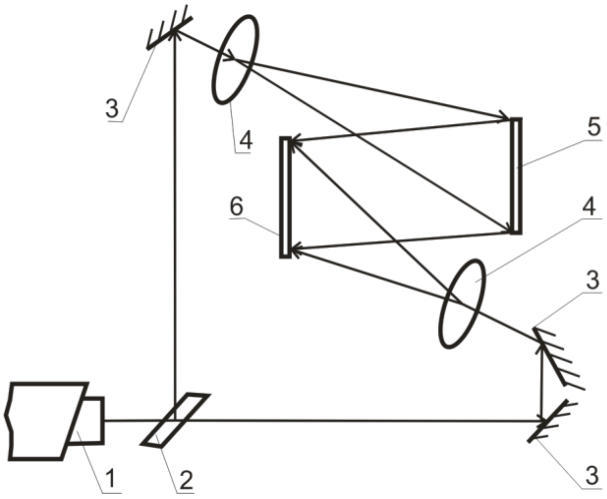

Fig. 3. A sketch of the holographic interferometry by double exposure method:
1 – laser ЛГ-38; 2 – divider; 3 – mirror; 4 – lens; 5 – the object; 6 – photographic plate

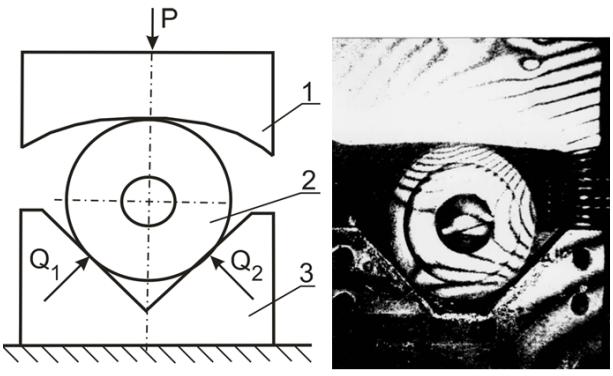

a *b*

Fig. 4. The scheme f the load (*a*) and the hologram of contact pair (*b*): 1, 2 – fixed and movable contacts; 3 – supporting prism

Determination of deformation performed by records taking into account the position of the zero-order fringe and displacement vector directed perpendicular to the surface of contact. The difference in compliance sections of the contact surfaces is clearly seen by the number of interference fringes. The closer their net, the more displacement. In this clearly indicates the difference of the bands on the steel prism and on contact.

Calculation of movement of the contact surface reduces to a multiplication of the interference maximum sequence number the numerical value of the wavelength of the radiation source (in this case 0.3162 μm). Conditionally designating by serial numbers light strips on the image, offset is determined by the formula

$$Z(x) = \frac{N\lambda}{2}.$$

where $Z(x)$ is the displacement, μm; N is the number of strips; λ is the wave length, μm.

Study of displacement of the contact surface is carried out in a static mode. During the experiment the force P was changed stepwise in the range of variation of the force of compression contacts of the real device. There was a possibility to supply transformer oil to the contact zone that simulate the conditions of work of contacts in the oil-filled switchgear. Data obtained by using the following methods, are shown in Table. 2.

Table 2

Maximal displacements of the contact surfaces at various load conditions, μm

Material	Load P, N			HardnessHB
	1300	2700	4000	
M1	0.632/1.264*	1.264/3.160*	4.100/8.010*	100-110
КМК-Б20	0.630/1.900*	1.900/6.320*	4.480/8.220*	120-150

* presence of transformer oil in the contact zone

According to the experimental results it can be seen that the comparison of the degree of deformation of the contact surfaces of the compact (cast) and powder materials in terms of their hardness is not quite correct, since deformation of the contact surface is greatly affected by homogeneity of the structure and porosity of the powder materials.

This method may determine the limit load for contact material without resorting to their destruction, as well as to predict the behavior of contacts for long term use.

Conclusions.

1. By the method of holographic interferometry it is possible to investigate the interaction of surfaces of breaking contacts of high-switching devices. The experimental results provide a more accurate picture of

the deformation of the contact surface, taking into account a variety of factors that can not be taken into account in the simulation.

2. The influence on the deformation of the contact surfaces of the external environment in the oil-filled switchgear that at high loads of more than twice the increases displacement of the contact surface without visible damage under compression is demonstrated.

3. The use of the experimental method of determining the movement of the region near contacts allows to optimize operation of breaking contacts from composite and powder materials. For example, it was found that for the contactor of the on-load tap-changing transformer PHTA 35/320 the compressive force shall not exceed 4,060 N, and the maximum deformation of the contact surface values of 8-11 μm.

REFERENCES

1. Taev I.S. *Elektricheskie apparaty upravleniia* [Electrical control apparatus]. Moscow, Vysshaia shkola Publ., 1984. 243 p. (Rus).

2. Butkevich G.V. *Osnovy teorii elektricheskikh apparatov* [Basic theory of electrical apparatus]. Moscow, Vysshaia shkola Publ., 1970. 600 p. (Rus).

3. Basov K.A. *ANSYS v primerakh i zadachakh* [ANSYS in examples and tasks]. Moscow, Komp'iuter Press Publ., 2002. 224 p. (Rus).

4. Merl V. *Elektricheskii kontakt. Teoriia i primenenie na praktike* [Electrical contact. Theory and practical application]. Moscow-Leningrad, Gosenergoizdat Publ., 1962. 82 p. (Rus).

5. Myshkin N.K. *Elektricheskie kontakty* [Electrical contacts]. Dolgoprudnyi, Intellekt Publ., 2008. 560 p. (Rus).

6. Kashcheev V.N. *Protsessy treniia v zone friktsionnogo kontakta metallov* [Friction process in metal contact frictional zone]. Moscow, Mashinostroenie Publ., 1978. 211 p. (Rus).

7. Ginzburg V.M., Stepanova B.M. *Golografiia. Metodyiapparatura* [Holography. Methods and equipments]. Moscow, Sovetskoe radio Publ., 1974. 376 p. (Rus).

Received 22.10.2015

O.G. Volkova[1]*, Candidate of Technical Science, Associate Professor,*
L.B. Zhornyak[1]*, Candidate of Technical Science, Associate Professor,*
[1] Zaporozhye National Technical University,
64, Zhukovsky Str., Zaporozhye, 69063, Ukraine.
phone +380 6127 698304, e-mail: volkova@zntu.edu.ua

How to cite this article:
Volkova O.G., Zhornyak L.B. Investigation of high-current interrupting contacts working surfaces mechanical interaction nature. *Electrical engineering & electromechanics*, 2016, no.1, pp. 12-16. doi: 10.20998/2074-272X.2016.1.02.

UDC 621.313:004.696 **doi: 10.20998/2074-272X.2016.1.03**

N.N. Zablodskii, V.E. Pliugin, A.N. Petrenko

USING OBJECT-ORIENTED DESIGN PRINCIPLES IN ELECTRIC MACHINES DEVELOPMENT

Purpose. To develop the theoretical basis of electrical machines object-oriented design, mathematical models and software to improve their design synthesis, analysis and optimization. Methodology. We have applied object-oriented design theory in electric machines optimal design and mathematical modelling of electromagnetic transients and electromagnetic field distribution. We have correlated the simulated results with the experimental data obtained by means of the double-stator screw dryer with an external solid rotor, brushless turbo-generator exciter and induction motor with squirrel cage rotor. Results. We have developed object-oriented design methodology, transient mathematical modelling and electromagnetic field equations templates for cylindrical electrical machines, improved and remade Cartesian product and genetic optimization algorithms. This allows to develop electrical machines classifications models, included not only structure development but also parallel synthesis of mathematical models and design software, to improve electric machines efficiency and technical performance. Originality. For the first time, we have applied a new way of design and modelling of electrical machines, which is based on the basic concepts of the object-oriented analysis. For the first time is suggested to use a single class template for structural and system organization of electrical machines, invariant to their specific variety. Practical value. We have manufactured screw dryer for coil dust drying and mixing based on the performed object-oriented theory. We have developed object-oriented software for design and optimization of induction motor with squirrel cage rotor of AIR series and brushless turbo-generator exciter. The experimental studies have confirmed the adequacy of the developed object-oriented design methodology. References 12, figures 2.

Key words: **electric machine, object-oriented, class, object, template, inheritance, hierarchy, designing, mathematical modeling, electromagnetic field, optimization, algorithm.**

Выполнен анализ применимости теории объектно-ориентированного анализа в проектировании и математическом моделировании электрических машин. Рассмотрены объектно-ориентированные модели электрических машин, синтез которых осуществляется как на основе положений теории электромагнитного поля, так и на основе дифференциальных уравнений электромагнитных переходных процессов. Обоснованы преимущества объектно-ориентированного подхода в проектировании. Определены основные принципы объектно-ориентированного проектирования. Библ. 12, рис. 2.

Ключевые слова: **электрическая машина, объектно-ориентированный, класс, объект, шаблон, наследование, иерархия, проектирование, математическое моделирование, электромагнитное поле, оптимизация, алгоритм.**

Introduction. Development and modernization of electric machines (EM) with high technical and economic performance is a priority for today's enterprises of electric machine industry [1, 2]. The development of new versions of EM is realized by an individual approach to each project.

However, the existing design methods based on the sequential organization of design stage, do not allow to implement the tasks associated with the following:

1) there is no possibility of the automated transfer of all or part of the project to create a new, which has both common features with the base, and their own;

2) there is no mechanism of inclusion in your existing project data dependencies of other projects;

3) it is impossible to apply modern methods of optimization based on an object-oriented representation of data;

4) the cost of resources for the design at the traditional sequential approach significantly inferior to the object-oriented systems.

In this connection, an important task is to validate such a design technique that will not only reduce the time of design work, but also to improve the process of creating of the EM due to the transfer of design techniques from the pre-formed database to a new combination of the EM components.

In [3-6] principles, methodology and implementation of object-oriented design (OOD), mathematical modeling and optimization of EM have been described. In this paper, the principles of object-oriented analysis (OOA) are considered in the realization of an integrated project of EM from calculation to optimization.

The goal of the work is the solution of the problem increasing the technical and economic parameters of EM and shortening their development by using OOD.

Problem definition. Traditional design is accompanied by so-called «procedural» approach to solving the problems of the calculation of the electrical machine. The project, built on the basis of a procedural method is divided into calculated blocks, each of which performs a certain sequence of actions completed and has clearly expressed-linkages with other units of the project. Calculations are divided into successively performed points with a set of formulas rigidly interconnected by input and output data. A large number of links between

the calculated blocks and data, in turn, gives rise to several problems: first, the complicated structure of the project; secondly, the project becomes difficult to make changes. The development costs of these projects are very high, which affects the additional material costs and higher cost of production. In this connection, such an organization of the EM design which would allow to increase the efficiency of the development of new projects, as well as modification of existing ones with minimal resource and time consuming, is of great importance in today's electrical machine industry.

Object-oriented design implements the concept of problem solving, using models based on the concepts of the real world. The fundamental elements are the class and object [7]. The classes allow to carry out the construction of individual components having simple tools. The object at the same time brings together a data structure (parameters with calculated procedures).

The underlying idea of the OOD is to join data and actions performed on that data, in a single unit, which is called an object. As an example, Fig. 1 shows the structure of the OOD to the DC motor.

Object-oriented project may be represented as «*Electrical Designer*» when from out-established blocks a new EM modification is assembled. Thus, Fig. 2 illustrates OOD of a screw motor with a massive rotor which is composed from modules of the induction motor (IM), machine with a massive rotor and screw.

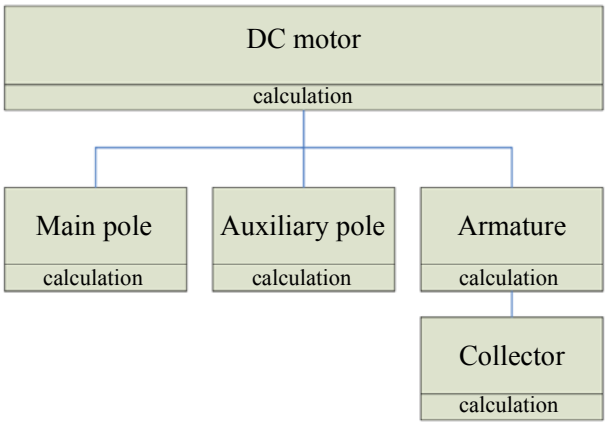

Fig. 1. Inheritance tree of DC motor in the OOD

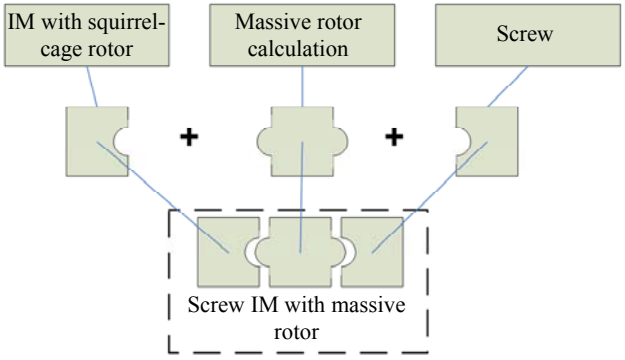

Fig. 2. Synthesis of the OO project of the screw IM with massive rotor

Creation of new projects at the OOD, as well as modification of existing ones is based on the experience of previous designs, resulting in a significant reduction in development time, reduces the probability of introducing errors into the new project.

Results of investigations. In OOD the project is represented as discrete objects, which contain the data and computational blocks with a set of formulas and logical connections [3, 7]. The characteristics and the basic *principles* of construction of the object in this case are: individuality; classification; inheritance; polymorphism.

Considering the theory of OOD, we go out from the point which assumes a basic class of generalized EM, descendants of which are well-known types of EM. By inheritance, using OOD principles discussed, added to or cut off those features which lead to the synthesis of a specific model of EM.

As the base, in terms of the OOD we accept Maxwell equations of classical electrodynamics [8]:

$$\begin{cases} \mathrm{rot}\vec{E} = -\dfrac{\partial \vec{B}}{\partial t}, \\ \mathrm{div}\vec{D} = \rho, \\ \mathrm{rot}\vec{H} = \vec{J} + \dfrac{\partial \vec{D}}{\partial t}, \\ \mathrm{div}\vec{B} = 0. \end{cases} \quad (1)$$

In (1) vectors of electric field strength $\vec{E}$ and magnetic field strength $\vec{H}$ are connected by the relations:

$$\vec{D} = \varepsilon\varepsilon_0\vec{E}, \quad \vec{B} = \mu\mu_0\vec{H}, \quad \vec{J} = \sigma\vec{E}, \quad (2)$$

with vectors of electric $\vec{D}$ and magnetic $\vec{B}$ inductions, vector of the electric current density $\vec{J}$, which represent the medium response on the presents of the electromagnetic field in it. Respectively, ρ is the volume density of the electric charge, ε_0 and μ_0 are electric and magnetic constants, σ is the conductivity, ε and μ are dielectric and magnetic permeabilities of the medium.

An analysis of the work performed shows that Maxwell equations (1), (2), which are fundamental to the theory of EM, fully confirm the stated principles of the OOD, thus proving the viability of the object-oriented approach in the design of EM. Thus, the development of theoretical bases of the OOD, in addition, that it improves the efficiency and quality of design does not contradict the principles of formation of electromagnetic structures in EM.

Practical implementation of the OOD has been made in the programming language Java [6]. In the project were implemented stages of the design, including electromagnetic calculation as well as thermal, reliability, economic.

Used object-oriented optimization algorithms, such as the Cartesian product of the sets (CPS) and genetic algorithm (GA), make it possible to perform calculations of the machine with all possible combinations of variable variables within specified limits and at a predetermined

step while changing simultaneously the variable parameters [9, 10].

To improve the efficiency of the algorithm of the CPS sampling procedure combinations authenticated the restrictions it has been modified by the authors that the increased performance of the algorithm is more than in 10 times [11].

Genetic optimization algorithm in the classical formulation was modified and practically realized by the authors for the EM data sample, and adding changes in the range of varied variables without invasion into the internal structure of the algorithm [12].

After the completion of the last phase of optimization automated parametric design of optimal motor in AutoCAD or COMPAS with automatic generation of design and drawing documentation is performed [6].

OOP principles allow not only synthesize the EM design techniques, but also consider their mathematical models of hereditary succession of the base class and descendant classes. This will go to the designing as a complex task, decisive problems of obtaining the parameters and characteristics of EM in steady-state and transient modes. Here, automated generation of mathematical model of a random kind of EM at the design stage is performed.

The system of equations of the EM of basic machine describes the energy conversion process and consists of four Kirchhoff equations, equations of the electromagnetic torque and movement. Based on the analysis mathematic models of different types of EM, a table of modifications, allowing to generate their model using OOD principles is built. Synthesis of models of EM was accompanied by the formation of the table of modifiers, which are the coefficients or terms, changing the matrix of basic parameters of the mathematical model [3].

Using a template class of generalized EM and selecting certain features, you can go to the object of particular EM [4]. A mathematical model of transient processes in at the OOD is formed on the base of the hierarchical tree of inheritance, modifiers tables compiled for the designed machine.

Practical implementation of the OOD of the EM is confirmed by the utilization at industrial enterprises of Ukraine.

The screw induction motor (SIM), manufactured by JSC «Pervomaisky Electromechanical Plant named after K. Marx» was developed and implemented in the production process of mixing and drying of coal sludge at JSC «Central Concentration Plant Selidovskaya».

For the SIM, the object-oriented design methodology was compiled, it was practically implemented in the programming language Java, object-oriented mathematical simulation of electromagnetic transients and the analysis of the distribution of the electromagnetic field were performed.

Using the principles of OOP techniques and a computer program in Java language for the optimal design and the study of transient modes of an induction motor for electric rolling stock have been developed. The results of calculations were the basis of field calculations in 2D and 3D formulations to improve the thermal performance of the motor.

As an object of design was also considered a multi-phase brushless synchronous exciter БТВ-12(15) (State Plant «Electrotyazhmash», Kharkiv) designed for systems of the brushless excitation of the turbine generator (BETG) of 80 MW. Object-oriented class structure of the BETG project was implemented in the form of software in Java.

As an object of design an asynchronous motor with a squirrel-cage rotor of АИР series was considered, developed at the company Special Design Bureau «Ukrelectromach». In the course of the work done object-oriented design was done, a computer program in Java was created, multi-criteria optimization of the IM using the CPS algorithm was made. As a result of optimization parameters of the IM with squirrel-cage rotor were obtained having improved in the comparison to the base case, the technical and economic performance.

Thus, the technique of the OOD of the EM was practically implemented in the projects that have received practical application in industry.

Conclusions.

1. Object-oriented design has allowed to realize the formation of project methods and mathematical models of EM by using information of base classes of the project using modifiers and operators of synthesis. Unified template allows to transfer elaborated project data to new versions of EM.

2. Object-oriented methodology of mathematical modeling of EM allows the synthesis of mathematical models of the existing types of EM, and to predict the possible modification of new structures.

3. The use of OOD principles leads to a significant reduction in terms of the design, along with opportunities to perform engineering design optimization, mathematical modeling of electromagnetic transients and the analysis of the distribution of the electromagnetic field of EM in the frame one project.

4. The use of object-oriented methods of optimization is allowed to raise such technical and economic performance of EM such as efficiency, cost, power factor, improve the performance of starting and operating characteristics.

REFERENCES

1. Expediting and validating development. Available at: http://www.iff.fraunhofer.de/en (accessed 12 September 2015).

2. R-Designed. Available at: http://blog.caranddriver.com/r-designed-2016-volvo-xc90-gets-the-sporty-r-design-treatment-still-isnt-on-sale-yet/ (accessed 12 September 2015).

3. Pliugin V.E. *Teoreticheskie osnovy ob'ektno-orientirovannogo rascheta i proektirovaniia elektromekhanicheskikh ustroistv* [Theoretical basis of electromechanical devices object-oriented calculation and design]. Alchevsk, Lado Publ., 2014. 200 p. (Rus).

4. Pliugin V., Milykh V., Polivianchuk A., Zablodskiy N. Using of object-oriented design principles in mathematic modeling of electric machines. *MOTROL – Motoryzacja i Energetyka Rolnictwa*, 2015, vol.15, no.2, pp. 25-32.

5. Pliugin V., Shilkova L., Letl J., Buhr K. Analysis of the electromagnetic field of electric machines based on object-oriented design principles. *Proceedings 36th PIERS*. Prague: Electromagnetic Academy, 2015, pp. 2522-2527.

6. Zablodskii M.M., Pliugin V.E., Buhr K. *SAPR elektromekhanichnykh prystroiv. – Navchalnyi posibnyk. Ch.2* [CAD of electromechanical devices. – Textbook. Vol.2]. Alchevsk, Lado Publ., 2013. 320 p. (Ukr).

7. Buch G. *Ob'ektno-orientirovannyj analiz i proektirovanie* [Object-oriented analysis and design]. Moscow, Binom Publ., 1998. 560 p. (Rus).

8. Beljaev E.F., Shulakov N.V. *Diskretno-polevye modeli elektricheskih mashin* [Discrete field models of electrical machines]. Perm, Perm State Technical University Publ., 2009. 457 p. (Rus).

9. Vereshhagin N.K., Shen' A. *Lekcii po matematicheskoj logike i teorii algoritmov. Nachala teorii mnozhestv* [Lectures on mathematical logic and theory of algorithms. Beginning of set theory]. Moscow, MCNMO Publ., 2008. 198 p. (Rus).

10. Emel'janov V.V., Kurejchik V.V., Kurejchik V.M. *Teorija i praktika evoljucionnogo modelirovanija* [Theory and practice of evolutionary modeling]. Moscow, Phizmatlit Publ., 2003. 432 p. (Rus).

11. Zablodskiy N., Pliugin V., Lettl J., Buhr K., Khomitskiy S. Induction motor optimal design by use of cartesian product. *Transactions on electrical engineering*, 2013, no.2, pp. 54-58.

12. Zablodskiy N., Pliugin V., Lettl J., Buhr K., Khomitskiy S. Induction motor design by use of genetic optimization algorithms. *Transactions on electrical engineering*, 2013, no.3, pp. 65-69.

Received 22.10.2015

N.N. Zablodskii[1]*, Doctor of Technical Science, Professor,*
V.E. Pliugin[2]*, Candidate of Technical Science, Associate Professor,*
A.N. Petrenko[3]*, Candidate of Technical Science, Associate Professor,*
[1] National University of Life and Environmental Sciences of Ukraine,
15, Heroyiv Oborony Str., Kyiv, 03041, Ukraine.
phone +38 044 5278242, e-mail: zablodskiynn@gmail.com
[2] National Technical University «Kharkiv Polytechnic Institute»,
21, Frunze Str., Kharkiv, 61002, Ukraine.
phone +38 057 7076600, e-mail: vlad.plyugin@gmail.com
[3] O.M. Beketov National University of Urban Economy in Kharkiv,
17, Marshal Bazhanov Str., Kharkiv, 61002, Ukraine.
phone +38 057 7061548, e-mail: petersanya2007@mail.ru

How to cite this article:
Zablodskii N.N., Pliugin V.E., Petrenko A.N. Using object-oriented design principles in electric machines development. *Electrical engineering & electromechanics*, 2016, no.1, pp. 17-20. doi: 10.20998/2074-272X.2016.1.03.

UDC 621.318 **doi: 10.20998/2074-272X.2016.1.04**

B.V. Klymenko, A.V. Eres'ko, I.S. Varshamova, N.A. Lelyuk

RESEARCH OF THE APPLICATIONS POSSIBILITY OF INTERFACE RELAY IN HYBRID SWITCHING SYSTEMS OF BISTABLE ACTUATORS WINDINGS

Purpose. ***Development of methods of experimental determination of action coordination characteristics of semiconductor and mechanical switching elements in systems of hybrid commutation of bistable actuators coils taking into account contact bounce of mechanical switching elements. Consideration of the application possibility of interface relay as mechanical switches, and the definition of the duration of the intervals to ensure coordination of the relay operation with semiconductor switches.*** ***Methodology.*** ***Experimental determination of the time intervals between the moments of switching transistor which controls the relay coil, and power transistor when the switching on and off operations using a hybrid switching device are performed; statistical processing of experimental results.*** ***Results.*** ***The durations of the time intervals between the moments of switching of semiconductor and mechanical switching elements in systems of actuator coils hybrid commutation are experimentally determined. A way of a significant reduction of the duration of the indicated time intervals is considered and experimentally confirmed.*** ***Originality.*** ***The scheme of the power circuit of the control system with hybrid commutation of the actuator coil circuit, which differs from the known schemes that the only semiconductor switching element performs functions of the current switching on and off, and electromechanical relay contact elements act as a router interconnecting electrical circuits during dead times.*** ***Practical value.*** ***The use of hybrid switches instead of switches with semiconductor switches will significantly reduce the cost of the actuators control system, as well as reduce their sizes.*** References 6, tables 1, figures 6.

Key words: **bistable actuators, interface relays, contact bounce, hybrid switching.**

Представлены результаты экспериментальных исследований дребезга контактов интерфейсных реле при выполнении операций их включения и отключения в нормальном режиме и в режиме ускорения срабатывания. Приводятся рекомендации по применению малогабаритных интерфейсных реле в системах управления коммутационных аппаратов с гибридной коммутацией электрических цепей обмоток бистабільных актуаторов. Библ. 6, табл. 1, рис. 6.

Ключевые слова: **бистабильные актуаторы, интерфейсные реле, дребезг контактов, гибридная коммутация**.

Introduction. Vacuum switching devices for medium voltage networks occupy a dominant position in the relevant market segment, and in the medium voltage contactors segment the share of vacuum devices is greater than 90 %. The invention of highly coercive permanent magnets (Masato Sagawa, 1982), as well as progress in the creation of microprocessor devices and high-power electrolytic capacitors allowed to create switching devices with highly reliable electromagnetic drives (e.g., devices by ABB – circuit breakers VM1 and contactors VSC), which provide the necessary power characteristics and practicallu do not consume energy after closing and opening operations. In these devices polarized bistable actuators with two coils are used [1], and to control their winding – a microprocessor system with semiconductor switching elements – power transistor and two thyristors (Fig. 1).

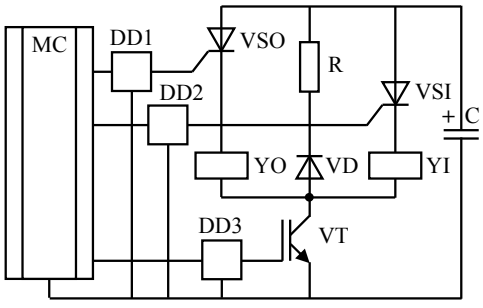

Fig. 1. Driving power circuit of activator windings control system of switching devices by ABB: YI, YO – windings on and off; VT – power transistor; VSI, VSO – thyristors, switching circuits of corresponding windings; VD – diode; R – resistor; DD1 ... DD3 – drivers; MC – microcontroller; C – electrolytic capacitor

In on operation, the microcontroller MC through driver DD3 injects the control signal to the gate of the transistor VT and through driver DD2 a short current pulse to the control electrode of the thyristor VSI, and as a result the actuator on winding YI connects to the power source, which role the role a storage electrolytic capacitor C performs, which is preliminary charged through the converter (not shown in the diagram) to the voltage U_C. In this thyristor remains open after the termination of the control pulse. At some time, the actuator armature starts moving and after the end of its movement by the command of the position sensor the controller stops supplying the control signal to the transistor, and as a result it is locked practically immediately, and the thyristor remains in the open state, since at this moment of time the diode VD opens and current in the winding YI, closing through the thyristor VSI, diode VD and resistor R, begins to subside by a curve close to exponential, until it drops below the level of the holding current of the thyristor VSI. At this moment, the thyristor VSI locked, simultaneously with it diode VD also locked, then the device is ready for the next operation – off operation, which is similar to on operation, but by connecting to a capacitor C of YO winding by using transistor VT and thyristor VSO.

Some disadvantage of the considered control system is the need to withstand some pause between operations that is between the moment of closing of one of thyristors (VSI or VSO) depending on the sequence of operations and transistor VT unlocking when performing a subsequent operation. It is difficult to check the fact of thyristor locking, so the algorithm of windings contrrol should assume quite a long pause (a few tens of milliseconds) between operations, else a command injection to unlock the transistor VT and thyristor VSO at

open thyristor VSI will not lead to the disconnection of the switching device and can cause a serious accident if it is necessary to disconnect the device immediately after switching it to a short circuit.

A polarized actuator with one coil [2] and the return spring is much simpler from designing and technological points of view, however, to perform on and off operations the coil must create oppositely MMF, which can be achieved either by winding two coils and control them alternately, either by using one coil included in the diagonal of the bridge formed by four power switching devices such as transistors. In the system shown in Fig. 2, to perform on operations (**I**) of the switching device, microcontroller MC through drives DD1 and DD2 injects signals to the gates of transistors VT2 and VT3, and performing the off operation (**O**) – to gates of transistors VT1 and VT4.

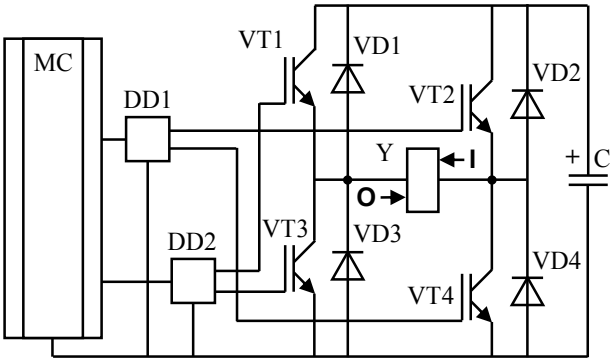

Fig. 2. Driving power circuit of actuator winding control system included in the diagonal of the bridge formed by four transistors: Y – actuator winding; VT1 ... VT4 – power transistors, controlled through drivers DD1 and DD2 (by one double driver for the half-bridge); VD1 ... VD4 – diodes, providing energy recovery, accumulated in the winding, in the electrolytic capacitor C after locking power transistors; MC – microcontroller

Power transistors and drivers for them are expensive elements, therefore of interest to consider the use of a hybrid switching of actuator windings circuits. With reference to the actuator control with one winding, a power circuit may appear, for example, as shown in Fig. 3.

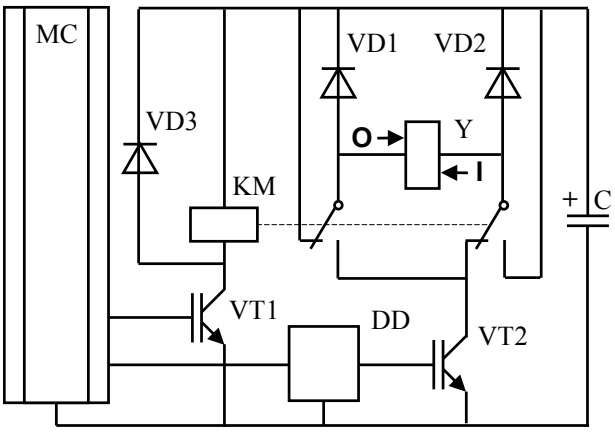

Fig. 3. Power circuit of a control system with hybrid switching of actuator winding circuit: Y – actuator winding; VT1 – low-power transistor controlled directly by the microcontroller MC; VT2 – power transistor controlled through the driver DD; VD1, VD2, VD3 – diodes; C – electrolytic capacitor; KM – relay with two change-over contact groups

Hybrid switching of electrical circuits, suggesting the presence in switching devices of both mechanical (contact) and semiconductor switching elements, is one of the most promising directions of development of electric apparatus [3 – 6], combining advantages of circuits switching by mechanical and semiconductor switching elements. In this hybrid switching is used primarily to increase the breaking capacity and electrical durability of apparatus that perform operations on and off. In hybrid switches unlike conventional switching devices, current on and off functions are performed by only the semiconductor switching element (transistor), and the mechanical switching elements (contact groups of relays) perform the functions of a router, switching electrical circuits during dead times. The use of hybrid switches of this type instead of the existing semiconductor switches will significantly reduce the cost of the actuators control systems, as well as reduce their sizes. This direction of hybrid switching is relatively new, so the study of the characteristics of the processes that occur in such switching, have some promise both in theoretical and in practical terms.

The aim of the work. The control algorithm of relay coil and power transistor given by the microcontroller must coordinate their work clearly and avoid interruptions in the opening relay contacts at the open transistor to prevent the occurrence of the arc on the relay contacts. Any switching operation in the electromagnetic relay is accompanied by contact bounce, which is due to the peculiarities of the structure of their contact systems. Coordination of the relay and power transistor operation has to take into account and this factor – the transistor should be open not earlier, what the end of contact bounce, that is not before the operation of the relay on or off will end completely. Relay manufacturers do not present in the specifications such the characteristic as duration of a fully completed operation on and off taking into account contact bounce, accompanying an operation that does not allow the use of relay in hybrid switching systems under the manufacturers warranty. Applying one or another relay in hybrid switching system, the manufacturer of the switching device should be based on reliable results of experimental investigations, taking into account the random components of the relay timing characteristics. Here, the experiment must be based on a certain method of experimental determination of the time intervals between the moments of switching transistor which controls the relay coil, and the power transistor at performing on and off operations of the switching device, the development of which is one of the goals of this work.

Another goal is to develop recommendations for the reduction of the duration of these intervals, because their reduction improves the breaker speed – one of the most important characteristics of the switching device.

A method of experimental determination of the time intervals between the moments of switching transistor which controls the relay coil, and the power transistor. The control algorithm for transistors VT1 and VT2 in the considered system (Fig. 3) implies that for any

switching state of the apparatus transistor VT1 initially have to be obligatory locked. This means that after the full completion of on operation of the switching device, if after this for a predetermined time interval Δt, sufficient to ensure that the current in the coil after the transistor VT2 locking decreased to near zero (this time is experimentally determined and in real apparatus does not exceed 100 ms) does not come the off command, the microcontroller closes transistor VT1, with the result that the relay is switched off, its contacts come in initial condition, preparing electrical circuits to carry out the subsequent on operation. The microcontroller continuously monitors the state of the switching device, and if the ion command comes when the apparatus is switched on, no action is taken, and if the the on command comes when the apparatus is switched off, the microcontroller performs two consecutive actions: 1) sends a signal to unlock the transistor VT1, whereby, the relay KM switches on, the relay contacts switching state is changed, the power circuit of the control system is prepared to perform the on operation of the apparatus, and 2) sends a signal for unlocking transistor VT2, whereby the actuator is activated and the apparatus switched on. At the on operation of the apparatus, the power transistor has to be opened no earlier than the end of relay contacts bounce, so the duration of the period of time between t_{bI} between the moments of unlocking transistors VT1 and VT2 should be guaranteed more than the interval between the moment of voltage supply to the relay coil KM and the moment of guaranteed end of contact bounce.

If the external command to off the apparatus comes when the apparatus before it was switched on longer than above mentioned duration of period of time Δt, the unlocking signal to the transistor VT2 controller issues immediately. If the off command comes during the on operation switching of the switching device, the controller has to interrupt the on operation, locking the transistor VT2, wait for the signal from the apparatus contact position sensor that its main contacts come into the open state (during this time current in the actuator coil will decrease to almost zero), after that to lock transistor VT1, and to give a signal to the transistor VT2 unlocking not earlier than in the time interval t_{bO} between transistor VT1 locking moment and the moment of guaranteed completion of the bounce of the break contact of the relay KM.

Durations of periods of time t_{bI} and t_{bO} depend on the characteristics of the relay selected for operation in a hybrid switching system. Interface relays intended mainly for switching automation circuits have attractively small dimensions and at the same time sufficiently large current ratings surpassing the possible values of the currents in the windings of medium voltage vacuum switchgear actuators. For example, the relay RT (Schrack, Austria) or relay RM84 (ABB, Relpol, Poland) with housing dimensions of 29 × 12.7 × 15.7 mm and weight 14 g allow holding current in continuous mode up to 8 A and peak currents up to 15 A. These relays have a sufficiently high speed – about 7 ms when switching on and 2 ... 3 ms when switching off. It should be borne in mind that in catalogues values of off time at mechanical opening of the relay coil circuit, which suggests that the energy stored in the winding is dissipated in the intercontact gap of the apparatus, switching this coil circuit and/or in the spark quenching circuit, connected in parallel to contacts of this device are indicated. If the switching operations are performed by a transistor interrupting the current almost immediately, the winding is required to be shunted by a «demagnetizating» diode, which opens automatically at the time of closing of the transistor shorting terminals of the winding, so that the current gradually decreases according to the law, which is close to an exponential and cumulative energy dissipates in winding resistance. As a result, the duration of fully completed operation of the switch off of the relay increases from 2 … 3 ms (at mechanical switching off) to 16 ... 20 ms. It is also important to consider the fact that there is a statistical spread of durations of periods of time t_{bI} and t_{bO} not only by comparing these characteristics at the relay from different parties, but even in the same relay. To determine t_{bI} и t_{bO} values the experiment was carried out, the scheme of which is shown in Fig. 4.

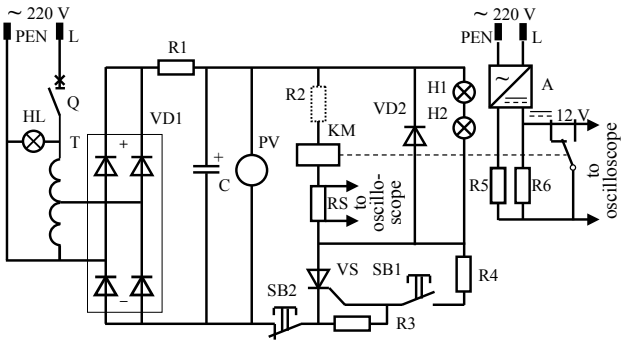

Fig. 4. The scheme of the experiment to determine the time intervals Δt_{bI} и Δt_{bO}: Q – switch quaranteeing protection against overloads and short circuits; HL – warning lamp; T – auto-transformer; VD1 – diode bridge; R1 – resistor, through which the capacitor C of high capacity (about 10,000 μF) charges; PV – voltmeter; KM – relay with two changeover contact groups (in the diagram one group is shown); R2 – auxiliary resistor (set if the voltage on the capacitor exceeds the nominative voltage relay coil); RS – shunt for current oscillography in the relay coil; VS – thyristor; VD2 – «demagnetizating» diode; R3, R4 – resistors of the thyristor control circuit; SV1, SV2 – buttons for the relay on and off; H1, H2 – incandescent lamps (thyristor load); A – changer; R5, R6 – divider (registrator of the bounce of relay contacts)

A method of experimental determination of the time intervals t_{bI} and t_{bO} includes the following sequence of actions.

1. Turn the switch Q.

2. Using the autotransformer T set the required voltage U_C of power supply of relay (capacitor C), which is controlled by the voltmeter PV.

3. Prepare the oscilloscope to the recording process.

4. Push the button SB1 and fix on the oscilloscope processes of change of current in the coil and the relay contact bounce when it is turned on.

5. Using the autotransformer T set the required voltage U_C of relay power supply.

6. Prepare the oscilloscope to the recording process.

7. Push the button SB2 and fix on the oscilloscope processes of change current in the coil and the relay contact bounce when it is turned off.

Typical oscillograms of the processes on and off the relay with the power supply voltage U_C which equals to the rated supply voltage of the relay coil U_S, in this case – 48 V are shown in Fig. 5,*a* and 5,*b*. From the oscillogramms it is shown that the time of relay on which is independent of the presence of «demagnetizating» diode approximatly corresponds to data of relay specification, and time off due to indivated diode is substantially greater than the value specified by the manufacturer.

Reducing the duration of intervals between the moments of switching transistor that controls the relay coil, and the power transistor. The duration of time intervals t_{bI} and t_{bO} can be significantly reduced if the relay coil with rated supply voltage U_S to connect to the source with a nominal voltage U_C, superior the value U_S, through a series resistor, the resistance of which is chosen so that in the steady state on the winding the established voltage equals to U_S. Besides, the time constant of the relay coil circuit will increase and the current in the coil during the process of the relay on will grow faster, and in the process of the relay off will decrease rapidly until the beginning of the movement of the armature. Although, as the results of experiments show, the speed and time of armature motion as well as the time of the contacts bounce remains approximately the same as when the relay operates in the «normal» mode, the total value of the duration of the time intervals t_{bI} and t_{bO} significantly reduce compared with the corresponding durations in «normal» mode.

For example, if a circuit consisting of the relay RT winding with rated supply voltage U_S = 48 V, and auxiliary resistor R2, whose resistance is six times higher than winding resistance, to connect to a source voltage 7 × 48 = 336 V, then in the steady state on the winding the established voltage will equal to 48 V. Here, typical oscillogramms of process on and off the relay and contact bounce will appear as shown in Fig. 5,*c* and 5,*d*. From the oscillogramms it is shown that time intervals t_{bI} and t_{bO} substantially reduce compared with «normal» mode, and this being primarily due to reduction of the time constant of the winding circuit, and the slope of change of current in the winding at the end of movement of the armature as well as the duration of contacts bounce still practically the same as they were in the «normal» mode.

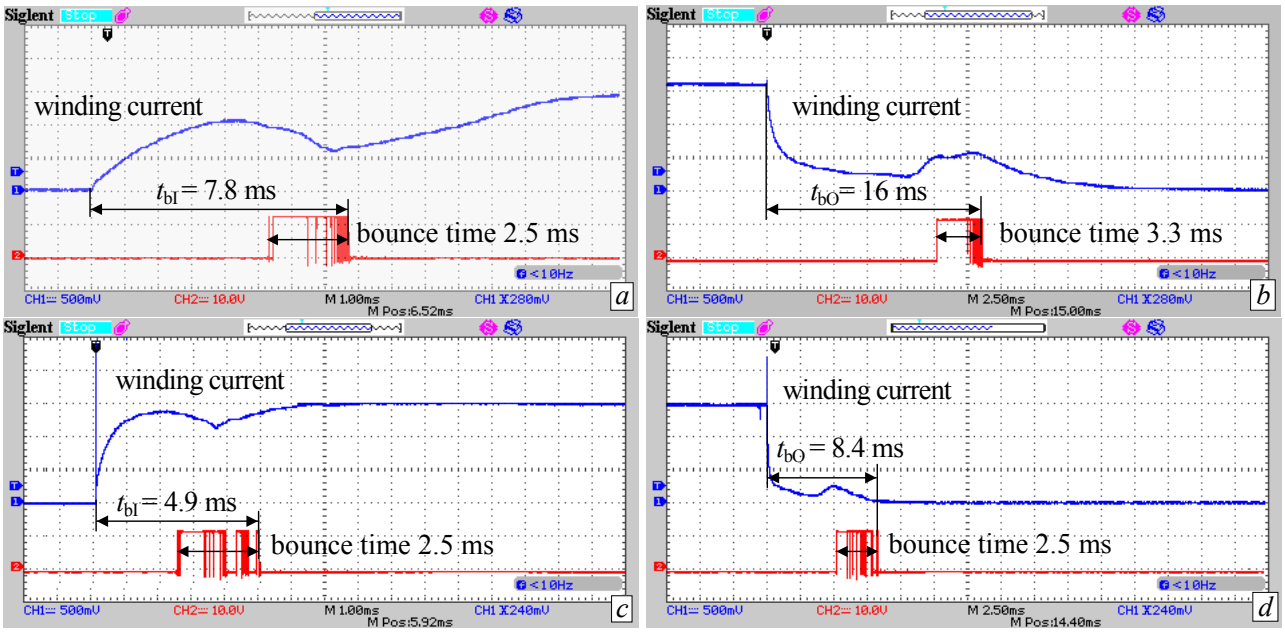

Fig. 5. Typical oscillogramms of the relay RT on and off with rated supply voltage U_S = 48 V:
a – relay on, voltage of the control circuit (source) U_C = 48 V; *b* – relay off, U_C = 48 V;
c – relay on, U_C = 336 V; *d* – relay off, U_C = 336 V

The temporal characteristics of the relay of the same type (even from the same batch) may differ significantly from each other. Therefore, in order to make a correct conclusion about the necessary duration of time intervals t_{bI} and t_{bO} in hybrid switching systems, it is necessary for the selected type of relay to perform measurements of indicated durations for sufficiently large number of relays and to carry out statistical processing of experimental results. We investigated the temporal characteristics (during on and off operations) of the RT relay with winding rated supply voltage U_S = 48 V at two values of the voltage of the control circuit (source) U_C = 48 V and U_C = 336 V. 20 relays were used in the experiment with two contact groups each for a total of 40 contact groups. The experimental results are shown in Fig. 6, where by dots cumulates are shown – accumulated frequencies of values of time intervals t_{bI} and t_{bO}, do not exceed the values (in ms) indicated on the *x*-axis.

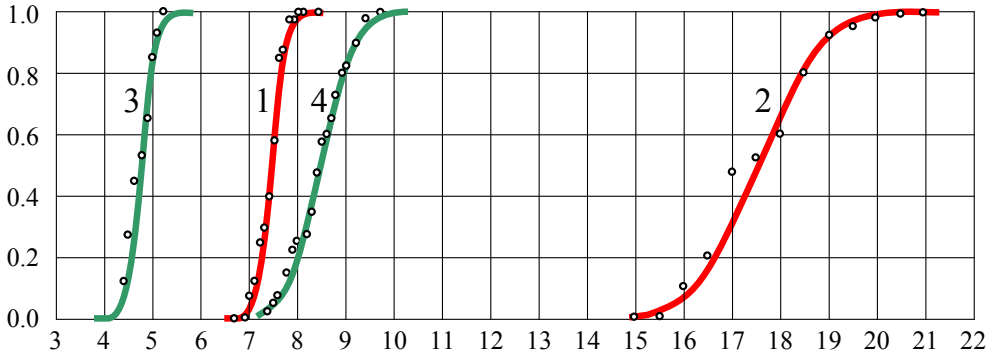

Fig. 6. Cumulates and normal distribution function, built on the results of experimental determination of the values of time intervals t_{bI} and t_{bO}, corresponding on and off operations of the RT relay with winding rated supply voltage U_S = 48 V: 1 – relay on, voltage of the control circuit (source) U_C = 48 V; 2 – relay off at U_C = 48 V; 3 – relay on at U_C = 336 V; 4 – relay off at U_C = 336 V

The solid lines in Fig. 6 show the normal distribution functions $F(t)$, built on the basis of expression

$$F(t) = \left[1 + \mathrm{erf}\left(\frac{t-\mu}{\sigma \cdot \sqrt{2}}\right)\right],$$

where t is the current value of the time interval (t_{bI} or t_{bO}); μ is the mathematical expectation (average value of the sample) of a random variable; σ is the root-mean-square deviation of distribution; erf is the error function. Results of calculations of the average (according to the experimental data) values, root-mean-square values, and the probable limit values of the duration of time intervals t_{bI} and t_{bO} for the RT relay with winding rated supply voltage U_S = 48 V are presented in Table. Cumulative curves in this case are very similar to the curves of normal distributions, therefore, with a high degree of reliability it can be argued that the coordination of operation of the relay RT and the semiconductor switch will be provided, if the interval between the moments of their switching will exceed the value of $\mu + 3 \cdot \sigma$, taken from the last column of the Table.

Table

Results of experiment for determination of duration of time intervals t_{bI} and t_{bO} for the RT relay with winding rated supply voltage U_S = 48 V

Quantity	U_C, V	μ	σ	$\mu + 3 \cdot \sigma$
t_{bI}	48	7.46	0.24	8.18
t_{bO}	48	17.3	1.06	20.5
t_{bI}	336	4.78	0.26	5.56
t_{bO}	336	8.51	0.56	10.2

Conclusions.

1. Switching of actuators windings circuits in which functions of the current on and off are assigned to the semiconductor switching element, and the mechanical switching elements perform the functions of routers, switching electrical circuits during the dead times, is a relatively new direction of the hybrid switching opening prospects of simplification, reduce the sizes and proce reduction of actuators control systems.

2. The hybrid switching of actuators coils circuits requires a clear coordination of moments of switching semiconductor and mechanical switching elements. The method of experimental determination of the time intervals between the moments of switching these elements taking into account contact bounce of mechanical elements is developed. The possibility of using the interface relays as mechanical switches is considered, the durations of the intervals to ensure coordination of the operation of these relays with semiconductor switches are determined.

3. A technique of a significant reduction of the duration of the intervals between the moments of switching semiconductor and mechanical switches in actuators control systems, providing the increase of speed of switching devices is considered and experimentally confirmed.

REFERENCES

1. Dullni E., Fink H., Reuber C. *A vacuum circuit-breaker with permanent magnetic actuator and electronic control*. Available at: https://library.e.abb.com/public/5e750b2ecc5b760ec1256ad4002d2c00/cired99_Nice_VM1.pdf (accessed 15 October 2015).

2. Klymenko B.V., Vyrovets S.V., Forkun Ya.B. *Elektromagnitnyi privod* [Electromagnetic actuator]. Patent Russian Federation, no. 2312420, 2007. (Rus).

3. Soskov A.G., Sabalaeva N.O. *Hibrydni kontaktory nyzkoi napruhy z pokrashchenymy tekhniko-ekonomichnymy kharakterystykamy: monohrafiia* [Hybrid contactors low voltage with improved technical and economic characteristics]. Kharkiv, National University of Urban Economy Publ., 2012. 268 p. (Ukr).

4. Meyer J.-M., Rufer A. A DC hybrid circuit breaker with ultra-fast contact opening and integrated gate-commutated thyristors (IGCTs). *IEEE Transactions on Power Delivery*, 2006, vol.21, no.2, pp. 646-651. **doi: 10.1109/tpwrd.2006.870981.**

5. Häfner J., Jacobson B. Proactive hybrid HVDC breakers – a key innovation for reliable HVDC grids. *Integrating supergrids and microgrids International Symposium in Bologna, Italy*. – 2011.

6. Kapoor R., Shukla A., Demetriades G. State of art of power electronics in circuit breaker technology. *2012 IEEE Energy Conversion Congress and Exposition (ECCE)*, 2012, pp. 615-622. **doi: 10.1109/ECCE.2012.6342764.**

Received 20.10.2015

B.V. Klymenko[1], *Doctor of Technical Science, Professor,*
A.V. Eres'ko[1], *Candidate of Technical Science, Associate Professor,*
I.S. Varshamova[1], *Assistant Lecturer,*
N.A. Lelyuk[1],
[1] National Technical University «Kharkiv Polytechnic Institute», 21, Bagaleya Str., Kharkov, 61002, Ukraine.
phone: +38 050 6534982; e-mail: b.v.klymenko@gmail.com

How to cite this article:
Klymenko B.V., Eres'ko A.V., Varshamova I.S., Lelyuk N.A. Research of the applications possibility of interface relay in hybrid switching systems of bistable actuators windings. *Electrical engineering & electromechanics*, 2016, no.1, pp. 21-25. doi: 10.20998/2074-272X.2016.1.04.

UDC 621.313:681.3 **doi: 10.20998/2074-272X.2016.1.05**

V.I. Milykh, N.V. Polyakova

DETERMINATION OF ELECTROMAGNETIC PARAMETERS AND PHASE RELATIONS IN TURBO-GENERATORS BY THE AUTOMATED CALCULATION OF THE MAGNETIC FIELD IN THE SOFTWARE ENVIRONMENT FEMM

The theoretical bases of calculation of electromagnetic quantities and time-phase relationship are presented for the turbo-generators. This is done by numerical calculations of the magnetic field in the software environment package FEMM (Finite Element Method Magnetics). A program which controls calculations and organizes the issuance of the results to a text file is created on the algorithmic language Lua. The program is universal in terms of a turbo-generator models, as well as steady-state modes of their work with a minimum of input data. The exciting current of the rotor and the phase currents of three-phase stator winding in accordance with their initial phase are given for the calculation of the magnetic field. The key function for the analysis of electromagnetic parameters is the calculated angular function of the magnetic flux phase stator winding. The expansion in the harmonic series is carried out and amplitude and initial phase are received for this function. Next, the phase EMF and voltage, phase shifts between all values, active power, electromagnetic torque, the magnetic flux in the gap and other parameters are determined. The presented Lua script is a prototype for a similar calculation software of electric machines of other types. References 9, figures 6.

Key words: **Finite Element Method Magnetics, program FEMM, turbo-generator, electromagnetic parameters, phase relationships, automated calculations, Lua script.**

Представлены теоретические основы расчета электромагнитных величин и их фазовых соотношений для турбогенераторов. Это реализуется путем численных расчетов магнитного поля в программном пакете FEMM. Расчеты автоматизированы посредством созданной программы на алгоритмическом языке Lua. Она управляет расчетами и организует выдачу результатов в текстовый файл. Представленный скрипт Lua универсален и может послужить прототипом аналогичного программного обеспечения для других типов электрических машин. Библ. 9, рис. 6.

Ключевые слова: **программа FEMM, турбогенератор, электромагнитные параметры, фазовые соотношения, автоматизированные расчеты, Lua скрипт.**

Introduction. Widely known software FEMM [1] is effective for the calculation of three-dimensional magnetic fields (MF) of electrical machines (EM), classic design with almost in-plane plane MF within their active part. For example, this applies to the turbo-generators (TG) [2]. This program is freed calculators from the development of implemented mathematical models and programming and has a fairly user-friendly interface.

An additional means of facilitating the work of users of the program FEMM are scripts in the algorithmic language Lua, integrated into it. For example, in [3] our program is described, which automated construction of simulation models of TG, in [4] the program of automated calculations of their electromagnetic processes is given. Efficiency of Lua script is that programs are written once, and used countless times, and by any number of users.

This paper continues the series of works started in [3, 4]. And its **purpose** is to present the script Lua, automating the preparation of a series of electromagnetic parameters and phase relations in EM by the numerical MP calculations in the software environment FEMM. It is made on the example of TG – one of the largest and responsible of their representatives [5].

Object of investigations. For illustration here, as in [3, 4], we have TG 340 MW. Its parameters are further presented in the file of initial data.

Electromagnetic system of the TG shown in Fig. 1 by its cross-section. Highlighted phase zones of a two-layer shortened three-phase stator winding A–A', B–B' and C–C'. Shown used rectangular (x, y) and polar (r, α) coordinate system, the longitudinal d transverse q axis of the rotor.

The basis of the developed Lua script is prepared in advance for the environment FEMM computational model of the electromagnetic system of the TG. We do this through a script Lua, presented in [3], and in the absence of such – in «manual» mode, in accordance with the instructions of the software FEMM.

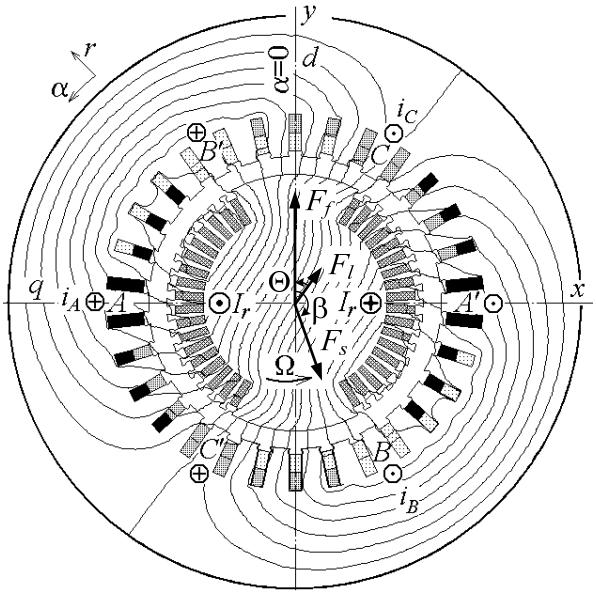

Fig. 1. Model of the electromagnetic system of the TG

in its cross-section

View on the computer screen in the environment FEMM (file type – Femme Document) of the calculation model of the TG presented as a whole in Fig. 2, and in Fig. 3 its fragment is presented. Visible marks of physical properties of the *blocks* – limited regions of the calculation area. Marks Fe1, Fe2 and Fe3 set the magnetization curves of ferromagnetic materials, m0 – permeability, m0 – magnetic permeability $\mu_0=4\cdot\pi\cdot10^{-7}$ H/m, marks iA, iB, iC – phase currents, Ir – rotor current. Addition of + or – to the mark of current indicates its direction: if the current at this time is positive, then at this point it is taken with the appropriate sign. The number after the colon indicates the number of effective conductors in this block. Circles around marks indicate the maximum size of the triangles in the structure of the finite elements formed by program FEMM.

The fragment in Fig. 3 is taken from the right half of a complete model from Fig. 2, the rest of all similarly formed in accordance with and model in Fig. 1. In particular, the left half of the signs of currents is opposite to that seen in Fig. 3.

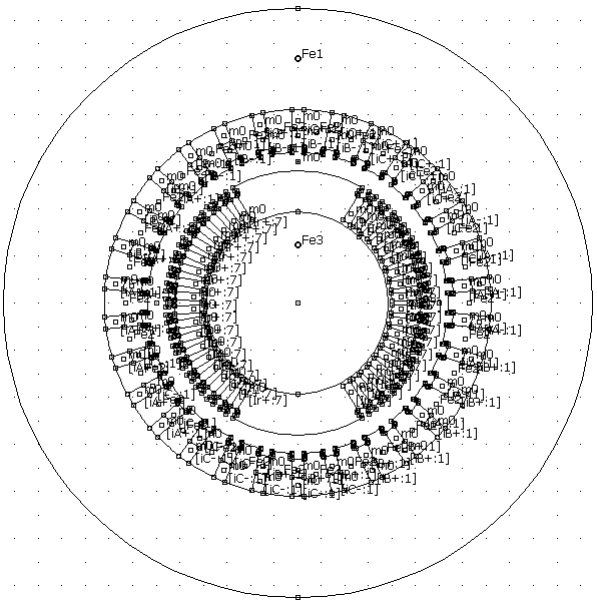

Fig. 2. Initial physico-geometrical model of the TG

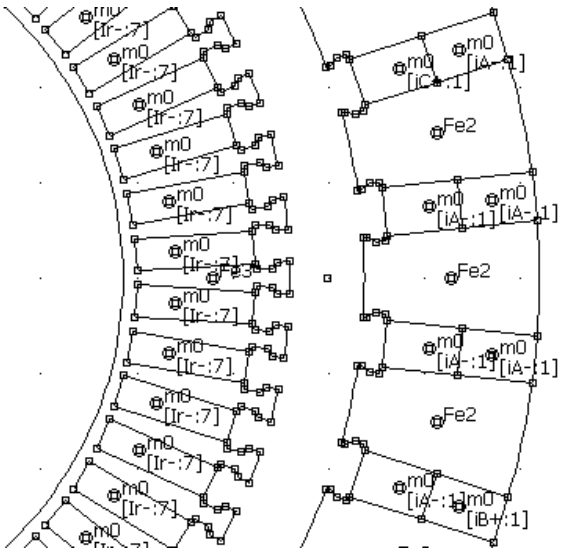

Fig. 3. Fragment of the physico-geometrical model of the TG

Mentioned blocks in the FEMM-model are combined in groups to operate with them as units of the calculation area. From the designated group number [3] is here used: 2, 3, 4, 5, 6, 7 – the phase zones A, B, C, A', B', C' of the stator winding, 9 – entire rotor (see Fig. 1).

Theoretical basics. The steady-state MF calculation by the program FEMM is carried out on the base of the numerical solution of the differential equation:

$$\mathrm{rot}\left[\frac{1}{\mu}\mathrm{rot}\left(\vec{k}\,A_z\right)\right]=\vec{k}\,J_z\,, \qquad (1)$$

where A_z, J_z are the axial components of the magnetic vector potential (MVP) and current density; μ is the absolute magnetic permeability; k is the ort.

On the external boundary of the calculation area for the MVP the know Dirichlet condition $A_z = 0$ is accepted.

In the model TG (Fig. 2) for calculating of the the instantaneous distribution of MP of the particular steady state mode it is necessary to have the corresponding currents. In generalizing load mode (LM) [9] is given a constant rotor current I_r and the instantaneous values of the symmetrical system of stator phase currents: $i_A=I_m\cos(\beta)$; $i_B=I_m\cos(\beta-2\pi/3)$; $i_C=I_m\cos(\beta+2\pi/3)$, where $I_m=\sqrt{2}\,I_s$ is their amplitude and I_s is the effective value; β is its initial phase [6-9] specifies the shift of the stator winding MMF F_s from rotor winding MMF F_f (Fig. 1). Here conditional resultant for the MMF at LM is given

$$\vec{F}_l=\vec{F}_f+\vec{F}_s\,. \qquad (2)$$

At no-load (NL) conditions only the rotor current is given, at steady mode of short circuit – only the stator currents. Directions of currents (Fig. 1) are regulated according to the system adopted in [7].

For TG the result is a distribution of MF in its cross-section as a function $A_z(x,y)$. Picture of MF in the calculation area is represented by a structure of field lines – lines of equal MVP $A_z=const$. An example of this for the TG at the mode to its rated load (RL) is shown in Fig. 1.

One of the key quantities in the analysis of electromagnetic parameters of the TG is the magnetic flux linkage (MFL) [2] and it is determined by the distribution of MVP. For example, for any of the six phase areas (Fig. 1) MFL is determined based on

$$\Psi=\frac{N_s l_a}{S_\varphi}\int_{S_\varphi}A_z dS\approx\frac{N_s l_a}{S_\varphi}\sum_{j=1}^{K_\varphi}A_{z,av,j}\Delta S_j\,, \qquad (3)$$

where S_φ is the section square by current-carrying elements of the phase zone; K_φ is the number of elements of its discretization; $A_{z,av,j}$ is the average MVP value in the j–th element.

In the formula (3) the active length of the TG l_a and the number of turns of the phase stator winding N_s are taken into account, and to determine S_φ and integral in Lua script there are appropriate procedures [1].

The initial basis for identifying the *phase relations* in any of the design modes is a temporary phase or direction of the vector MFL of the phase winding A–A'. MMF of this base winding in Figure 1 is oriented along the longitudinal axis of the rotor d.

The direction of the vector MFL of the phase

winding $A–A'$ 'is determined by the structure of a particular MF of the actual calculated mode. So, in Fig. 1 this direction is becomes apparent by orientation of field lines of the MP and generally corresponds to the direction of the vector MMF F_l (2). But as long as the vector is constructed a priori, taking into account the results that will be obtained even further based on the methodology, which was published in [4-6]. Here, it shall be presented briefly to understand the meaning of the developed and submitted further the Lua script.

The mentioned techniques will be described with reference to the NL conditions, and then it will be effective for any other mode. Specifically, we assume that the MF at the NL conditions is calculated by the program FEMM. The structure of this field is shown in Fig. 4.

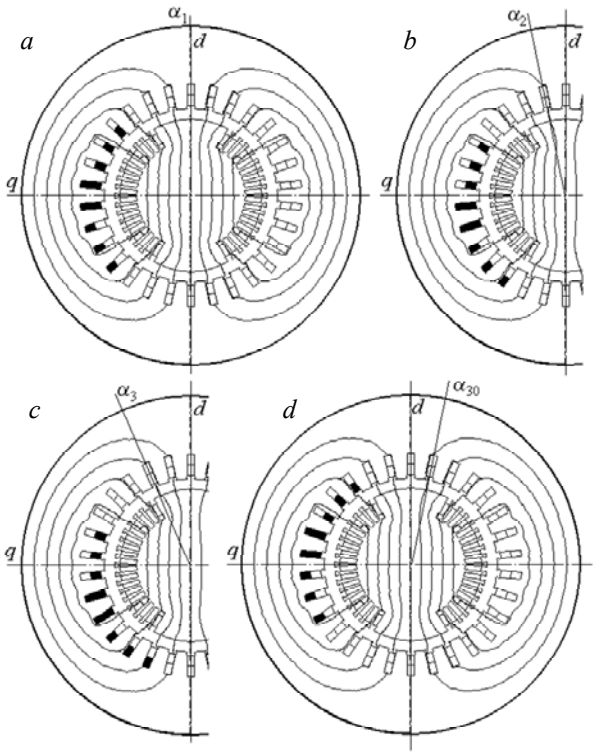

Fig. 4. Displacement of the phase zone of the stator winding against a background of the calculated MF to select the MFL values

In the initial angle position α_1 of the phase zone A in Fig. 4,*a* on the basis of formula (3) the MFL Ψ_1 is determined. Now move this zone conditionally on the tooth division to the position α_2 (Fig. 4,*b*) and find the corresponding value of the MFL Ψ_1. The same repeat $\alpha 3$ at position α_3 (Fig. 4,*c*), etc. – until the position α_{30} (Fig. 4,*d*). In general, the number of positions equals to the number of stator slots Q_s. A phase shift of each phase zone is made on angle $\Delta\alpha=360/Q_s$ (in degrees).

As a result we will have a discrete angular function of the MFL of one phase zone at its period T, i.e.

$$\Psi_k(\alpha_k); \quad \alpha_k=(k-1)\cdot\Delta\alpha; \quad k=1,\,2,\,3,\ldots\,Q_s, \quad (4)$$

where k are number of angular positions of this zone.

For each position of the phase zone between 1 and $Q_s/2$ there is a diametrically opposite position between $Q_s/2+1$ to Q_s. They mutually create a conditionally movable phase winding $A–A'$, for which the angular function of the MFL at its half-period:

$$\Psi_{A,k}=\Psi_k-\Psi_{k+Q_s/2}; \quad k=1,2,3,\ldots Q_s/2. \quad (5)$$

By obtaining results, taking into account the periodicity of values in the TG type $\Psi(\alpha+T/2)=-\Psi(\alpha)$ we supplement the half-period of the MFL (5) to full period:

$$\Psi_{A,k+Q_s/2}=-\Psi_{A,k}; \quad k=1,2,3,\ldots Q_s/2. \quad (6)$$

The number series of the MFL (5) is illustrated in Fig. 5 by set of highlighted points on the curve of the NL in the range of k from 1 to 15. On the basis of (6) the curve is extended to a full period (points 16 to 30) and point 31 repeated the first point (point 1) through a period T.

Similar actions were carried out and after calculating the MF at the RL mode, and the results are presented by the RL curve in the same Fig. 5. To display the initial phases of functions of the MFL the curves are continued to the left.

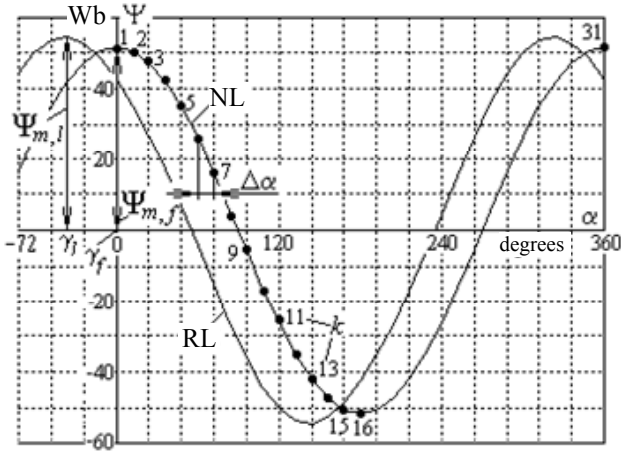

Fig. 5. Angular dependences of the MFL of the TG phase winding

Obtained numerical full angular function $\Psi_{A,k}(\alpha_k)$, $k=1,2,3,\ldots Q_s$, can be presented as harmonic series expansion [6, 7]. Because of typical for the TG periodic condition $\Psi(\alpha+T/2)=-\Psi(\alpha)$ in this series there is no constant component and even harmonics. Assumed in [6] cosine series for the MFL is the following

$$\Psi_A=\sum_{\nu=1,3,5,\ldots}\Psi_{m,\nu}\cos(\nu\alpha+\gamma_\nu), \quad (7)$$

There amplitudes and arguments (initial phases)

$$\Psi_{m,\nu}=\sqrt{s_\nu^2+c_\nu^2}\,; \quad \gamma_\nu=-\mathrm{arctg}\frac{s_\nu}{c_\nu} \quad (8)$$

Are obtained by sinus-cosine coefficients:

$$s_\nu=\frac{2}{Q_s}\sum_{k=1}^{Q_s}\Psi_{A,k}\sin(\nu\alpha_k)\,; \; c_\nu=\frac{2}{Q_s}\sum_{k=1}^{Q_s}\Psi_{A,k}\cos(\nu\alpha_k).$$

In (8) arctangent function $\mathrm{arctg}(s_\nu/c_\nu)$ should be extended to give a value in the range of –180° до +180° depending on the signs c_ν and s_ν. In Lua there is a corresponding function *atan2*(s_ν,c_ν).

In EM including TG analysis of the phase relationships is carried out for the first harmonics. For the first cosine harmonic of the MFL (7) at the NL the amplitude and initial phase Ψ_{mf}=51.97 Wb and γ_f =0, at

the RL – $\Psi_{m,l}$ =53.89 Wb and γ_l = –35.75° are obtained (in the notation we do not show the harmonic number). The remaining harmonic, in principle, were negligible.

Illustration of angles γ_f and γ_l is presented in Fig. 5, where we see that the amplitude and hence the vector of the MFL at the RL mode are shifted toward negative value of the angle α relatively to the MFL at the NL mode.

The shift angle $\Theta = \gamma_f - \gamma_l$ is a load angle of the TG (in this case, it has a positive value). The vectors F_l and F_f in Fig. 1 have a similar shift.

Taking into account that in the TG the rotation angle is connected with time, i.e. $\alpha=\Omega \cdot t$, where Ω is the angular velocity, it is possible to go to the common temporal vector diagrams (VD) to illustrate and other phase relationships and the definition of other parameters. Such a VD is shown in Fig. 6, where as the origin of the angles vertically disposed longitudinal axis of the rotor *d*, as well as the angles in Fig. 1 is taken.

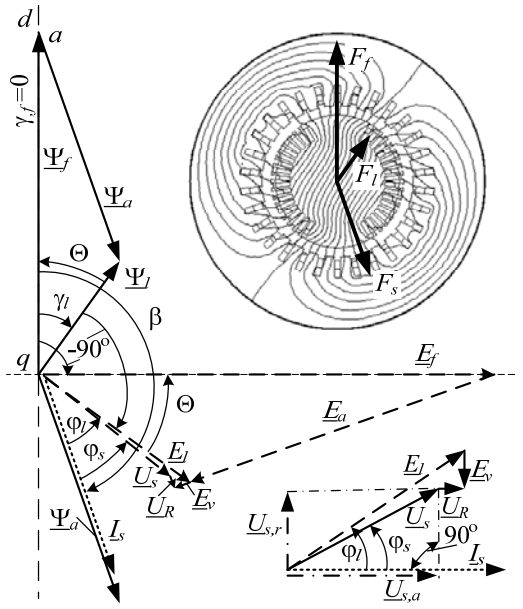

Fig. 6. Vector diagram corresponding the load mode of the TG

Phase current vector $\underline{I}_s$ is produced relatively the *d*-axis with respect to the previously caused β angle (in this case, it equals to –160.43°). The vector of the MFL Ψ_a phase windings, caused by the MF of the armature reaction corresponding to the vector F_s has the same direction. Vectors of the MFL Ψ_f from the rotor winding and the resulting MFL Ψ_l are carried out under already determined angles γ_f and γ_l.

Actually, selection of Ψ_a и Ψ_f from the MFL Ψ_l is conditional at the LM, and here the value Ψ_f is completely different compared to the NL mode. Parts of the MFL are determined by the procedure adopted here.

Namely, we adopt a base already defined MFL Ψ_l and from the end of its vector draw a line parallel to the vector Ψ_a to the intersection with a line oriented as Ψ_f at an angle γ_f. This intersection in the point *a* and identifies specific length of vectors Ψ_a and Ψ_f and their values in the scale of the vector Ψ_l.

Based on the known theory [2] by the amplitude of the MFL at frequency f_s we have root-mean-square value of the first harmonic of the phase EMF, including and at the LM:

$$E_l = \sqrt{2}\,\pi f_s \Psi_{m,l}\,. \qquad (10)$$

The vector of this EMF, as it is known, behind the vector of its MFL Ψ_l at –90 °. Vectors of the EMF E_a and E_f from the MFL Ψ_a and Ψ_f are defined and constructed similarly.

It turns out that the triangle of the EMF E_l, E_a and E_f is similar to the triangle of the MFL Ψ_l, Ψ_a and Ψ_f.Therefore, between the vectors E_l and E_f will be the same angle of the load Θ.

In order to determine phase voltage U_s, it is necessary to take into account the voltage drop $\underline{U}_R=R_s \underline{I}_s$ at the active resistance R_s and EMF $\underline{E}_v= -jX_v \underline{I}_s$ from the flux of the phase winding end leakage, where X_v is the corresponding inductive reactance.

Obviously, the vector $\underline{U}_R$ is parallel to the vector $\underline{I}_s$, and the vector $\underline{E}_v$ – perpendicular (in the direction of lag). So they are attached to the end of the vector E_l and give as a result the vector of the phase voltage Us = $\underline{U}_s = \underline{E}_l + \underline{E}_v - \underline{U}_R$.

It is known that in the TG the U_R value is negligible compared with E_l и U_s, but here they appear to demonstrate the full-factor approach.

From the geometric relationships on the VD, a fragment of which in the rotated form is shown in detail below on the right (without observing proportions), the active and reactive components of the voltage U_s, its root-mean-square value and the phase shift from the vector of current $\underline{I}_s$:

$$U_{s,a} = E_l \cos\varphi_l - U_R;\; U_{s,r} = E_l \sin\varphi_l - E_v; \qquad (11)$$

$$U_s = \sqrt{U_{s,a}^2 + U_{s,r}^2};\;\; \varphi_s = \operatorname{arctg}(U_{s,r}/U_{s,a})\,, \qquad (12)$$

Where by the VD he angle between $\underline{I}_s$ and $\underline{E}_l$ equals to $\varphi_l = -\beta - 90 + \gamma_l$.

As a result, by the field calculation a lot of already considered electromagnetic parameters as well as active electric power of the TG are determined:

$$P_a = m_s U_s I_s \cos\varphi_s\,. \qquad (13)$$

Besides, it is possible to determine the electromagnetic torque of the TG which is made by the tensor of magnetic tension [2] in the correspondence with the formula

$$M_{em} = \frac{l_a}{\mu_0 (r_s - r_r)} \int_0^{2\pi} \int_{r_r}^{r_s} r \cdot B_r \cdot B_\alpha \cdot r \cdot dr \cdot d\alpha\,, \qquad (14)$$

where r_r and r_s are radii of circles limiting the gap from the sides of rotor and stator; B_r и B_α are radial and angular components of the magnetic flux density.

The magnetic flux through a surface bounded by the contour *l*, has the expression [2]:

$$\Phi = \left(A_{z1} - A_{z2}\right) \cdot l_a\,, \qquad (15)$$

where A_{z1}, A_{z2} are the MVP values at the points 1 and 2 in a plane of calculation, through which in the axial direction lateral sides of the mentioned circuit *l* pass.

To automate all conditioned calculations, the presented further Lua script according to the purpose of

this work is intended.

File of initial data of the TG for the Lua script.

Requirements to create the program, as in [3, 4] are its flexibility in terms of the geometry and dimensions of the TG, as well as steady-state modes of operation – with a minimum of input data.

The values of various parameters of the TG and serving local constants and variables can be defined directly in the Lua script, or input from a pre-prepared text files. In this work, all the parameters that characterize this problem and perhaps changing for different variants of the TG, entered from a separate file.

Text files of Lua-scripts and data files are written in the editor *Notepad*.

Here is a data file that may have any name with the extension txt. Data have a form of numbers or text strings in quotation marks " " and accompanied by commentaries. To mark the beginning of comments the colon been have chosen.

Text of the file of initial data.

"FemC_TG340" : name_fem – name of the model in FEMM
"RezC_TG340" : name_rez – name of the file of results
3 : ms – number of stator winding phases
1 : p – number of pairs of poles
50 : fs – frequency, Hz
-160.47 : beta – initial phase of the stator currents, degree
3151.4 : Ir – rotor excitation current, A
11547 : Is – stator phase current, A
0.8 : bs – relative stub of the stator winding
0.00266 : Rs – active resistance of the stator winding, Ω
0.063 : Xv – inductive reactance of the end part of the stator winding, Ω
0.0 : gf – initial phase of the MFL at the NL mode, degree
30 : Qs – number of rotor slots
10 : Ns – number of series turns in the stator phase
1 : as – number of parallel branches of the stator winding
5.308 : la – turbo-generator active length, m
637.5 : rsi – radius of the stator core bore, mm
699 : rv – average radius of the upper layer of the stator winding, mm
778 : rn – average radius of the lower layer of the stator winding, mm

General characteristics of Lua language. Language Lua, as well as other programming languages, can create loops, conditional statements, procedures, perform calculations on mathematical formulas for standard and created their own functions. There are functions: *sqrt* – square root; *sin*, *cos*, *atan2* – sine, cosine, arctangent, and others. There is built-in π number – Pi. Trigonometric functions operate with radians, but when dealing with geometric objects Lua uses degrees, rectangular coordinates are measured in millimeters, which are predetermined in the formulation of the problem in FEMM menu *Problem*, what has been done in [3].

The Lua script commands that begin with mo_ or mi_ are its procedures. Their description can be found via the *Help* button in the working window of FEMM, then entered the section *Lua Scripting* [1].

Strings of the program or the right side, starting with a double hyphen - - are comments and do not affect its work.

External data file name Lua script asks after its launch by the operator with a "tip":

```
File_dan=prompt("Введите имя файла")
```

This name is entered from the keyboard and entered by press Enter. Script opens the file for reading (`"r"`) and assign it internal name `f_d`, i.e.

```
f_d = openfile(File_dan .. ".txt","r")
```

Reading operator read(f_d, "*n", "*l")
from the next line reads valus of numeric and string data, how many times in it the option "* n" appears, and the option "* l" will make a transfer to a new line, i.e. remaining in the string any text is ignored and used by the user as a comment (we separate by symbol :).

In operators write to write to the results file the option "\ r \ n" gives a pass to new line, and the use of symbols such as % 6.3f is the format (format) of printing, i.e. in this case 6 position are reserved for the number, including 3 – for a fractional part.

Further a program is presented that after its call in the environment FEMM organizes input of the initial information and the calculation of the MF, forms an angular function of the MFL of the phase winding, determines its amplitude and the initial phase, as well as a number of electromagnetic parameters and phase relationships of different values in the TG.

Lua script.

```
--Definition of the file of initial
--data
File_dan=prompt("Input the file name")
--Opening of the data file
f_d = openfile(File_dan .. ".txt","r")
--INITIAL DATA from the text file
name_fem=read(f_d,"*n","*l")
--nameFEMM
--File name for the results writing
name_rez=read(f_d,"*n","*l")
ms=read(f_d,"*n","*l")
 --number of phases
p=read(f_d,"*n","*l") --pole pairs
fs=read(f_d, "*n", "*l")  --frequency
```

By the same way all data from the above-mentioned file are read till `rn`, i.e.*:*

```
rn=read(f_d,"*n","*l")
-- average radius of the lower layer
--of the stator winding
closefile(f_d) --closing the data file
--Organization of the file of results
writeto(name_rez) --name_rez file name
--Name of geometrical
--model of TG-type fem
name_fem=name_fem .. ".fem"
mi_saveas(name_fem) --to store model
   --ADDITIONAL DATA FOR CALCULATION:
gr=Pi/180 --multiplier degree=>radian
beta=beta*gr --value of angle beta, rad
Ur=Rs*Is --voltage drop on Rs
Ev=Xv*Is --voltage drop on Xv
ts=360/Qs --angle of stator tooth step
tp=Qs/(2*p) --pole step in
```

```
--tooth division
qsp=tp/ms --slot number per pole and
--phase
qsn=0.5*(qsp-tp*(1-bs)) --slot number
-- of the lower layer of the stator
-- winding under q-axis
qsv=qsp-qsn -- slot number
-- of the upper layer of the stator
-- winding under q-axis
--Angle of the first lower bar of the
-- phase A
an1=180-(qsn-0.5)*ts
--Angle of the first upper bar of the
-- phase A
av1=180-(qsv-0.5)*ts
Im=Is*2^0.5/as --amplitude of the phase
-- current in the parallel branch
--Writing of some TG parameters
write("TG exciting data","\r\n")
write(format(" Is= %5.0f",Is),
format(" Ir= %5.0f",Ir),
format(" beta=%7.2f",beta/gr),"\r\n")
F = {} --massive creation to store
     -- MFL values of phase winding
--Phase currents of the stator winding
c=2*Pi/3  Ia=Im*cos(beta)
Ib=Im*cos(beta-c) Ic=Im*cos(beta+c)
--Definition of currents of phases and
-- rotor in FEMM
mi_modifycircprop("iA+",1,Ia)
mi_modifycircprop("iA-",1,-Ia)
mi_modifycircprop("iB+",1,Ib)
mi_modifycircprop("iB-",1,-Ib)
mi_modifycircprop("iC+",1,Ic)
mi_modifycircprop("iC-",1,-Ic)
mi_modifycircprop("Ir+",1, Ir)
mi_modifycircprop("Ir-",1,- Ir)
--In FEMM-model there are names of
--marks of currents
--MF calculation in FEMM and path to
--demonstration and extraction of
--calculation results
mi_analyze(1)    mi_loadsolution()
--Cycle of conditional displacement of
--the phase zone A with slot step ts
for k=1,Qs,1 do   ak=(k-1)*ts --angle
--Cycle of calculation of conductors
--angles of phase A
for i=1,qsp,1 do  ai=ak+(i-1)*ts
--Calculation of coordinates of
--conductors of lower layer and their
--extraction
ani=(an1+ai)*gr  x=rn*cos(ani)
y=rn*sin(ani)   mo_selectblock(x,y)
--Calculation of coordinates of
--conductors of upper layer and their
--extraction
avi=(av1+ai)*gr  x=rv*cos(avi)
y=rv*sin(avi)    mo_selectblock(x,y)
end   --end of the cycle by i
--Reading of allocated blocks square
S = mo_blockintegral(5)
--MVP integral's value by square S
A = mo_blockintegral(1)
mo_clearblock() -allocation emptying
--MFL of the phase zone of winding A
F[k] = Ns*A/S
end -end of slot steps by k
--MFL of phase winding obtaining by
--MFL of phase zone and prolongation
--on period
q2=Qs/2 --a half of phase zone
-- positions
for i=1,q2,1 do F[i]=F[i]-F[i+q2]
             F[i+q2]=-F[i]  end
--Amplitude and phase shift
-- calculation
--MFL first harmonic by Fourier series
Fsin=0 Fcos=0 --storages nulling
for k=1,Qs,1 do --cycle by MFL array
ak=ts*(k-1)*gr --angular position
--Aplitudes of sin and cos components
Fsin=Fsin+2*F[k]*sin(ak)/Qs
Fcos=Fcos+2*F[k]*cos(ak)/Qs
end  --sweep of k array elements
Fm1=sqrt(Fsin^2+Fcos^2) --amplitude
gl=atan2(Fsin,Fcos) -initial phase
   --Electromagnetic parameters of TG
--RMS value of the phase EMF
El=Pi*2^0.5*fs*Fm1
--phase shift EMF El from current Is
fil=-(beta+Pi/2-gl)
--active and reactive components of
--phase voltage
Usa=El*cos(fil)-Ur Usr=El*sin(fil)-Ev
--RMS value of phase voltage
Us=sqrt(Usa^2+Usr^2)
--phase shft between Us and Is
--TG power ratio
fis=atan(Usr/Usa)  cosfi=cos(fis)
teta=gf*gr-gl  --TG load angle
Pa=ms*Us*Is*cosfi --active power
   --Results writing to file
write("  MFL, phase shifts,  EMF,
voltage and active power","\r\n")
--Angles recalculation (radians to
-- degrees)
gl=gl/gr fil=fil/gr fis=fis/gr
teta=teta/gr  beta=beta/gr
write(format(" Fm1=%5.2f",Fm1),
format(" gl=%7.2f",gl),"\r\n")
write(format(" El=%5.0f",El),
format(" fil=%7.2f",fil),"\r\n")
write(format("  gf=%4.1f",gf),
format(" teta=%6.2f",teta),
format(" Us=%5.0f",Us),"\r\n")
write(format(" fis=%7.2f",fis),
format(" cosfi=%4.2f",cosfi),
format(" Pa=%6.1f",Pa*1e-6),"\r\n")
write("Electromagnetic torque
and power","\r\n")
--Rotor block groups allocation
mo_groupselectblock(9)
--Electromagnetic torque reading
Mem=mo_blockintegral(22) Mem=Mem*1e-3
mo_clearblock()--allocation emptying
--Electromagnetic power
Pem=Mem*2*Pi*fs*1e-3
write(format("Mem=%5.0f",Mem)," кN*m",
format("Pem=%6.1f",Pem)," MW","\r\n")
--Magnetic flux per pole
--in gap on the stator bore
```

```
--Cycle of angular steps in da degrees
for i=1,180,1 do   da=1
--Coordinates of two neighbor points
ai=da*(i-0.5)*gr  ai0=da*(i+0.5)*gr
x=-rsi*sin(ai)  y=rsi*cos(ai)
x0=-rsi*sin(ai0)   y0=rsi*cos(ai0)
--MVP reading in two points
A=mo_getpointvalues(x,y)
A0=mo_getpointvalues(x0,y0)
--MVP maximum search on the circle
if A0<A then Pot=2*A*la  i=181 end
end --sweep of I points by the circle
write("Magnetic flux per pole, Wb",
format(" Pot=%5.3f",Pot),"\r\n")
writeto()--Results file closing
mi_close()--Closing of documents of
 --magnetism preprocessor
```

Indications on the program utilization.

To use the script of the field calculation of parameters and phase relationships of the TG it is necessary:

1. The script file with the extension *.lua and file with initial data with the extension *.txt should be in the same folder on the computer disk.

2. Run the program FEMM – the TG model. Editor Lua is called from the working window in FEMM by the «key» *Open Lua Script* in menu *File*, and then in the window that opens, the desired file *lua* is started.

3. At the request of the program in the opened window we enter the data file name and press the button Enter. Further action the program executes itself.

4. The calculation results are in a text file with a name given in the data file with name RezC_TG340 and are read by the editor *Notepad*.

Content of the file of results.

The data presented correspond to the NL mode and are already illustrated in Fig. 5 and Fig. 6. For convenience of representation in the format of this paper the text of the file of results is partially reformatted.

```
TG excitation data
Is=11547  beta=-160.43  Ir=3153
MFL, phase shifts, EMF, voltage and
active power
Fm1= 53.89   gl= -35.75
El=11971 fil=  34.68
gf= 0.0   teta= 35.75   Us=11547
fis= 31.79 cosfi=0.85  Pa=340.0
Electromagnetic torque and power
Mems=-1086 кN*m;   Pems=-341.2 MW
Magnetic flux per the stator pole, Wb
Pot=6.608
```

In the full version of the Lua script other results are calculated in inputted to the text file, too.

Conclusion. The presented theoretical basics and Lua scripts provide wide opportunities for users of the program FEMM for automated obtaining of electromagnetic parameters and phase relations of the TG on the basis of the calculation of the magnetic field. This script is universal in terms of the structure of the electromagnetic system of the TG within their wide-spread structure, and steady-state modes of their operation. Designed Lua script may be a prototype for similar software for calculations of EM of other types.

REFERENCES

1. Meeker D. *Finite Element Method Magnetics. FEMM 4.2 32 bit 11 Oct 2010 Self-Installing Executable.* Available at: www.femm.info/wiki/OldVersions (accessed 10 March 2014).

2. Milykh V.I., Polyakova N.V. Numerically-field calculations of the electromagnetic parameters of turbogenerators. *Visnyk NTU «KhPI» – Bulletin of NTU «KhPI»*, 2014, no.38(1081), pp. 3-18. (Rus).

3. Milykh V.I., Polyakova N.V. Automated formation of calculation models of turbogenerators for software environment FEMM. *Elektrotekhnika i elektromekhanika – Electrical engineering & electromechanics*, 2015, no.4, pp. 7-14. (Rus).

4. Milykh V.I., Polyakova N.V. Automated calculations of the dynamics of turbogenerator electromagnetic processes in software environment FEMM. *Elektrotekhnika i elektromekhanika – Electrical engineering & electromechanics*, 2015, no.6, pp. 24-30. (Rus).

5. Titov V.V., Hutoreckij G.M., Zagorodnaja G.A., Vartan'jan G.P., Zaslavskij D.I., Smotrov I.A. *Turbogeneratory* [Turbogenerators]. Leningrad, Energiia Publ., 1967. 895 p. (Rus).

6. Milykh V.I., Polyakova N.V. Analysis of phase relationships of electromagnetic parameters in a turbogenerator on the basis of numerical calculation of magnetic fields. *Elektrotekhnika i elektromekhanika – Electrical engineering & electromechanics*, 2003, no.4, pp. 59-64. (Rus).

7. Milykh V.I., Polyakova N.V. A system of directions and phase relationships for electromagnetic parameters at numerical calculations of magnetic fields in a turbogenerator. *Elektrotekhnika i elektromekhanika – Electrical engineering & electromechanics*, 2011, no.5, pp. 33-38. (Rus).

8. Milykh V.I., Polyakova N.V. Bases of numerical analysis of phase correlations of electromagnetic sizes are in a turbogenerator. *Elektrika – Electrician*, 2012, no.3, pp. 31-33. (Rus).

9. Milykh V.I., Polyakova N.V. Organization of numerical calculation of turbogenerator magnetic field under load with specified output parameters control. *Elektrotekhnika i elektromekhanika – Electrical engineering & electromechanics*, 2012, no.1, pp. 36-41. (Rus).

Received 22.07.2015

V.I. Milykh[1]*, Doctor of Technical Science, Professor,*
N.V. Polyakova[1]*, Engineer,*
[1] National Technical University «Kharkiv Polytechnic Institute», 21, Frunze Str., Kharkiv, 61002, Ukraine.
тел/phone +38 057 7076514, e-mail: mvikemkpi@gmail.com

How to cite this article:
Milykh V.I., Polyakova N.V. Determination of electromagnetic parameters and phase relations in turbo-generators by the automated calculation of the magnetic field in the software environment FEMM. *Electrical engineering & electromechanics*, 2016, no.1, pp. 26-32. doi: 10.20998/2074-272X.2016.1.05.

UDC 620.92+621.311+621.548 **doi: 10.20998/2074-272X.2016.1.06**

V.I. Panchenko, D.V. Tsyplenkov, A.M. Grebeniuk, M.S. Kyrychenko, O.V. Bobrov

MACHINE-TRANSFORMER UNITS FOR WIND TURBINES

Background. Electric generators of wind turbines must meet the following requirements: they must be multi-pole; to have a minimum size and weight; to be non-contact, but controlled; to ensure the maximum possible output voltage when working on the power supply system. Multipole and contactless are relatively simply realized in the synchronous generator with permanent magnet excitation and synchronous inductor generator with electromagnetic excitation; moreover the first one has a disadvantage that there is no possibility to control the output voltage, and the second one has a low magnetic leakage coefficient with the appropriate consequences. Purpose. To compare machine dimensions and weight of the transformer unit with induction generators and is an opportunity to prove their application for systems with low RMS-growth rotation. Methodology. A new design of the electric inductor machine called in technical literature as machine-transformer unit (MTU) is presented. A ratio for estimated capacity determination of such units is obtained. Results. In a specific example it is shown that estimated power of MTU may exceed the same one for traditional synchronous machines at the same dimensions. The MTU design allows placement of stator coil at some distance from the rotating parts of the machine, namely, in a closed container filled with insulating liquid. This will increase capacity by means of more efficient cooling of coil, as well as to increase the output voltage of the MTU as a generator to a level of 35 kV or more. The recommendations on the certain parameters selection of the MTU stator winding are presented. The formulas for copper cost calculating on the MTU field winding and synchronous salient-pole generator are developed. In a specific example it is shown that such costs in synchronous generator exceed 2.5 times the similar ones in the MTU. References 3, figures 2.

Key words: **wind power, wind turbines, inductor electric machine, transformer-machine unit, pole, stator winding, generator.**

В работе предложена новая конструкция индукторной электрической машины, которая в технической литературе называется – машинно-трансформаторный агрегат (МТА). Для такого агрегата получено соотношение для определения расчетной мощности. На конкретном примере показано, что при одинаковых габаритах расчетная мощность МТА может превышать таковую для обычных синхронных машин. Конструкция МТА позволяет разместить катушки обмотки статора на некотором расстоянии от подвижных элементов машины, а именно, в закрытой емкости, заполненной электроизоляционной жидкостью. Это позволит увеличить мощность за счет более эффективного охлаждения обмотки, а также повысить выходное напряжение МТА как генератора до уровня 35 кВ и более. Библ. 3, рис. 2.

Ключевые слова: **ветроэнергетика, ветроэнергетические установки, индукторная электрическая машина, машинно-трансформаторный агрегат, полюс, обмотка статора, генератор.**

Introduction. Electric generators of wind turbines should meet the following requirements: they must be multi-polar, have a minimum size and weight, but be guided contactless, while working on the electrical system to provide maximal possible output voltage.

Problem definition. Multi-polarity and contactlessness are relatively simply realized in synchronous generators with excitation from permanent magnets and the inductor synchronous generator with electromagnetic excitation, and at first, as a drawback – no ability to control output voltage, the second – small (up to 0.4) utilization factor of magnetic flux of excitation.

State of the problem. In [1] the new design of electric machines – machine-transformer unit, which is non-contact, has electromagnetic excitation type inductor generator and a greater relative to the last utilization of magnetic flux is proposed. But the design of the unit, especially in three-phase version, is complex and, in addition, requires a significant copper consumption for stator windings. In [2] an improved design of machine-transformer unit with vertical shaft in three-phase design is presented.

Materials of investigations. A considered machine-transformer unit consists of two parts – the machine (Fig. 1,*a* above) and transformer (Fig. 1,*a* below), which have a common external magnetic core (stator) in a longitudinal package 1 of isolated plates electrical steel. On the machine shaft 2 of the rotor hub 3 is fixed on the outer surface of which is placed radial toothed packages 4 and 5, also made of insulated electrical steel plates and are relatively shifted in the axial direction. Teeth in these packages are oriented toward the gap between the rotor and the stator longitudinal packages and mutually displaced in the tangential direction geometric angle π/z_2, where z_2 is the number of teeth in one package of the rotor. Between toothed package contains 6 annular excitation coil attached on its outer surface to the longitudinal stator packs. Winding divided into two sections, located nearby. Each of the leading bands wound in mutually opposite directions, and the sections are interconnected at the end of the part winding rotor. Longitudinal package 1 along the length of the machine unit fixed by fill gaps between nonmagnetic alloy, which also forms part of the housing 7. In the radial direction packs 1 are based on the cylindrical sidewall 8 and 9, which made holes for their passage. In sidewalls constipation Leno-bearings 10 and 11 are seated on the shaft bearings 2. Outside bearings are closed by lids.

Width of each of the packages 1 is made less than width corresponding groove in its outer rotor (radial) side. The packages of the transformer, in extreme along the length of the working areas mounted coil windings interconnected respective schemes – «triangle» or «star». The lower end oppression packages to the ring yoke 13 wound with insulated ferromagnetic tape. Package 1 of

the transformer coils 12 and 13, yoke placed in a closed container 14, which is filled electrical insulating fluid. The outside of the containers secured cooling device 15 combined with the internal volume of the pipes 16.

At supply of the excitation winding 6 by DC magnetic system unit, a magnetic flux, which is obtained, for example, tine rotor pack 4 and included in those packages stator longitudinal area «overlap» and whose maximum rotor teeth (in Fig. 1 direction magnetic excitation flow shows by arrows). Next, the magnetic flux of 1 packet enters the ring yoke 13 and then – in other packages stator 1, and it is in those areas «overlap» which package and rotor teeth 5 maximum. Then, with a package of one stator magnetic flux enters the rotor pack teeth 5 and the sleeve 3 again in package 4 of the rotor.

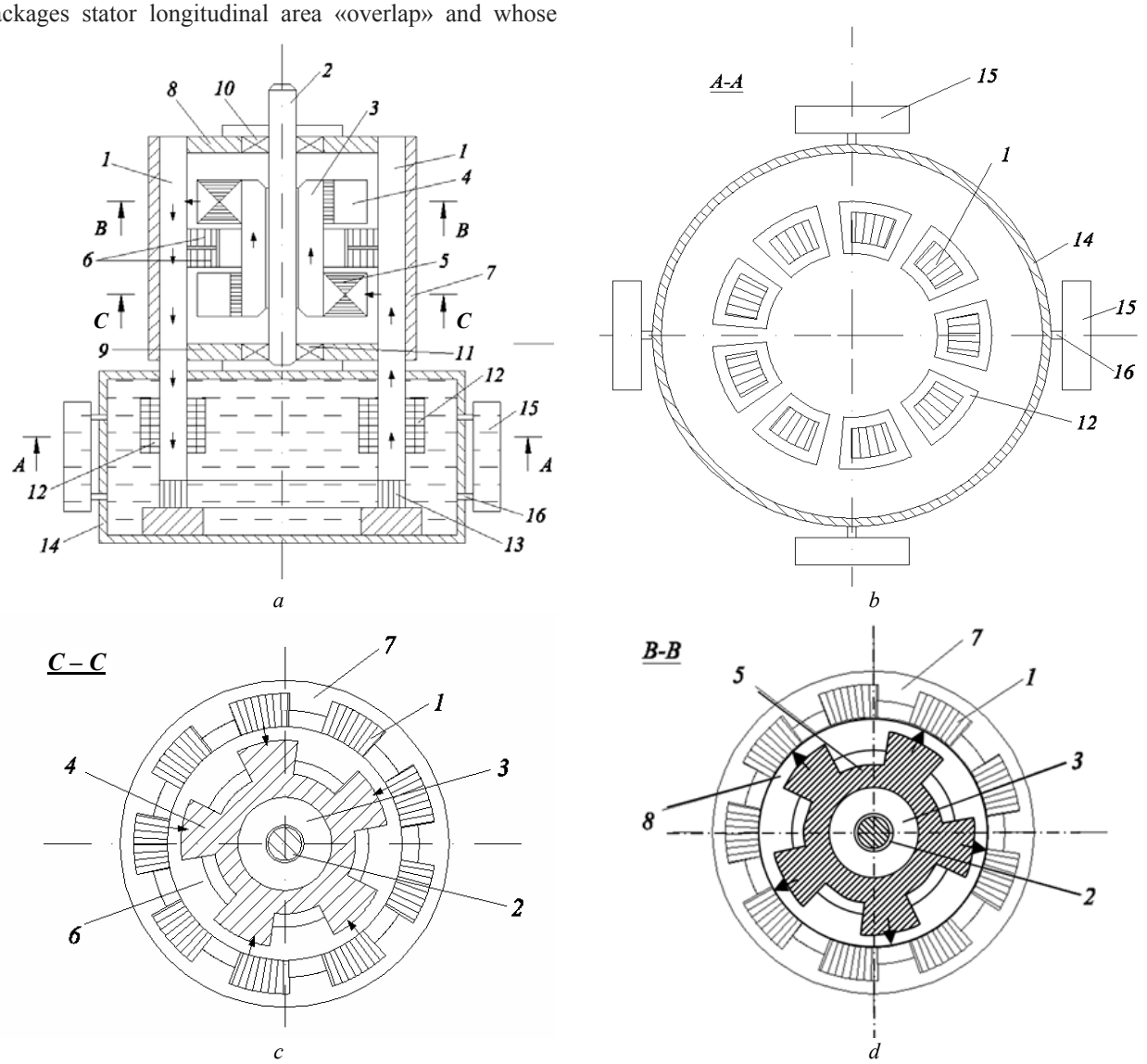

Fig. 1. Machine-transformer unit design
(*a* – longitudinal axial section; *b*, *c*, *d* – cross-sections in different places in height)

As the rotor rotates, for example by the wind turbine its teeth continuously change their position relative to the longitudinal stator packs, which leads to changes in the size and direction of the magnetic flux in the past. These flows permeate the working coil winding 12 that it causes the electromotive force (EMF) with frequency $f = z_2 n/60$, where n is the rotor rotation speed, rev/min.

Design power of the machine-transformer unit (MTU):

$$P' = mE_1 I_1 \ , \qquad (1)$$

where m is the number of phases of the stator winding; E_1 is the electromotive force (EMF) of the phase; I_1 is the phase current.

On each package longitudinal magnetic stator coil one phase is placed. Number of coils per phase will be $z_{ph} = z_1/m$, respectively, EMF of the phase

$$E_1 = z_{ph} E_c K_r = z_{ph} E_c K_r / m,$$

where z_1 is the total number of packages загальна кількість пакетів; E_c is the EMF of one coil; K_r is the distribution ratio that takes into account the mutual phase shift vector EMF coils phase.

Figure 2 conventionally shows the relative position of the stator packs and rotor teeth at some initial time and after displacement of the rotor on the pole notch $\tau = 0.5t_2$, where t_2 is the tooth division of the rotor.

The magnetic flux which penetrates the coil turns, $\Phi_c = \Phi_{z1} - \Phi_{12}$ where Φ_{z1} is the flow, part of the package of the stator tooth rotor; Φ_{12} is the flow that of the stator package includes a groove adjacent rotor package.

Average EMF of the coil

$$\langle E_c \rangle = w_c \frac{\Delta\Phi}{\Delta t} = w_c \frac{2\Phi_c}{T/2} = 4 f w_c (\Phi_{z1} - \Phi_{12}), \quad (2)$$

where w_c is the number of windings of the coil; $\Delta\Phi = 2\Phi_c$ is the magnetic flux change through the coil during time $\Delta t = 0.5T$, corresponding to a distance of displacement of the rotor relative to the initial position. $T = 1/f$ is the EMF period; f is its frequency.

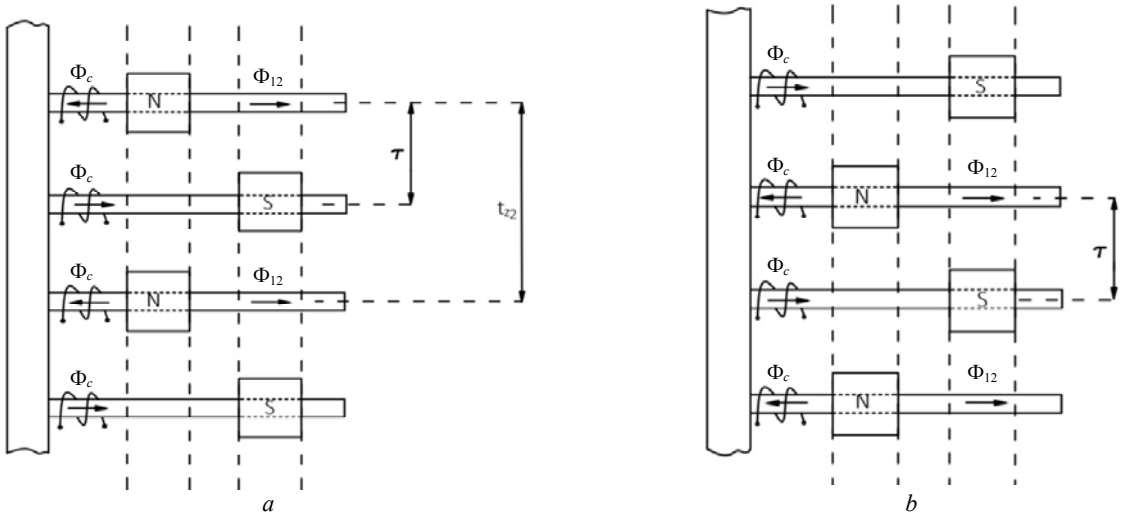

Fig. 2. Schemes of relative position of stator packets and rotor teeth at different times

Magnetic flux values:

$$\Phi_{z1} = \frac{\mu_0 F_\delta S_{z1}}{\delta_1}; \ \Phi_{12} = \frac{\mu_0 F_\delta S_{12}}{\delta_2},$$

where μ_0 is the magnetic constant; F_δ is the magnetomotive force (MMF) winding one air gap; δ_1, δ_2 are the air gaps between the package and the stator tooth and rotor, respectively, between the package and the stator slot rotor; S_{z1}, S_{12} are the area magnetic flux between the tooth and the package and between package and groove, and, $S_{z1}=b_{z1}l_{z2}$; $S_{12}=b'_{g2}l_{z2}$, where b_{z1} is the width package; l_{z2} is the axial length (thickness) wave rotor; b'_{g2} is the estimated width of the groove of the rotor.

After the substitutions above formulas in expression (2) we have:

$$\langle E_c \rangle = 4 w_c f B_\delta l_{z2} b_{z_1} \left(1 - \frac{\delta_1 b'_{g2}}{\delta_2 b_{z_1}}\right), \quad (3)$$

where B_δ is the magnetic flux density in the air gap between the stator package tooth and rotor (maximum value).

We write: $b_{z1}=\alpha_\delta\tau$, where α_δ is the pole arc ratio. As a result, the corresponding calculations obtained ratio $(b'_{g2}/b_{z1})=1.2$. The machine that analyzed by the rotor has two packages; area of the excitation magnetic flux action in the axial direction is the active length of the core, i.e. $l_\delta = 2l_{z2}$. We write the expression in parentheses of the formula (3) as follows:

$$\left(1 - \frac{\delta_1}{\delta_2}\frac{b'_{g2}}{b_{z_1}}\right) = \left(1 - \frac{1{,}2\delta_1}{\delta_2}\right) = K_\sigma,$$

where K_σ is the coefficient taking into the magnetic leakage flux.

In view of the above we write the expression for the current value of the EMF of the coil

$$E_c = K_f \langle E_c \rangle = 2 K_f \alpha_\delta K_\sigma w_c f B_\delta l_\delta \tau, \quad (4)$$

where K_f is the shape factor of the excitation magnetic flux.

Stator winding coils similar in design to the same bars of power transformers. As for transformers we write ratio for linear load: $A = I_1 w_c / l_c$ where l_c is the axial length of the coil. From here the phase current

$$I_1 = \frac{A l_c}{w_c}. \quad (5)$$

Substituting relation (3), (4), (5) in the formula (1) taking into account the fact that: $f = pn/60$ and $\tau = \pi D/(2p)$, where p is the number of pairs of poles of the machine, which is the number of rotor teeth z_2 in one package; D is the diameter bore on which stator packets placed; n is the rotor rotation speed, rev / min we receive:

$$P' = \frac{\pi}{60D} \alpha_\delta K_f K_r K_\sigma B_\delta A D^2 l_\delta l_c z_1 n. \quad (6)$$

Let's consider in detail the expression for the linear load:

$$A = \frac{I_1 w_c}{l_c} = \frac{j_a S_c w_c}{l_c} = \frac{j_a h_c l_c K_d}{l_c} = j_a h_c K_d,$$

where h_c is the length of the coil; K_d is the filling factor of the copper coil longitudinal section; j_a is the current density in the coil.

The interval between packets in a circle on the stator diameter D denote as b_{g1}, and $b_{g1} = t_1 - b_{z1}$, where t_1 is the tooth division of the stator. It is desirable to ensure $b_{g1} = 0.5t_1$. Then, the thickness of the coil $h_c \approx 0.45 b_{g1} \approx \approx 0.23 t_1$. The value in the next product of formula (6) will be the following:

$$\frac{A l_c z_1}{D} = 0{,}72 j_a l_c K_d.$$

After substituting the last value in (6) we obtain:

$$P' = 3{,}8 \cdot 10^{-2} \alpha_\delta K_f K_\sigma K_r K_d B_\delta j_a D^2 l_\delta l_c n. \quad (7)$$

Regarding the coefficient $\alpha_\delta = b_{z1}/\tau$:

- the width of the stator package $b_{z1} = t_1 - b_{g1} = 0.5t_1$;
- the pole dividing $\tau = \pi D/(2z_2)$.

So

$$\alpha_\delta = \frac{t_{z_1}}{t_{z_2}} = \frac{z_2}{z_1}.$$

To make the machine as 3-phase one it is necessary to provide:

$$z_1 = 2z_2 + K,$$

where K = 1, 2, 3 …, then

$$\alpha_\delta = \frac{z_2}{2z_2 + K} = \frac{1}{2 + K/z_2} < 0.5.$$

The formula for the design power of classical synchronous machines with electromagnetic excitation is the following [3]:

$$P_s' = 0{,}164\alpha_i K_f K_w B_{\delta_c} A_s D^2 l_\delta n. \quad (8)$$

Design power ratio for the same overall dimensions

$$\frac{P'}{P_s'} = \frac{0{,}23\alpha_\delta K_r K_\sigma K_d B_\delta j_a l_c}{\alpha_i K_w B_{\delta_c} A}. \quad (9)$$

Perform by the last formula calculations (generators in the power range up to 1000 kVA).

Assume: α_δ=0.45; K_r=0.95; K_d=0.58; B_δ=1.5 T; $j_a = 4\cdot10^6$ A/m^2; α_i=0.85; K_w=0.92; $B_{\delta s}$=0.9 T; A_s=4·10^4 A/m.

As a result of calculations obtain:

$$\frac{P'}{P_s'} = \frac{0{,}23\cdot0{,}45\cdot0{,}95\cdot0{,}58\cdot1{,}5\cdot4\cdot10^6}{0{,}85\cdot0{,}92\cdot0{,}9\cdot4\cdot10^4} l_c = 11{,}2 l_c.$$

When l_c = 0.1 m we have P' = 1.12P_s', i.e. the estimated capacity of the MTU exceed this for conventional synchronous generator. Selecting the l_c value, you can change the size of the power within the allowable heat load stator windings. It should be noted that the induction in the air gap B_δ of the MTU is limited only by magnetic saturation of the stator electrical steel package, i.e. $B_\delta \le$1.8 T, which is significantly higher compared with classical generators.

Spatial distribution transformer and machine parts in the MTU will post stator coil windings at some distance from moving parts, such as in a closed container filled with electrical insulating fluid. This provides more efficient cooling of the stator winding in operation, which makes it possible to increase the current density in the winding and, therefore, power MTU compared with the case of air cooling. On the other hand, placing windings in electrical insulating fluid will increase the output voltage in generator mode MTU to the level of 35 kV and above and thus refuse the use of power transformer, which increases voltage before feeding electricity into the high-voltage network.

MTU stator winding consists of individual coils attached to the longitudinal packets. Reels are concentrated, which will provide the minimum length frontal parts. In conventional synchronous generator stator teeth number is selected according to the formula: z_1=2pmq, where $q\ge2$. For low-speed generators, for example, when n = 150 rev/min, f = 50 Hz, q = 2 must provide p = 20 and z_1 = 2·20·3·2=240. This is complicated by the stator performance and forced to increase the size of the generator. Consider the opportunity to realize three-phase machine (MTU) where z_1=2z_2+K. The magnetic field provides excitement in the air gap of each packet number of rotor pole pairs $p = z_2$. Mutual angle γ (in electrical degrees) of two coils located on adjacent stator packets in this magnetic field will be:

$$\gamma = \frac{2\pi p}{z_1} = \frac{2\pi(z_1 - K)}{2z_1} = \pi - \frac{K\pi}{z_1}.$$

Neighboring packets belonging to one of the phases and coil these packages are interconnected in series opposite, the electrical angle between the vectors EMF coils will be the following

$$\gamma_c = \pi - \gamma = \frac{K\pi}{z_1}.$$

Number of packages in the three-phase stator electric machine $z_1 = am$, where a = 2, 3, 4 ... are the packets numbers per phase. In the formula $z_1 = 2z_2 + K$ the K number denotes the number of branches winding of one phase, connected in series or parallel. Number of coils in one winding branch is:

$$a_b = \frac{z}{Km} = \frac{a}{K}.$$

Electric angle that they occupy by the coil bore of one branch

$$\gamma_b = a_b\gamma_c = \frac{z_1}{K\cdot m}\cdot\frac{K\cdot\pi}{z_1} = \frac{\pi}{m} = 60^\circ \text{ el.}.$$

The last formula confirms the possibility of creating asymmetrical three-phase windings with 60 degree phase zone. From the preceding considerations it follows that the number a_b and K must be whole. Connection between them describes by the relationship:

$$a_b = \frac{z_1}{K\cdot m} = \frac{2z_2/(K+1)}{m}. \quad (10)$$

The value of K is desirable minimal. Consistently increasing the value of K, starting with one, we find from formula (10) ah appropriate value as the first whole number. For example, when n = 150 rev/min, f = 50 Hz, z_2 = 20, m = 3, then only at K = 2 we will obtain a_b =7. Then: z_1 = 2·20 + 2 = 42, $a = z_1/m$ = 42/3 = 14.

As noted earlier, the excitement of the MTU provides one fixed ring winding. Define the cost of copper for the creation of such winding. For magnetic circuit through which the excitation flow passes, the fair equation:

$$2\delta H_\delta K_F = I_f w_f = F_f,$$

where H_δ is the magnetic field strength in the air gap pack size δ_1 between stator and rotor teeth; $K_F > 1$ is the coefficient taking into account ferromagnetic of the chain; I_f and w_f are the current and number of turns of winding; F_f is the magnetomotive force (MMF) of the winding.

Consider the following: $H_\delta = B_\delta/\mu_0$; $I_f w_f = j_f S_f w_f = S_d w_f$ where j_f is the current density in the winding; S_f is the pre sectional area of the conductor; $S_d = S_f w_f$ is the sectional area of copper windings, and

$$S_d = \frac{F_f}{j_f} = \frac{2\delta B_\delta K_F}{\mu_0 j_f}.$$

Taking into account that the average length of the coil $\langle l\rangle = \pi(D - h_0)$, where h_0 is the radial thickness of winding, winding copper volume is as follows:

$$V_d = S_d \langle l \rangle = \frac{2\pi D\delta B_\delta K_F}{\mu_0 j_f}\left(1-\frac{h_0}{D}\right) = \frac{2V_\delta B_\delta K_F}{\mu_0 j_f}\left(1-\frac{h_0}{D}\right),$$

where $V_\delta = \pi D\delta$ is the volume of the air gap between stator packages and rotor teeth.

For comparison, we determine the cost of copper for the excitation winding of synchronous salient-pole generators. We write the equation of magnetic equilibrium magnetic circuit which passes through two adjacent poles,

$$2\delta H_{\delta_c} K_F K_\delta = 2I_c w_c = 2F_c ,$$

where K_δ is the coefficient taking into account the stator toothness; I_c and w_c are the current and number of turns of the pole winding; $F_c = I_c w_c$ is the EMF of the winding.

Cross-sectional area of copper of the coil

$$S_d = S_f w_c = \frac{F_c}{j_c} = \frac{\delta B_{\delta_c} K_F K_\delta}{\mu_0 j_c} ,$$

where j_c is the current density in the coil.

Volume of copper of the coil

$$V_d = S_d \langle l' \rangle ,$$

where <l'> is the intermediate winding length.

It is about <l'> = 2,5(l_δ+b_p); l_δ is the length of the stator core; b_p is the width of the pole core.

Usually $b_p \approx 0.35\tau$. We write:

$$\langle l' \rangle = 2{,}5(l_\delta + 0{,}35\tau) = 2{,}5D\left(l_\delta/D + 0{,}55/p\right) = 2{,}5D\left(\lambda + 0{,}55/p\right),$$

where $\lambda = l_\delta/D$. Then

$$V_d = \frac{0{,}8V_\delta B_{\delta_c} K_F K_\delta}{\mu_0 j_c}\left(\lambda + 0{,}55/p\right).$$

The total volume of copper of the excitation winding consisting of 2p coils, taking into account the recommendation to the choice $\lambda = 0.8/p^{1/2}$, will be the following

$$V_{ds} = 2pV_d = \frac{0{,}9V_\delta B_{\delta_c} K_\delta K_F}{\mu_0 j_c}\left(1{,}45\sqrt{p}+1\right).$$

The ratio of the volume of copper windings excitation with the same volume of air gap, current density in the windings and magnetic cores saturation:

$$\frac{V_{ds}}{V_d} = \frac{0{,}45B_{\delta_c} K_\delta \left(1{,}45\sqrt{p}+1\right)}{B_\delta\left(1-h_0/D\right)} .$$

For example, for $p = z_2 = 20$; $B_\delta = 1.5$ T; $B_{\delta s} = 0.9$ T; $K_\delta = 1.2$; $h_0/D = 0.05$, we will obtain: $V_{ds}/V_d = 2.5$.

Conclusion.

1. A synchronous electrical machine in the form of a machine-transformer unit because of silent-pole design and large magnetic flux density in the air gap will permit to increase the design power and reduce the cost of copper on the excitation winding compared to a classical synchronous machine with electromagnetic excitation.

2. Placement of transformer part of the unit in a closed container filled by electrical insulation fluid will permit to increase the output voltage in the generator mode as well as the power of the unit.

REFERENCES

1. Svecharnyk D.V. *Mashinno-transformatornyi agregat* [Machine-transformer unit]. Patent Russian Federation, no.2096893, 1997. (Rus).

2. Panchenko V.I. *Mashynno-transformatornyi ahrehat* [Machine-transformer unit]. Patent UA, no.103685, 2013. (Ukr).

3. Goldberg A.D., Gurin Y.S., Sviridenko Y.S. *Proektirovanie elektricheskikh mashin* [Designing of electric machines]. Moscow, Vyssh. shk. Publ., 1984. 431 p. (Rus).

Received 27.11.2015

V.I. Panchenko[1],
D.V. Tsyplenkov[1], *Candidate of Technical Science, Associate Professor,*
A.M. Grebeniuk[1], *Candidate of Technical Science, Associate Professor,*
M.S. Kyrychenko[1], *Assistant Lecturer,*
O.V. Bobrov[1], *Candidate of Technical Science,*
[1] State Higher Education Institution «National Mining University»,
19, K. Marksa Avenue, Dnipropetrovsk, 49005, Ukraine.
phone +38 056 3730743, e-mail: nmu.em@ua.fm

How to cite this article:
Panchenko V.I., Tsyplenkov D.V., Grebeniuk A.M., Kyrychenko M.S., Bobrov O.V. Machine-transformer units for wind turbines. *Electrical engineering & electromechanics*, 2016, no.1, pp. 33-37. doi: 10.20998/2074-272X.2016.1.06.

UDC 621.313.333.2 **doi: 10.20998/2074-272X.2016.1.07**

V.S. Petrushin, L.Y. Bielikova, Y.R. Plotkin, R.N. Yenoktaiev

COMPARISON OF ADJUSTABLE HIGH-PHASE ORDER INDUCTION MOTORS' MERITS

Purpose. *Development of mathematical models of adjustable electrical drives with high-phase order induction motors for their merits analysis at static and dynamical modes.* ***Methodology.*** *At the mathematical modeling main kinds of physical processes taking place in the high-phase order induction motors are considered: electromagnetic, electromechanical, energetic, thermal, mechanical, vibroacoustic ones. Besides, functional as well as mass, frame and value indicators of frequency converters are taking into account which permits to consider technical and economical aspects of the adjustable induction electrical drives. Creation of high-phase order induction motors' modifications in possible on the base of a stock 3-phase motors of basic design. Polyphase supply of induction motors is guaranteed by a number of the adjustable electrical drives' power circuits.* ***Results.*** *Modelling of a number of adjustable electrical drives with induction motors of different phase number working on the same load by its character, value and required adjustment range is carried out. At the utilization of the family of characteristics including mechanical ones at different adjustment parameters on which loading mechanism's characteristics are superimposed regulation curves representing dependences of electrical, energetic, thermal, mechanical, vibroacoustic quantities on the motors' number of revolutions are obtained.* ***Originality.*** *The proposed complex models of adjustable electrical drives with high-phase order induction motors give a possibility to carry out the grounded choice of the drive's acceptable variant. Besides, they can be used as design models at the development of adjustable high-phase order induction motors.* ***Practical value.*** *The investigated change of vibroacoustic indicators at static and dynamical modes has been determined decrease of these indicators in the drives with number of phase exceeding 3.* References 10, tables 2, figures 4.

Key words: **adjustable high-order induction motor, semiconductor frequency converter, mathematical modelling, regulation curves, stator winding, vibroacoustic indicators.**

Обоснована возможность создания модификаций многофазных асинхронных двигателей на базе серийных трехфазных. Рассмотрен ряд силовых схем регулируемых электроприводов, в которых обеспечивается многофазное питание асинхронных двигателей. Анализируется работа приводов на определенную по величине и характеру нагрузку и заданным диапазоном регулирования. В результате математического моделирования определено, что температуры перегревов обмоток статоров рассматриваемых двигателей не превышают допустимых значений соответственно классу нагревостойкости изоляции. Выполнено сравнение технико-экономических показателей рассматриваемых схем и двигателей, дающее возможность осуществить приемлемый выбор варианта. Установлены закономерности изменения фазных токов многофазных двигателей в диапазоне регулирования. Исследовано изменение виброакустических показателей в статических и динамических режимах. Определено снижение этих показателей в двигателях с числом фаз, превышающим три. Библ. 10, табл. 2, рис. 4.

Ключевые слова: **многофазный регулируемый асинхронный двигатель, полупроводниковый преобразователь частоты, математическое моделирование, регулировочные характеристики, обмотка статора, виброакустические показатели.**

Introduction. Adjustable high-phase order induction motors (AIM) are used in medical and domestic equipment, electrical car industry, textile industry, boats' electrical propulsion systems [1, 2]. It is useful to use them in special ventilation systems and complexes where increased motor's reliability at low noise and vibration levels is required [3]. AIMs have decreased torque and speed pulsations at the motor's shaft as well as increased reliability at decreased noise and vibration levels. Besides, division of electrical power to phases makes AIM's regulation curves more critical to the asymmetry by the amplitude and phase of the supply voltage that at the increase of the number of phases (m) simplifies finally the control system and increases the reliability [4, 5]. Systems of electrical drive (ED) with high-phase order AIM are realized at using frequency converters with a few autonomous voltage inverters (AVI) which creates a symmetrical voltage system with a time shift which equals to the spatial phase shift of high-phase order motors (see Fig. 1).

High-phase order induction motors can be developed on the base of stock 3-phase ones of basic modification. In some cases it is realized at presence of a few parallel loops in the 3-phase network. Decreasing their number we obtain a polyphase modification (in two times – 6-phase one, in 3 time – 9-phase one, etc.). And here the active part's geometry, number of turns in the phase and winding wire's section are not changed. Besides, it is necessary to take into account number of slots per the pole and the phase.

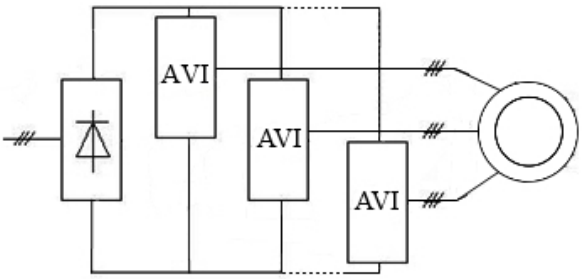

Fig. 1. Circuits of adjustable ED with high-phase order AIM

If such a problem solution is impossible it is necessary to change number of effective turns in the phase w_p and a wire's section d_w. Using an expression $w_p = \frac{Z_1}{2 \cdot m} \cdot \frac{U_c}{a}$ by variation of number of parallel loops (a), number of conductors in the slot (U_c) and number of turns they achieve the conservation of the value of magnetic flux. Here it is necessary to check the coefficient of the slot filling [6].

Problem definition. To build models of electrical drives with high-phase order AIMs it is necessary to input

a few initial data which determine functional properties as well as indicators of mass, frame and value. Last ones give a possibility to consider economical aspects of various ED's variants. Indicators of mass, frame and value of multiphase frequency transducers increase approximately in 30 % at the transition from the 3-phase modification to the 6-phase one, in 60 % at the transition to the 9-phase one, etc. Increase of production expenses results in the change of high-phase order motors' value.

To compare the ED's variants it is necessary to use some indicators including the effectiveness averaged in the range [7] which reflects the AIM's energetic in all adjustment range given from n_1 to n_2 and is determined as equivalent one averaged for this range.

$$\eta_{atrIM} = \frac{1}{n_2 - n_1}\int_{n_1}^{n_2} \eta_{IM}(n)dn.$$

The generalized criterion of the adjusted present expenses (APE) takes into account production value and operation expenses. Expenses depend on the efficiency and the power ration, therefore the generalized criterion of the adjusted present expenses has different values in different points of the range, and it is expediently to determine the range value of this criterion, i.e. equivalent averaged value for all range.

It is necessary to note that at the AIM operation in modern variable-frequency electrical drives the drive's power ratio is near 1 and as a result from the expression for the electrical drive's APE the component corresponding the value of the reactive energy compensation can be excluded. So

$$APE_{ED} = ved\,[1 + T_n(k_d + k_s)] + C_{eED},$$

where *ved* is the total electrical drive's value which consists of the values of the AIM and the transducer, USD; $C_{eED} = C_{apl}P_{1ED}(1{,}04 - \eta_{atrED})$ is the value of the electrical energy losses during the year, USD; T_n is the normative term of the motor's cover of expenditure, years; k_d is the part of expenses for depreciation charges; k_s is the part of service expenses during the motor's operation; C_{apl} the coefficient taking into account the value of the active power losses representing the product of the value of the production of the 1 kW·h of electrical energy during the drive's service life (USD 0.1 for 1 kW·h), number of hours of the motor's operation during the year (2100), number of years of the operation till the major overhaul (5 years), and the coefficient of the relative motor's loading (accepted 1); P_{1ED} – active power consumed by the drive, kW, η_{artED} – the drive's effectiveness averaged in the range. For adjustable induction motors the values T_n = 5 years, k_d = 0.065, k_s = 0.069 are accepted the same as for general industrial IM [8].

Results of investigations. The modeling of adjustable electrical drives (AED) with coupled consideration of transducers, motors and loads [9] can be carried out by the code DimasDrive [10] developed at the Department for Electric Machines, Odessa Polytechnic University.

As a base motor the 4A200M6 3-phase motor working with the frequency transducer Altivar 58HD33N4 (USD 3650, 34 kg, η_{tr} = 0.94) is selected. Changing the winding data, the 6-phase (number of turns w_p = 114, number of parallel loops a = 2, the effective conductor's section q_{ef} = 1.76 mm^2, the insulated winding wire's diameter d_w = 1.585 mm) and the 12-phase (number of parallel loops a = 1, the rest of data are the same as for the 6-phase one) modifications have been carried out.

The frequency control low U/f = const has been considered. As a load the traction one has been used, P_{load} = 18 kW with maximal torque of 140 N·m. At the given constant value of the load, the required adjustment range (200-1600 RPM) in the AED systems can be guaranteed by the considered electric motors.

Regulation curves representing dependences of electrical, energetic, thermal, mechanical, vibroacoustic quantities on the number of revolutions can be obtained by using a family of characteristics including mechanical ones at different adjustment parameters on which loading mechanism's characteristics are superimposed. In Fig. 2 a family of the mechanical characteristics and given load corresponding the AED with the 3-phase AIM is presented. Families of the mechanical characteristics for the AED with the 6-phase and 12-phase motors have the same form.

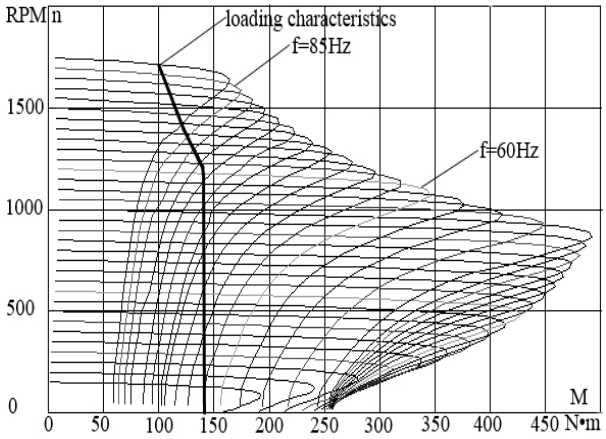

Fig. 2. A family of mechanical characteristics

At this composition of mechanical characteristics and loads the presence of three zones takes place. Within all of zones the monotonous change of mechanical characteristics and loading characteristics takes place. Temperatures of the considered motors stator windings do not exceed the values permitted by the class F of the thermal resistance at the selected load in the given adjustment range.

In Fig. 3 some regulation curves of the considered AED representing dependences of motors' consumption current and vibroacoustic indicators of electromagnetic nature on the number of revolutions are presented.

In Table 1 values of the considered AEDs' indicators including the effectiveness averaged in the range (η_{atr}) and adjusted present expenses (APE) as well as indicators of mass, frame and value for motors and drives are presented.

It is possible to carry out the calculation of the active energy losses value during the year.

$$C_a = V_a \cdot T_n \cdot K_l \cdot P_{mech} \cdot (1 + 0{,}04 - \eta_{AED}) / \eta_{AED},$$

where V_a = USD 0.1 is the value of the 1 kW·h; T_n = 2100 is number of hours of the AED's operation during the year; K_l is the coefficient of loading (accepted to be equal to 1.0); 0.04 is the relative value of losses in the customer's distribution network.

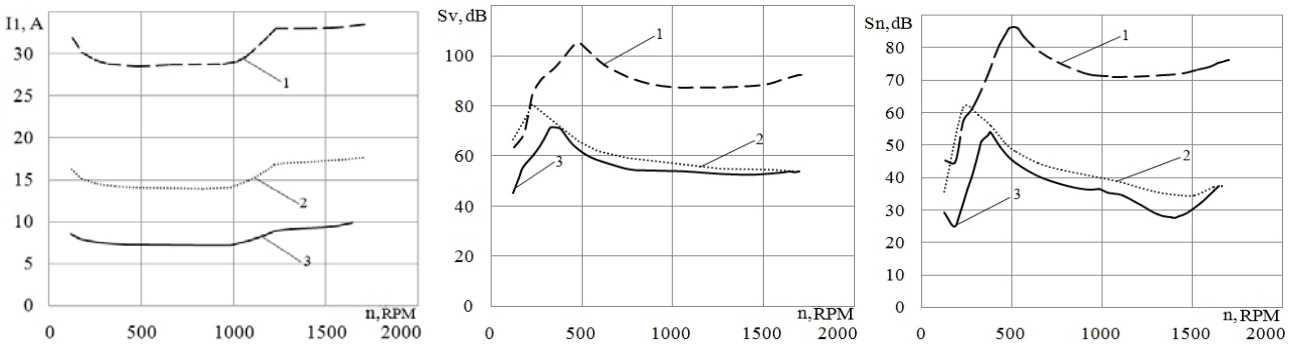

a *b* *c*

Fig. 3. Change of the consumption current (*a*), vibration speed (*b*) and noise of electromagnetic nature (*c*) in the adjustment range: 1 – AED with a stock 3-phase IM, 2 – AED with a 6-phase IM, 3– AED with a 12-phase IM

Table 1

Comparison of different AEDs' indicators

Indicators and parameters \ AED	With 3-phase AIM	With 6-phase AIM	With 12-phase AIM
η_{atr} of IM, %	82.97	82.41	81.70
η_{atr} of AED, %	81.34	80.79	80.10
APE of IM, USD	5729	5844	6034
APE of AED, USD	11991	13935	17779
Value of IM, USD	1994	2016	2069
Mass of IM, kg	254	254	254
Volume of IM, dm^3	19	19	19
Mass of AED, kg	288	298	318
Volume of IED, dm^3	56	101	275
Value of AED, USD	5644	6761	9004

Comparison of the considered AED's variants by the active energy losses value during the year is carried out (see Table 2). Besides, modeling for each AED's circuit design at the operation on the given tachogram (2 s – 200 RPM, 2 s – 600 RPM, 2 s – 1200 RPM) taking into account transients is carried out.

Table 2

Comparison of the active energy losses value for various AED

Indicators and parameters \ AED	With 3-phase AIM	With 6-phase AIM	With 12-phase AIM
η_{atr} AED, %	81.34	80.79	80.10
Active energy losses value during the year, USD	1001	1036	1073

In Fig. 4 changes of currents, vibration speeds and noises of electromagnetic nature at the considered motors' operation on the given tachogram are presented.

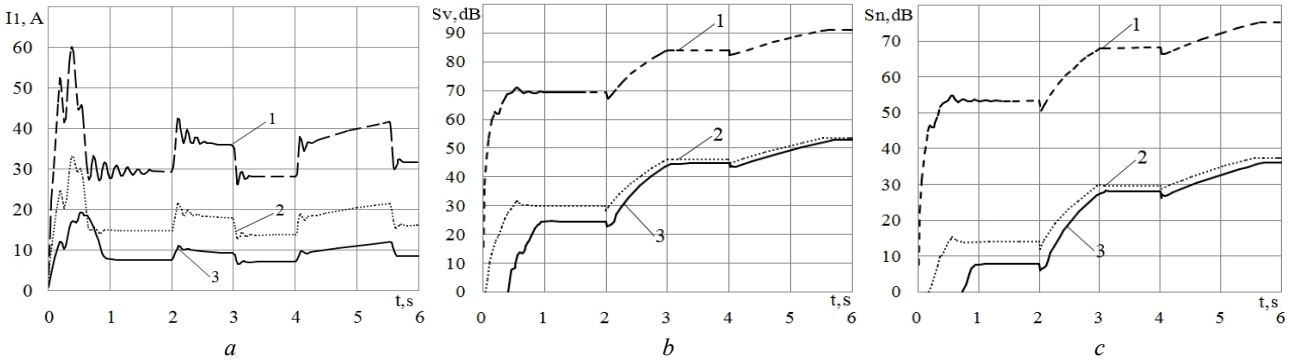

a *b* *c*

Fig. 4. Change of the consumption current (a), vibration speed (b) and noise of electromagnetic nature (c) in the adjustment range: 1 – AED with a stock 3-phase IM, 2 – AED with a 6-phase IM, 3– AED with a 12-phase IM

Conclusions.

1. High-phase order AIMs' consumption current decreases in proportion to the number of phases in the comparison with the 3-phase motor's current.

2. Essential decrease of the vibroacoustic indicators of electromagnetic nature at the transition from the 3-phase AED to the high-phase order ones takes place. This decrease is irregular and minimal in the initial part of the range. Besides, resonant phenomena take place. In addition, for the considered AED the difference between these indicators for the 6-phase and 12-phase AIM is not so essential. Therefore, for this design problem the 6-phase AIM is preferable because the 12-phase one essentially is more expensive, has increased mass and volume at practically equal energetic indicators.

3. Comparison of the considered AEDs' the active energy losses value during the year permits to conclude that the AED with 3-phase IM has a little bit better indicators in the comparison with other considered variants.

4. Results of modeling of dynamical dependences of consumption current, vibration speed and noise of electromagnetic nature confirm lows elicited at static modes.

REFERENCES

1. Datskovskii L.Kh., Rogovoi V.I. Current status and trends in asynchronous variable frequency drives. *Elektrotekhnika – Electrical Engineering*, 1996, no.10, pp. 20-24. (Rus).

2. Soustin B.P. Single-phase inverter asynchronous electric. *Nauka proizvodstva – Science production*, 2000, no.3, pp. 10-16. (Rus).

3. Sidelnikov B.V. Six-phase variable-frequency high power asynchronous motors. *Izvestiya RAN. Energetika – News Russian Academy of Sciences. Energetics*, 2000, no.3, pp. 31-38. (Rus).

4. Mustafa T.M., Volkov S.V., Ershov A.M., Sentsov Yu.M., Minaev G.M. Frequency converter for the propeller motor. *Elektrotekhnika – Electrical Engineering*, 2014, no.1, pp. 46-54. (Rus).

5. Golubev A.N., Ignatenko C.B. Influence of the number of phases of the stator winding of the induction motor on its vibronoise characteristics. *Elektrotekhnika – Electrical Engineering*, 2000, no.1, pp. 28-31. (Rus).

6. Golubev A.N., Zykov V.V. A mathematical model of a multi-phase induction motor stator and rotor windings. *Elektrotekhnika – Electrical Engineering*, 2003, no.7, pp. 35-40. (Rus).

7. Petrushin V.S. Range of optimality criteria for the design of controlled asynchronous motors. *Trudy Odesskogo politekhnicheskogo universiteta – Proceedings of Odessa Polytechnic University*, 2001, no.1(13), pp. 81-86. (Rus).

8. Petrushin V.S. These costs asynchronous motors in the drive frequency for different control laws. *Elektromashinostoenie i elektrooborudovanie – Electrical Engineering and Electric Equipment*, 2001, no.56, pp. 51-54. (Rus).

9. Petrushin V.S. *Asinhronnye dvigateli v reguliruemom elektroprivode: Uchebnoe posobie* [Induction motors in adjustable electric: Textbook]. Odessa, Nauka i tehnika Publ., 2006. 320 p. (Rus).

10. Petrushin V.S., Rjabinin S.V., Jakimec A.M. *Programmnyj produkt «DIMASDrive». Programma analiza raboty, vybora i proektirovanija asinhronnyh korotkozamknutyh dvigatelej sistem reguliruemogo elektroprivoda* [Program performance analysis, selection and design of asynchronous cage motors controlled drive systems]. Patent UA, no.4065. (Ukr).

Received 27.11.2015

V.S. Petrushin[1]*, Doctor of Technical Science, Professor,*
L.Y. Bielikova[1]*, Candidate of Technical Science, Associate Professor,*
Y.R. Plotkin[2]*, Candidate of Technical Science, Professor,*
R.N. Yenoktaiev[1]*, Postgraduate Student,*
[1] Odessa National Polytechnic University,
1, Shevchenko Avenue, Odessa, 65044, Ukraine.
e-mail: victor_petrushin@ukr.net, Conda@ukr.net, rostik-enok@inbox.ru
[2] HWR Berlin,
Alt Friedrichsfelde 60, 10315 Berlin, Germany.
e-mail: juriy.plotkin@hwr-berlin.de

How to cite this article:
Petrushin V.S., Bielikova L.Y., Plotkin Y.R., Yenoktaiev R.N. Comparison of adjustable high-phase order induction motors' merits. *Electrical engineering & electromechanics*, 2016, no.1, pp. 38-41. doi: 10.20998/2074-272X.2016.1.07.

UDC 621.3.013.22 **doi: 10.20998/2074-272X.2016.1.08**

E.I. Sokol, M.M. Rezinkina, E.V. Sosina, O.G. Gryb

NUMERICAL COMPUTATION OF ELECTRIC FIELDS IN PRESENCE OF CURVILINEAR INTERFACE BETWEEN CONDUCTIVE AND NON-CONDUCTIVE MEDIA

Purpose. To elaborate a method of electric field numerical calculation in systems with curved boundaries between conductive and non-conductive media at final volume method usage and application of the rectangular grids. Methodology. At electric field calculation in quasi-stationary approximation, potential of the whole conductive object (rod) is constant. At final difference scheme writing, presence of the curved part of the boundary between conducting and non-conducting media has been taking into account as follows. It was supposed that curved section complements the closed loop on which integration of the solvable equation is done instead of a straight section which extends within a conducting medium. Usage of this approach allows taking into account square of the curved sections of the boundary and distance between surface of non-conductive medium and nearest nodes of the computational grid. Results. Dependence of the maximum electric field intensity on the height and radius of curvature peaks rods has been got with the help of calculations. As a result, a polynomial approximation for the analytical expression of the external electric field intensity, upon which application to the conductive object of a certain height and radius of curvature of its top, corona discharges will develop. References 13, figures 4.

Key words: **rounded tops, curvilinear borders, finite volume method, calculated grid, electric field intensity.**

Описаны принципы учета криволинейных границ раздела при использовании метода конечных объемов для расчета усиления электрического поля на вершинах проводящих стержней. С помощью проведенных расчетов получена зависимость максимальной напряженности электрического поля от высоты и радиуса скругления вершин стержней. В результате аппроксимации данной зависимости полиномом записано аналитическое выражение для напряженности внешнего электрического поля, при приложении которого к проводящему объекту определенной высоты и радиуса скругления вершины на нем развивается коронный разряд. Бібл. 13, рис. 4.

Ключевые слова: **скругленные вершины, криволинейные границы, метод конечных объемов, расчетная сетка, напряженность электрического поля.**

Introduction. In a number of practically important cases information on the distribution character and level of the maximum electric field (EF) intensity in the surrounding of tops of conductive rods is required. Application of systems containing conductive rods, is one of the possible ways of practical realization of metamaterials, which are widely spread in recent years [1]. Systems «rod – plane» are used in high-voltage pulse engineering for initiation discharges in different media [2]. This category of objects is elements of power facilities that can be modeled by peaks with rods of various shapes. In particular, information about the intensity of external electric field intensities, at application of which corona discharges arise is necessary.

Typically, tops of rods used in engineering are rounded. In calculating the EF in such systems problem of taking into account the curvature of the surface of tops of rods arises. The application in this case of the finite element method does not solve problem fully because the elements used (e.g., triangles) have corners, which means that when calculating the intensity of the EF will be too high compared with the actual values. Taking into account that the main part of the rod is straight for the calculation it is appropriate to apply the finite-difference methods [3]. However, it is known that using the rectangular calculated mesh to describe the EF in systems with curved surfaces leads to a significant increase in the calculated levels of the EF intensity that has no place in reality [4]. Moreover, utilization of the more fine mesh only worsens the situation. To solve this problem, different techniques, such as representation of derivatives in the form of polynomials, not finite differences, are used [5]. However, this approach is linked to the complexity of the problem, so advantaged of the finite-difference methods such as simplicity and possibility to take into account nonlinear parameters of media are lost. To calculate electromagnetic fields in such systems so-called conformal schemes are used providing averaging of material parameters of media in volumes of cells located at their curved interfaces [6]. Utilization of this approach to media which material parameters differ not more than in 5-10 times, gives very good results [6-8]. But if these values differ by several orders of magnitude (for example, at the location of conducting rod in the air), then, as it will be shown below, using this method is ineffective.

The goal of the work is development of a simplified method of incorporation of curved boundary interfaces between conductive and non-conductive media using the calculated rectangular meshes for calculating electromagnetic fields in the respective systems and the use of this method to assess by what radius should be rounded the sharp edges on objects that are in the area of electric fields impact, so that there are not there corona discharges on them.

Electric field modeling at presence of curvilinear interfaces. We consider the cases where the distance at which the EF is changing significantly exceed the typical size of the objects under consideration, so the calculation can be done in quasi-stationary approximation. The equations that describe the distribution of the EF, we obtain in the following manner. We write Maxwell equations in the form [9]:

$$\text{rot}\,\vec{H} = \gamma\vec{E} + \frac{\partial\vec{D}}{\partial t}, \qquad (1)$$

where $\vec{H}$, $\vec{E}$ are the intensities of magnetic and electric fields, respectively; $\vec{D} = \varepsilon_0\varepsilon\vec{E}$; $\varepsilon_0 = 0.885\cdot10^{-11}$ F/m; ε is the relative electric permeability; γ is the conductivity.

We use for the numerical calculation the finite volume method, at the use of which to the considered area the rectangular mesh is applied, and the solved differential equation is obtained by using conservation laws. To do this, we take the divergence of both parts of (1) taking into account that at the steady-state mode the second term on the right side is close to zero. Then we integrate the obtained equation by elementary cell volumes, into which the estimated region is divided, and use the substitution $\vec{E} = -\text{grad}\,\varphi$ (where φ is the electrical potential). Finally, we obtain:

$$\oint_S -\frac{\partial\varphi}{\partial n}\cdot\gamma ds = 0, \qquad (2)$$

where S are the sides of the parallelepiped, which divide in half the distances between neighboring nodes; n is the direction of the normal to the integration contour.

Let us describe in detail the calculation of the EF near the rounded tops of rods. When using the finite volume method nodes in which values of potentials are calculated should be placed at the boundaries between interfaces [8]. This allows take into account boundary conditions automatically, without setting their individual equations.

It is proposed to use this approach to obtain solutions for intensities of the EF near curved surfaces of interfaces. We take into account that the system considered includes conductive (rod) and non-conductive (air) media. Moreover, in the quasi-stationary case the conductive object potential can be considered as constant. We consider three-dimensional objects. First, we consider the case of rectilinear interfaces (see Fig. 1,*a*).

The section Z = const of closed contour of the square S by which of the solved equation (2) is carried out may be presented in the form of four planes perpendicular to components of the intensity of the EF: S_{1x} and S_{2x} – in the direction parallel to the axis Ox, and S_{1y} and S_{2y} – in the direction parallel to the axis Oy.

This is possible because integration of (2) by the surfaces S_{1x}^B and S_{2x}^B which are located close to the interface between media on both sides of it, in this case, can be replaced by integration by S_{1x} and S_{2x}.

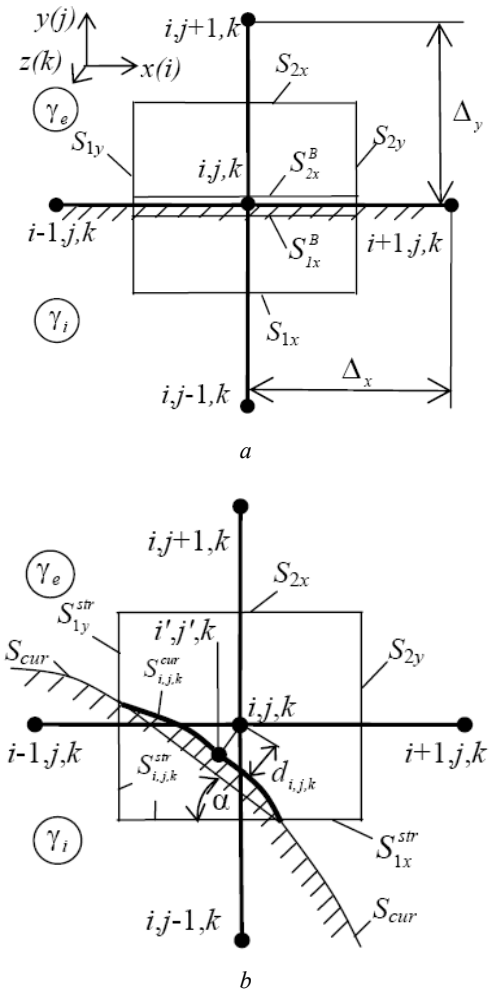

Fig. 1. Section of the calculating scheme by plane Z=const in the case of rectilinear (*a*) and curved (*b*) interfaces

Such a substitution is possible because squares by which integration is carried out are equal: $S_{1x}^B = S_{1x} = S_{2x}^B = S_{2xr} = \Delta_x$ (where Δ_x is the step by space in the direction of the axis Ox), and differential analogs of y-components of the EF intensities by both sides of the interface: $Ey_{i,j}^+$ and $Ey_{i,j}^-$ are determined by similar expressions: as derivatives at step back or step forward in the integration by S_{1x}^B and S_{2x}^B or as central derivatives at integration by S_{1x} and S_{2x}:

$$Ey_{i,j,k}^+ = -\frac{\partial\varphi}{\partial y} \approx -\frac{\varphi_{i,j+1,k} - \varphi_{i,j,k}}{\Delta_y},$$

$$Ey_{i,j}^- = -\frac{\partial\varphi}{\partial y} \approx -\frac{\varphi_{i,j,k} - \varphi_{i,j\text{-}1,k}}{\Delta_y}, \qquad (3)$$

where $\varphi_{i,j,k}$ is the potential of the node (i, j, k); Δ_y is the step by space in the direction of the axis Oy.

Let us write (2) in the differential form as a sum of integral by squares perpendicular to axis Ox and Oy, taking into account that $\gamma_e << \gamma_i$, and, therefore, $\gamma_i + \gamma_e \approx \gamma_i$ (where γ_i, γ_e are conductivities of conductive and non-conductive media, respectively):

$$\oint_S -\frac{\partial \varphi}{\partial n}\cdot \gamma ds \approx (F_{y2}-F_{y1})+(F_{x2}-F_{x1}), \quad (4)$$

де $F_{y1} = -\gamma_i \cdot \frac{\varphi_{i,j,k}-\varphi_{i,j-1,k}}{\Delta_y}\cdot S_{1x}$; (5)

$$F_{y2} = -\gamma_e \cdot \frac{\varphi_{i,j+1,k}-\varphi_{i,j,k}}{\Delta_y}\cdot S_{2x}; \quad (6)$$

$$F_{x1} \approx -0.5\cdot \gamma_i \cdot \frac{\varphi_{i,j,k}-\varphi_{i-1,j,k}}{\Delta_x}\cdot S_{1y}; \quad (7)$$

$$F_{x2} \approx -0.5\cdot \gamma_i \cdot \frac{\varphi_{i+1,j,k}-\varphi_{i,j,k}}{\Delta_x}\cdot S_{2y}. \quad (8)$$

We now consider (*i*,*j*,*k*)-th cell of the calculated system for which the *S*-contour of integration (2) includes a part $S^{cur}_{i,j,k}$ of curved interface S^{cur} (see Fig. 1,*b*). In order to take into account the presence of this area when writing the difference scheme, we assume that $S^{cur}_{i,j,k}$ complements *S* to closed contour instead of straight part $S^{str}_{i,j,k}$ that runs inside a conductive medium. As noted above, at the assumptions adopted the potential of all conductive object (rod) is the same, denoted by U_0. With that, the potential value in the nodes located inside a conductive medium, are obtained from the solution automatically when setting the level of potential $\varphi = U_0$ on the corresponding part of the outer boundary of the calculated area. Denote by *En* the EF intensity near the surface of the rod directed perpendicular to this surface. Since the potentials of all nodes located inside and on the surface of a conductive medium are the same, we assume that at the determination of *En* as a potential difference instead of nodes inside a conductive medium (in our case (*i*–1,*j*,*k*) і (*i*,*j*–1,*k*) – see. Fig. 1,*b*) can be used the node (*i*′,*j*′,*k*′) located on the interface at the place of contact of the perpendicular to the surface of the node (*i*,*j*,*k*):

$$En_{i,j,k} = -\frac{\partial \varphi}{\partial n} \approx -\frac{\varphi_{i,j,k}-\varphi_{i',j',k'}}{d_{i,j,k}} = -\frac{\varphi_{i,j,k}-U_0}{d_{i,j,k}}, \quad (9)$$

where $d_{i,j,k}$ is the distance from the node (*i*,*j*,*k*) to the curved interface.

Taking into account that the curvature in the direction of the axis *Oz* is small, we expand *En* on the *x* and *y* components, considering that the region is inclined to the horizontal at an angle α (see Fig. 1,*b*):

$$-\frac{\partial \varphi}{\partial x} = E_x \approx En\cdot\sin\alpha,$$
$$-\frac{\partial \varphi}{\partial y} = E_y \approx En\cdot\cos\alpha. \quad (10)$$

Then the terms F_{x1} and F_{y1} in (4), for which the integration contour of equation (2) includes, in particular, curved planes of the interface, are written as:

$$F_{x1} \approx -\gamma_e \cdot \frac{\varphi_{i,j,k}-U_0}{d_{i,j,k}}\cdot\left\{\sin\alpha\cdot S^{str}_{1y}\cdot\left[k_x+(1-k_x)\right]+k_x\cdot S^{cur}_{i,j,k}\right\}, \quad (11)$$

$$F_{y1} \approx -\gamma_e \cdot \frac{\varphi_{i,j,k}-U_0}{d_{i,j,k}}\cdot\left\{\cos\alpha\cdot S^{str}_{1x}\cdot\left[k_y\cdot+(1-k_y)\right]+k_y\cdot S^{cur}_{i,j,k}\right\}, \quad (12)$$

where $k_x = \begin{cases}0, & if \quad \alpha<\pi/4\\ 1, & if \quad \alpha>\pi/4\end{cases}$; $k_y = \begin{cases}0, & if \quad \alpha>\pi/4\\ 1, & if \quad \alpha<\pi/4\end{cases}$;

S^{str}_{1x}, S^{str}_{1y} are the squares of straight parts of the contour of integration *S*; $S^{cur}_{i,j,k}$ is the square of the curvilinear part *S* (see Fig. 1,*b*).

In writing (11), (12) a simplified approach is used when it is assumed that when $\alpha>\pi/4$ the part $S^{cur}_{i,j,k}$ together with part S_{1y} or S_{2x} (in our case this is a part S^{str}_{1y}) complements the part of the integration contour, parallel to the axis *Oy*. If $\alpha<\pi/4$, the curve $S^{cur}_{i,j,k}$ is considered as a part of the integration contour, supplementing with parts S_{1x} or S_{2x} (in our case this is a segment S^{str}_{1x}) a part of integration contour, parallel to axis *Ox*. For the considered cell (see Fig. 1,*b*) terms F_{y2} and F_{x2} in (4) are determined by the expressions (6) and (8) as at their obtaining the curved parts are not included to the integration contour. Finding the length of the curved part $S^{cur}_{i,j,k}$, straight segments S^{str}_{1x}, S^{str}_{1y} as well as $d_{i,j,k}$ does not present significant difficulties and could be done, for example, numerically as a result of more fine dividing of cells that lie on the interface. And, by the proposed approach near-boundary cells located inside a conductive medium, are virtually displaced on it at the EF determination in non-conductive medium. This «displacement» does not affect the determination of EF inside a conductive medium because its potential is constant.

Generally, at the use of finite difference methods curvilinear boundary between media is replaced by a step approximating surface [6]. However, this causes the appearance at the calculation of local areas with increased intensity of the EF that really has no place [4]. Moreover, the level of EF intensity in the areas adjacent to the corners of rectangular cells approximating the curved surface will be greater, the smaller step of the spatial calculation mesh. The proposed method allowed tavoid this problem. Fig. 2 shows the EF intensity distributions on the conductive sphere surface areas that is in the homogeneous EF calculated by using the described approach (see the dotted curve 2).

Calculation is carried out at the step of the mesh $\Delta = 0.02\cdot R$ (where *R* is the radius of the sphere). Levels of the EF intensity modulus in the (*i*,*j*,*k*)-th node are determined by calculated potentials in the nodes of the mesh as average values by the cell volume:

$$|\vec{E}| = \sqrt{Ex^2_{i,j,k}+Ey^2_{i,j,k}+Ez^2_{i,j,k}}, \quad (13)$$

де $Ex_{i,j,k} \approx -0.5 \cdot \left(\frac{\varphi_{i+1,j,k} - \varphi_{i,j,k}}{\Delta_x} + \frac{\varphi_{i,j,k} - \varphi_{i-1,j,k}}{\Delta_x} \right)$;

$$Ey_{i,j,k} \approx -0.5 \cdot \left(\frac{\varphi_{i,j+1,k} - \varphi_{i,j,k}}{\Delta_x} + \frac{\varphi_{i,j,k} - \varphi_{i,j-1,k}}{\Delta_y} \right)$$

$$Ez_{i,j,k} \approx -0.5 \cdot \left(\frac{\varphi_{i+1,j,k+1} - \varphi_{i,j,k}}{\Delta_z} + \frac{\varphi_{i,j,k} - \varphi_{i,j,k-1}}{\Delta_z} \right).$$

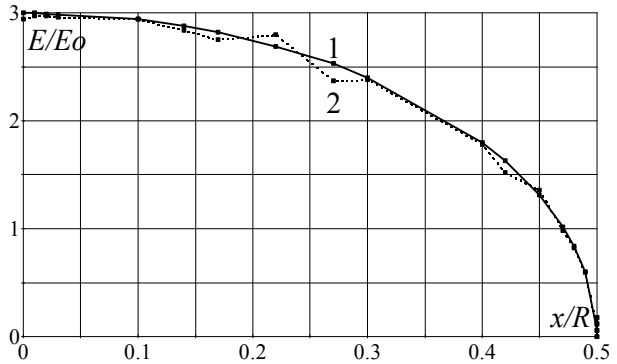

Fig. 2. Calculated EF intensity distributions on the surface of the conductive sphere of radius R in the homogeneous external EF of intensity E_0: 1 – analytical solution, 2 – solution by proposed method

For comparison, in the same figure (see curve 1) the analytical solution for the conductive sphere in a homogeneous external EF is shown [10]. As can be seen from a comparison of curves 1 and 2, the relative differences in the intensity of the EF for these two cases are very small, they do not exceed 3 %. As the calculations with the same step in space demonstrate, at the step approximation of the interface the relative differences reach almost 30%.

As noted above, to address this problem, a number of methods are used [4-6]. They are rather bulky, which greatly complicates their practical implementation in contrast to the described approach, not associated with the introduction of non-orthogonal mesh or increase the order of approximation of derivatives.

Thus, the use of the proposed approach allows take into account the square of curved sections of interfaces as well as the distances between the non-conductive medium between arranged in near-boundary medium nodes of computational mesh and the interface. This is possible due to the use to obtain the solved equations of the conservation law (in this case, for charge) through the integration of initial differential equations on contours of cells of the calculated taking into account configuration of the interface within each cell.

As the calculations are shown, the EF intensity values obtained using the conformal scheme [6] coincide fully with those obtained using the step approximation. This is because with such a large difference between the values of conductivity of conductive and non-conductive media (more than 5-6 orders) the reduce by several times of the equivalent conductivity of cells located at the interface and containing conductive and non-conductive medium practically does not influence impact on calculated levels of potentials.

Calculation of EF in the neighborhood of a cylindrical wire rod. The approached described above permit to perform the calculation of the electric field in the neighborhood of the conductive cylindrical rod that is in the vertically directed external EF of intensity E_0. The calculated system that includes a conductive cylindrical rod with rounded top 1 is shown in Fig. 3.

Analytical solutions for EF intensity in systems containing cylindrical rods with rounded tops are absent. To find the distribution of EF we use the numerical finite volume method [11] and the above proposed approach. Due to the axial symmetry of the system under consideration the cylindrical coordinate system was used. It is assumed that the axis Oz coincides with the axis of the rod 1 and perpendicular to the ground surface 2 (see Fig. 3). It is also assumed that the calculation area is limited by a rectangle with sides $z = 0$, $z = Z_{max}$, $r = R_{max}$, $r = 0$ (see Fig. 3) and is divided into elementary rectangular cells.

In order to reduce the calculation region on its boundaries the so-called well-matched layers (PML) [6] (see 3 and 4 in Fig. 3) are introduced. These layers perform a supporting role and are need for guarantee the rapid and reflectionless decrease of the distortion of the EF caused by the presence of the considered objects when approaching the calculation region's boundaries.

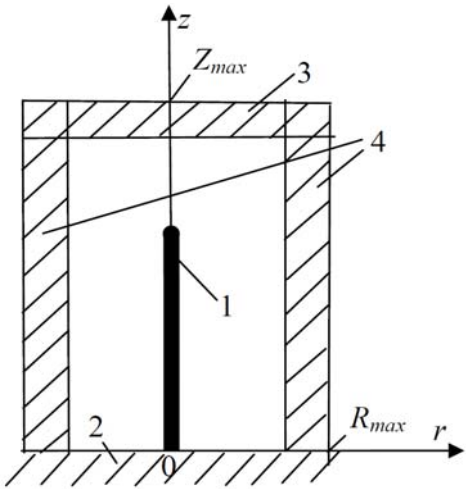

Fig. 3. Section $z = 0$ of the considered calculation system, including conductive rod. 1 – rod; 2 – ground; 3, 4 – PML

Distribution of the EF in the PML is not included in the results of the calculation. It is supposed that the electrical conductivity in this layer of thickness d is a tensor, has different values in the directions of the coordinate axes Or, Oz and varies in depth of the layer according to the polynomial law. Thus, for PML, which is perpendicular to the axis Or (see 4 in Fig. 3), changing

the r-th – $\gamma_r^{PML}(r)$ and the z-th – $\gamma_z^{PML}(r)$ components of the conductivity tensor in the direction of the axis Or is written as [6]:

$$\gamma_r^{PML}(r) = \gamma_0 \cdot k_r(r),\ \gamma_z^{PML}(r) = \gamma_0 / k_r(r),$$

where $k_r(r)=1+(k_{max}-1)\cdot(r/d)^m$; k_{max} is the maximal value of k_r on the external boundary of the PML-layer; m is the power; γ_0 is the value of the conductivity of the medium adjacent with internal boundary of the PML.

Values of the conductivity tensor components in PML which is perpendicular to the axis Or (see 4 in Fig. 3) are the following:

$$\gamma_z^{PML}(z) = \gamma_0 \cdot k_z(z),\ \ \gamma_r^{PML}(z) = \gamma_0 / k_z(z),$$

where $k_z(z) = 1 + (k_{max}-1)\cdot(z/d)^m$.

The values of electric conductivity in the areas of PML-layers crossing are found by multiplication of the respective components in each of the layers.

The conditions at the boundaries of the calculation area (see Fig. 3) are the following: $\varphi=0$ on the ground surface ($z=0$); $\partial\varphi/\partial n = 0$: at $R=0$ and at $r=R_{max}$ (on the external boundary of the calculation area). In order to take into account that on the upper boundary of the calculation after the PML-layer the intensity of the applied EF equals to E_0, at $z = z_{max}$ the condition $\partial\varphi/\partial n = k_{max}\cdot E_0$ is used (for details, see [8]).

Comparison with analytical solution for a sphere in the homogeneous EF is showed that using ten layers of PML with parameters $m = 5$, $k_{max} = 500\cdot\gamma_0$ the relative error of calculation of intensity and potential of the EF no more than 3 % is provided.

The influence of the geometry of rods with rounded tops on the maximum intensity of the EF. In order to assess the effect of height of rods on the possibility of corona discharge development from them distributions of the EF at different heights of rods were calculated.

Preliminary calculations in sequential increasing size of the limited by PML calculation area in the direction of the coordinate axes, as well as reducing the computational mesh's step have been carried out. It was believed that the solution adequately describes the distribution of the EF, when the values of intensities and potentials stop to change at sequential twice reduction of the step of the calculation grid and increasing its size. An analysis of the data made the following conclusions: so that the relative error does not exceed 3%, size of the calculation area in the radial direction should be not less than the height of the rod (H) and in the vertically – in 1.2 times more than H; the step of the calculation grid mesh be no more than $R/10$ (where R is the radius of rod rounding).

The case is considered when it can be supposed that the uniform EF is applied to the rod. According to the literature (see, for example, [12, p. 188 and further]) at the discharges in systems «rod – plane» a so-called critical radius of the rod is. It is determined by the condition of the identity of the character of rupture in systems with rods, radius of which is less than the critical radius: $R \le R_{cr}$, because at this condition the breakdown voltage does not depend on the value of R because of the corona. The case where the value of the radius of the rod equals to the critical radius is considered – $R = R_{cr} = 0.1$ m [12].

Fig. 4 shows the results of numerical calculation of the dependence of E_{max} – maximal intensity levels of the EF in the vicinity of the conductive rods tops located in the external uniform field of strength E_0 (see curve 1) on their height H. The calculation was performed at the following of the calculation mesh: $\Delta_r = \Delta_z = R/10$, $Z_{max} = 1.2\cdot H$, $R_{max} = H$, $H = var$.

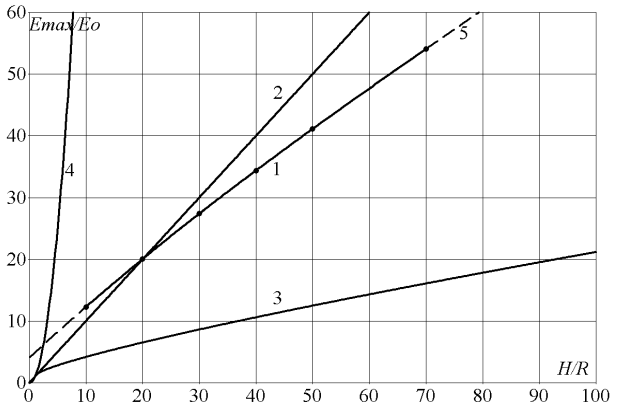

Fig. 4. Dependence of the maximal intensity of the EF in the vicinity of the conductive rod on its height H: 1 – numerical calculation by using the described approach; 2 – dependence $E_{max}=E_0\ H/R$; 3, 4 – analytical solutions for conductive prolate ellipsoid at a distance from the top $l=0$ (3) and $l=R=0.1$ m (4); 5 – polynomial approximation of the curve *1*

The Figure also presents results of engineering estimates for E_{max} (curves 2 – 4). Curve 2 corresponds to the assessment of E_{max} as ratio of the potential of the EF at the height of the top of the grounded rod to its radius (R):

$$E_{max} = E_0 \cdot H / R.$$

Curves 3 and 4 are obtained as a result of the use of analytical expression for the intensity of the EF above the ellipsoid on its axis (see, for example, [13]) at a distance from its top $\Delta = R_{cr}$ (curve 3) and $\Delta = 0$ (curve 4). As can be seen from a comparison of curves 1 – 4, the values $E^*_{max} = E_{max}/E_0$ obtained with real shape of the rod (cylinder whose vertex is rounded) occupy an intermediate position relative to the smallest levels (curve 3) that correspond to the distance from the rod which is equal to critical radius R_{cr} and maximal levels that match a point on the top of the equivalent ellipsoid (curve 4). In Fig. 4 curve 5 shown by a dotted line corresponds to a polynomial approximation of the curve 1.

For the range of the change of the ratio of the height of core (H) to its top rounding radius (R) within $10<H/R<70$ the calculated curve of the dependence $E^*(H/R)$ can be approximated by a more simple function with which for object which is in the area of the electric

field impact with intensity E_0 [V/m] it is possible to find a boundary value for the ratio of the radius of rounding of its top to its height, which ensures guarantees suppression of the corona at this object:

$$R/H>0.7/(3\cdot10^6/E_0–6.08).$$

Conclusions.

1. The proposed method of taking into account the curved interface between media based on the finite volume method utilization permits to calculate the electric field distribution on the surface of the sphere and in its vicinity with relative error not exceeding 3%, at the step of the calculation mesh not more than $0.1\cdot R$ (where R is the radius of the sphere).

2. Using the proposed method of taking into account the curved interface between media dependences of maximum electric field strength at the tops of the rods on the ratio between their diameter and height are calculated.

3. An expression to assess by which radius they should round off the sharp edges on objects of the height H, located in the area of the EF action of intensity E_0 so that they are not there corona discharge.

4. It is shown that the use of analytical solutions for conductive prolate ellipsoid leads to substantial error at placement of levels of maximum intensity near the tops of the rods.

REFERENCES

1. Toal B., McMillen M., Murphy A., Atkinson R., Pollard R. Tuneable magneto-optical metamaterials based on photonic resonances in nickel nanorod arrays. *Materials Research Express*, 2014, no.1, pp. 1-11. **doi: 10.1088/2053-1591/1/1/015801**.

2. Bazelian E.M., Razhanskii I.M. *Iskrovoi razriad v vozdukhe* [Spark discharge in air]. Novosibirsk, Nauka Publ., 1988. 165 p. (Rus).

3. Samarskii A.A. *Teoriia raznostnykh skhem* [Theory of difference schemes]. Moscow, Nauka Publ., 1989. 616 p. (Rus)

4. Popov E., Nevière M., Gralak B., Tayeb G. Staircase approximation validity for arbitrary-shaped gratings. *Journal of the Optical Society of America A*, 2002, vol.19, no.1, pp. 33-42. **doi: 10.1364/josaa.19.000033**.

5. Gjonaj E., Lau T., Schnepp S., Wolfheimer F., Weiland T. Accurate modeling of charged particle beams in linear accelerators. *New Journal of Physics*, 2006, no.8, pp. 1-21. **doi: 10.1088/1367-2630/8/11/285**.

6. Taflove A., Hagness S. *Computational electromagnetics: the finite difference time domain method*. Boston – London: Artech House, 2000. – 852 p.

7. Rezinkina M.M. The calculation of the penetration of a low-frequency three-dimensional electric field into heterogeneous weakly conducting objects. *Elektrichestvo – Electricity*, 2003, no.8, pp. 50-55. (Rus).

8. Rezinkina M.M. Numerical calculation of the magnetic field and magnetic moment of ferromagnetic bodies with a complex spatial configuration. *Technical Physics*, 2009, vol.54, no.8, pp. 1092-1101. **doi: 10.1134/S1063784209080027**.

9. Tamm I.E. *Osnovy teorii elektrichestva* [Bases of the theory of electricity]. Moscow, Nauka Publ., 1989. 504 p. (Rus).

10. Stretton Dzh.A. *Teoriia elektromagnetizma* [Theory of electromagnetism]. M.-L.: OGIZ, Gostekhizdat Publ., 1948. 539 p. (Rus).

11. Patankar S. *Chislennye metody resheniia zadach teploobmena i dinamiki zhidkosti* [Numerical methods of solution of problems of heat exchange and dynamics of liquid]. Moscow, Energoatomizdat Publ., 1984. 150 p. (Rus).

12. Cooray V. *Lightning Protection.* London: The Institution of Engineering and Technology, 2010. 1036p.

13. Kuchinskii G.S., Kizevetter V.E., Pintal' Iu.S. *Izoliatsiia ustanovok vysokogo napriazheniia* [Isolation of installations of high tension]. Moscow, Energoatomizdat Publ., 1987. 368 p. (Rus).

Received 29.10.2015

E.I. Sokol[1]*, Doctor of Technical Science, Professor,*
Corresponding Member of the National Academy of Science of Ukraine,
M.M. Rezinkina[2]*, Doctor of Technical Science,*
E.V. Sosina[1]*, Postgraduate Student,*
O.G. Gryb[1]*, Doctor of Technical Science, Professor,*
[1] National Technical University «Kharkiv Polytechnic Institute», 21, Frunze Str., Kharkiv, 61002, Ukraine.
e-mail: elenasosina09@gmail.com
[2] State Institution «Institute of Technical Problems of Magnetism of the NAS of Ukraine», 19, Industrialna Str., Kharkiv, 61106, Ukraine.
e-mail: marinar2@mail.ru

How to cite this article:
Sokol E.I., Rezinkina M.M., Sosina E.V., Gryb O.G. Numerical computation of electric fields in presence of curvilinear interface between conductive and non-conductive media. *Electrical engineering & electromechanics*, 2016, no.1, pp. 42-47. doi: 10.20998/2074-272X.2016.1.08.

UDC 621.3.022: 621.319.53 **doi: 10.20998/2074-272X.2016.1.09**

M.I. Baranov, S.V. Rudakov

EXPERIMENTAL INVESTIGATIONS OF ELECTRO-THERMAL RESISTIBILITY OF CONDUCTORS AND CABLES TO ACTION OF RATIONED ON THE INTERNATIONAL STANDARD IEC 62305-1-2010 APERIODIC IMPULSE OF CURRENT OF ARTIFICIAL LIGHTNING

Purpose. *Experimental researches of electro-thermal resistibility of cable-explorer products, applied in the power electric circuits of objects of electric-power industry, to action on its copper and aluminum parts bearings a current rationed on the International Standard of IEC 62305-1-2010 aperiodic impulse 10/350 μs of current of artificial lightning.* ***Methodology.*** *Electrophysics bases of technique of high tensions and high pulsed currents (HPC), and also scientific and technical bases of planning of devices of high-voltage impulsive technique and measuring HPC in them.* ***Results.*** *Experimental a way the quantitative levels of maximal values maximum of possible and critical closenesses of aperiodic impulse 10/350 μs of current of artificial lightning with rationed on the international standard of IEC 62305-1-2010 peak-temporal parameters and admittances on them in copper (aluminum) parts bearings a current of send-offs and cables with a polyethylene (PET) and polyvinylchloride (PVCH) isolation.* ***Originality.*** *First in world practice on the unique powerful high-voltage generator of HPC of artificial lightning experimental researches of resistibility to lightning of pre-production models of send-offs (cables) are conducted with copper (aluminum) tendons, PET and PVCH by an isolation, in-use in power electric circuits of electric-power industry objects.* ***Practical value.*** *The use in practice of protecting from lightning of the got results will allow substantially to promote functional and fire-prevention safety of engineering communications of objects of industrial electroenergy in the conditions of action on them of short shots of linear lightning.* References 16, figures 12.

Key words: **high impulsive current of lightning, wires and cables of electric chains of objects of electric-power industry, generator of high pulsed current of artificial lightning, electro-thermal resistibility to lightning of cable-conductor products.**

Приведены результаты экспериментальных исследований электротермической стойкости образцов ряда проводов и кабелей электрических цепей объектов промышленной электроэнергетики с медными (алюминиевыми) жилами (экранами), поливинилхлоридной и полиэтиленовой изоляцией к действию короткого удара большого импульсного тока искусственной молнии с нормированными по международному стандарту IEC 62305-1-2010 амплитудно-временными параметрами и допусками на них. Библ. 16, рис. 13.

Ключевые слова: **большой импульсный ток молнии, провода и кабели электрических цепей объектов электроэнергетики, генератор большого импульсного тока искусственной молнии, электротермическая молниестойкость кабельно-проводниковой продукции.**

Introduction. One of the ways for reliable electro-thermal and fire protection from direct (indirect) lightning power facilities (PF) and their utilities is the informed choice of cables and wires installed in their primary and secondary circuits, and complies with strict conditions of lightning resistance. According to the requirements of existing International and national Standards [1-6] with a short lightning in the wire and cable power circuits of the PF can occur pulse currents of positive polarity amplitude I_{mL}, with aperiodic temporary form τ_f/τ_p=10 μs/350 μs, where τ_f, τ_p are, respectively, the acceleration time between the levels $(0.1 – 0.9)I_{mL}$ and duration of the current pulse at the level $0.5I_{mL}$. In [1-6], the normalized amplitude-time parameters (ATP) and the tolerances are specified for the aperiodic impulse lightning current corresponding to I-IV levels of protection against lightning of the PF and their utilities. Thus, for example, a lower level IV of the lightning protection of the PF set of ATPs and other characteristics affecting the current pulse are aperiodic 10/350 μs lightning characterized by the following normalized quantitative values [1-7]: τ_p = 350 μs (with a tolerance of ± 10%); I_{mL} = 100 kA (with a tolerance of ± 10%); specific energy (the integral of the action of the lightning current) J_L=2.5·10^6 A^2·s (with a tolerance of ± 35%); fluxed charge q_L=±50 C (with a tolerance of ± 20%). With regard to the numerical value of τ_f, it is, with a tolerance of ± 20% is according to [1-7] and the secondary character may be in the range 10 μs ≤ τ_f ≤ 15 μs. Furthermore, the time t_m≈1,6τ_f, corresponding to a current amplitude I_{mL}, according to the requirements [1-5] must not exceed 25 μs, and by [6] – 50 μs. Currently there are no methodological and other data that can be used to select the specified wire and cable electrical circuits of the PF that meets the existing requirements [1-6]. In this regard the holding of a high-current high-voltage equipment in the experimental studies on the definition of electrothermal lightning resistance of cables and wires of the PF is an actual scientific and technical problem.

Problem definition. Consider widely used in electrical power circuits of the PF wires and cables with copper (aluminum) conductor (screen) in polyvinylchloride (PVC) and polyethylene (PET) insulation. For their

electrothermal tests on lightning resistance we use straight test samples (TS) of given wires (cables) with length of 0.5 m, rigidly clamped in a high-current discharge circuit of the generator of the pulsed lightning current (GPLC). As GPLC we select created in 2014 by the Institute «Molniya» of the NTU «KhPI» a powerful high voltage generator ГИТМ-10/350 [7], which reproduces at low impedance and low-inductive electrical load aperiodic current pulses 10/350 μs artificial lightning with positive polarity normalized ATP and tolerance to them, meet the requirements of existing International and national Standards [1-6]. During consideration of experimental studies on the generator ГИТМ-10/350 containing in its structure four concurrent high-voltage pulse current generator (PCG) it is required as a first approximation to determine at room temperature $\theta_0 = 20$ °C maximum limit values δ_{m1d} and critical δ_{m1k} densities of the aperiodic current pulse 10/350 μs of the artificial lightning with normalized ATP [1-6] in the current-carrying parts of mentioned TS of wires and cable of electrical circuits of the PF.

Electrical circuit and parameters of the powerful high-voltage generator ГИТМ-10/350. Fig. 1 shows a circuit diagram of the generator ГИТМ-10/350 used for electrothermal tests on the lightning resistance of the TS of chosen wire and cable of power circuits of the PF.

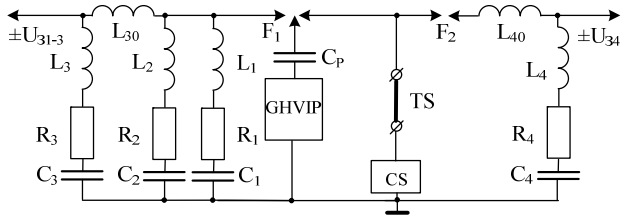

Fig. 1. Circuit diagram of high-current discharge circuits of the generator ГИТМ-10/350 for forming in the TS of wires (cables) of electrical circuits of the PF aperiodic current pulses 10/350 μs of the artificial lightning with normalized ATP and tolerance to them (GHVIP – generator of high-voltage ignitor microsecond pulses of voltage of amplitude up to ± 100 kV; F_1, F_2 – respectively three and two-electrode high-voltage air-spark switches PCG-1 – PCG-4; C_p≈180 pF – blocking capacity for pulse voltage up to ± 120 kV of the GHVIP circuit controlling the actuation of the spark switches F_1 and F_2; TS – test sample of the wire (cable), CS – coaxial shunt type ШК-300 for measuring of pulse current of artificial lightning amplitude from ± 10 A to ± 300 kA; $\pm U_{31\text{-}3}$, $\pm U_{34}$ – charging voltage, respectively of PCG-1 – PCG-3 and PCG-4; $L_1 - L_4$, $R_1 - R_4$ and $C_1 - C_4$ – respectively intrinsic inductances, resistances and capacitances of discharge circuits of PCG-1 – PCG-4; L_{30}, L_{40} – forming inductances of discharge circuits of PCG-3 and PCG-4) [7]

It can be seen that its four individual PCG (PCG-1 – PCG-4) work in parallel on the total electrical load – tested TS of wires and cables. Note that the PCG-1 – PCG-3 were collected on the basis of 171 parallel included high-voltage pulse capacitor ИК-50-3 (16 for PCG-1, 44 for PCG-2 and 111 for PCG-3), and PCG-4 – on the basis of 288 high-voltage pulse capacitors ИМ2-5-140 consistently included two in each of its 144 connected in parallel sections [7, 8]. Intrinsic electrical parameters of the generator type ГИТМ-10/350 are the following [7]: for PCG-1 − R_1≈0.375 Ω; L_1≈1 μH; C_1≈48 μF; for PCG-2 − R_2≈0.136 Ω; L_2≈1.3 μH; C_2≈132 μF; for PCG-3 − R_3≈0.057 Ω; L_3≈2.5 μH; C_3≈333 μF; for PCG-4 – R_4≈0.083 Ω; L_4≈1.5 μH; C_4≈10.08 μF. Forming inductance L_{30} in the discharge circuit of the PCG-3 is about 40 μH, and forming inductance L_{40} in the discharge circuit of the PCG-4 – about 7 μH.

The nominal value of stored electrical energy in a generator-type ГИТМ-10/350 at a charging voltage for capacitors $U_{31\text{-}3}$ of PCG-1 – PCG-3 at ± 50 kV and a charging voltage for capacitors U_{34} of PCG-4 at ± 5 kV is about 1145 kJ [7]. And, for the PCG-1 – 60 kJ, for PCG-2 – 165 kJ, for PCG-3 – 416 kJ, for PCG-4 – 504 kJ. These data highlight the high levels of energy consumption such as capacitor banks generator ГИТМ-10/350, and point to «hidden» from the reader difficulties for maintenance personnel with such powerful energy storage [9, 10]. To avoid devastating consequences in capacitor banks generator type ГИТМ-10/350 and ensure safe working conditions for maintenance of their personnel in the emergency mode of its work due to electrical breakdown at the stage of the charge (discharge) of the inner or outer insulation of at least one of its 459 capacitors all high-voltage output pulse capacitors in PCG-1 – PCG-4 were installed protective resistance made on the basis of parallel connected high graphite-ceramic volume fixed resistors ТВО-60 with par value of 24 Ω at DC voltage up to ± 25 kV [10, 11]. Parallel operation of PCG-1 – PCG-4 in the mode of the high-current discharge of high-voltage capacitor oscillator type ГИТМ-10/350 on the TS wires (cables) is provided as shown in Fig. 1 simultaneous actuation of the high-voltage three-electrode-managed air switch F_1 with graphite main electrodes having a hemispherical working surface at a nominal voltage of ±50 kV [12] and the high-voltage two-electrode air switch F_2 with graphite rectangular electrodes containing a flat working surface, for a rated voltage of ±10 kV [13]. Synchronous actuation of switches F_1 and F_2 in the presented in Fig. 1 circuit diagram is performed by applying a high voltage across the capacitance C_p dividing by the average graphite spherical electrode F_1 switch from generator of high-voltage ignitor microsecond pulse (GHVIP) of microsecond duration pulse voltage amplitude up to ± 100 kV [7, 10]. When electrical breakdown due to the work of the GHVIP of one of the two air gaps switch F_1 and its subsequent activation occurs surge voltage to the TS of the wire (cable) results simultaneously with F_1 triggered and switch F_2, subsequent discharge to a load (TS) of charged capacitors PCG-1 – PCG-4 and the flow of

simulated lightning current pulse with the required ATP through the samples studied wires (cables).

The results of tests of wires and cables for resistance of the PF to current pulse 10/350 μs of the artificial lightning. Fig. 2 is a perspective view of the working table of the generator ГИТМ-10/350 is rigidly fixed to its high-current discharge circuit solid round copper wire diameter of 3.5 mm and a cross-section mm^2 S_1≈9.6 mm^2 of the TS of the RF coaxial cable РК Д2-3,5/9 [14] to the flow by it of the aperiodic current pulse 15/335 μs of the artificial lightning amplitude of about I_{mL}≈85.6 кА.

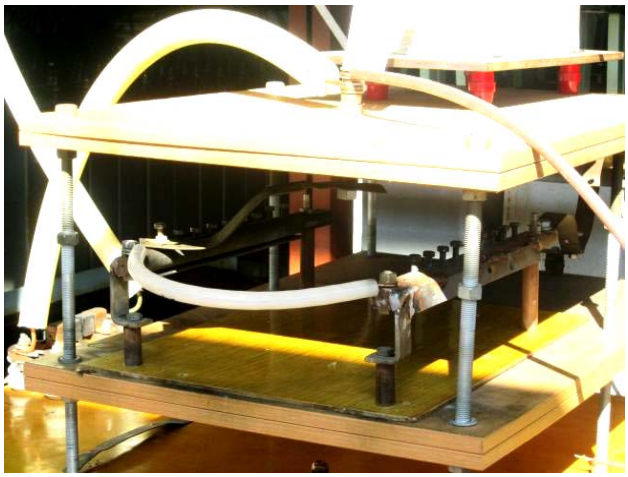

Fig. 2. The view of the workingtable of thepowerful high-voltage generator ГИТМ-10/350 with rigidly fixed to its massive steel electrodes solid round copper wire cross-section of S_1≈9.6 of the TS of the RF coaxial cable РК Д2-3,5/9 with semi-air PET insulation of length of 0.5 m, removed protective sheath and PET twisted copper screen before exposure to the aperiodic current impulse 15/335 μs of the artificial lightning with amplitude I_{mL}≈85.6 кА ($U_{31\text{-}3}$≈16.5 кV; U_{34}≈4.2 кV)

Fig. 3 presents fixed with the help of calibrated by the state metrological service of the measuring shunt type ШК-300 [7, 10] and DSO Tektronix TDS 1012 aperiodic waveform current pulse 15/335 μs of artificial lightning flowing in the discharge circuit of the generator ГИТМ-10/350 via the copper core of the TS of the mentioned cable of the length of 0.5 m. After exposure to the amplitude of the current pulse I_{mL}≈85.6 кА the TS of the RF coaxial cable РК Д2-3,5/9 was visually as a whole and, accordingly, electrodynamically and electrothermally not damaged.

The maximum current density in the copper conductor on the particular cable was about δ_{m1}≈I_{mL}/S_1≈8.9 kA/mm^2. Found in a copper conductor RF cable РК Д2-3,5/9 with PET insulation for the case (I_{mL}≈85.6 кА; J_L≈2·10^6 A^2·s) calculated by taking into account [15] The peak value of the maximum permissible density δm1d current pulse 15/335 μs of the artificial lightning from the ratio δ_{m1d}≈1.353·10^8·$I_{mL}/(J_L)^{1/2}$ is approximately equal to δ_{m1d}≈8.2 кА/mm^2. It is known that at this average density δ_{m1d} pulsed current in a copper conductor of said cable, the maximum permissible short-term temperature heating θ_{1k} it will not exceed 120 °C [15, 16]. From the obtained approximate data that the calculated value of the current density δ_{m1d}≈8.2 кА/mm^2 different from its experimental value δ_{m1d}≈8,9 кА/mm^2 about 8%.

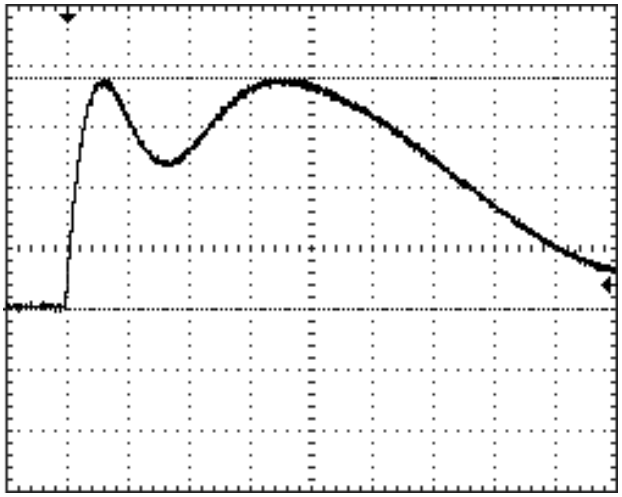

Fig. 3. Oscillogram of the aperiodic artificial lightning current pulse generator circuit type ГИТМ-10/350 in the discharge of its PCG-1 – PCG-4 on the solid round copper conductor of cross-section S_1≈9.6 mm^2 of the RF cable brand РК Д2-3,5/9 with semi-air PET insulation of the length of 0.5 m, and removal of the protective sheath of PET and twisted copper screen (I_{mL}≈85.6 kA; δ_{m1}≈I_{mL}/S_1≈8.9 kA/mm^2; τ_f≈15 μs; t_m≈25 μs; τ_p≈335 μs; J_L≈2·10^6 A^2·s; q_L≈42 C; $U_{31\text{-}3}$≈16.5 kV; U_{34}≈4.2 kV; vertical scale – 22.52 kA / cell; the horizontal scale – 50 ms / cell)

Fig. 4 shows a working table of the generator ГИТМ-10/350 with electrodes attached to his split round copper conductor cross-section of S_1≈3.2 mm^2 of the TS of the RF coaxial cable РК 50-7-11 with solid PET insulation [14] of the length of 0.5 m before exposure to the current pulse of 15/335 μs of the artificial lightning amplitude up I_{mL}≈85.6 кА.

Fig. 5 shows the initial stage of the electrical explosion (EE) of the copper conductor of the cross-section of S_1≈3.2 mm^2 tested in the discharge circuit of the generator type ГИТМ-10/350 of the TS of the RF coaxial cable РК 50-7-11 with a solid of length of 0.5 m. Filming of the EE of the indicated copper wires made with the help of a digital camera s Canon M307E with its subsequent storyboard. The examination of the investigated TS after its electrothermal test indicates total sublimation of its copper from the interior of PET belt insulation cylindrical configuration of radio frequency coaxial cable РК 50-7-11.

Fig. 4. The view of the working table of the generator ГИТМ-10/350 with rigidly fixed to its massive steel electrodes split round copper conductor with cross-section S_1≈3.2 mm^2 of the TS of the RF coaxial cable РК 50-7-11 with a solid PET insulation of the length of 0.5 m and «plugged» with electrothermal tests its braided copper shield-up exposure to the aperiodic current pulse 15/335 μs of the artificial lightning amplitude of about I_{mL}≈85.6 кА ($U_{31\text{-}3}$≈16.5 кV; U_{34}≈4.2 кV)

Fig. 5. The initial stage of EE of the copper conductor with cross-section of S_1≈3.2 mm^2 of the TS of the RF coaxial cable РК 50-7-11 with a solid PET insulation of the length of 0.5 m in the high-current discharge circuit of the generator ГИТМ-10/350

Fig. 6 shows in enlarged form an end cutting of the TS of the RF coaxial cable РК 50-7-11 with solid PET insulation of length of 0.5 m after exposure to the test current pulse 17/310 μs with amplitude I_{mL}≈82.9 кА according to the oscillogram, shown in Fig. 7 and EE of its split round copper conductor cross-section of S_1≈3.2 mm^2. The average peak value of pulse current density in the exploding electrical copper conductor was in this case δ_{m1}≈I_{mL}/S_1≈25.9 кА/mm^2.

Fig. 6. View of the end cutting of the TS of the RF coaxial cable РК 50-7-11 with a solid PET insulation of the length of 0.5 m after passing on his split round copper conductor of the cross-section of S_1≈3.2 mm^2 of the test current impulse 17/310 μs by the artificial lightning from the generator ГИТМ-10/350 and its EE with complete sublimation of copper (I_{mL}≈82.9 кА; δ_{m1}≈I_{mL}/S_1≈25.9 кА/mm^2; τ_f≈17 μs; t_m≈28 μs; τ_p≈310 μs; J_L≈1.76·10^6 A^2·s; q_L≈37.9 C)

The calculated estimation for this electro-thermal case (I_{mL}≈82.9 кА; J_L≈1.76·10^6 A^2·s) of the maximum value of the critical density of the current pulse 17/310 μs of the artificial lightning ratio δ_{m1k}≈4.416·10^8·$I_{mL}/(J_L)^{1/2}$ [15] indicates that δ_{m1k}≈27,6 кА/mm^2. It can be concluded that for copper conductor cable brand РК 50-7-11 estimated value of the current density δ_{m1k}≈27.6 кА/mm^2 from its experienced values δ_{m1k}≈25.9 кА/mm^2 differs by about 6%.

We note that used in Fig. 3, 6 and 7, the value passed through the current-carrying parts of the TS wires and cables in the discharge circuit of the generator type ГИТМ-10/350 electric charge q_L was determined by the ratio q_L≈$k_L I_{mL}$(1.32τ_p+0.27t_m), where k_L is the normalizing factor for changing our experience in the range (1.092 – 1.112).

Fig. 8 captures the moment of preparation for electrothermal tests in high-current discharge circuit from the generator ГИТМ-10/350 of the TS of the wire ПНП 2×2,5 with PVC insulation of the length of 0.5 m, comprising two parallel connected to the massive steel electrodes desktop used high voltage pulse current solid round copper conductor of the cross-section of S_1≈5 mm^2.

Fig. 9 shows of the wire ПНП 2×2,5 with a PVC insulation, experienced the impact of its two parallel-connected to the discharge circuit of the generator type ГИТМ-10/350 solid round copper conductor of the total section of S_1≈5 mm^2 of the aperiodic current pulse 17/335 μs of the artificial lightning amplitude I_{mL}≈83.8 кА. The average peak value of pulse current density of large veins in the copper wires of the test in this case was equal to about δ_{m1}≈I_{mL}/S_1≈16.8 кА/mm^2.

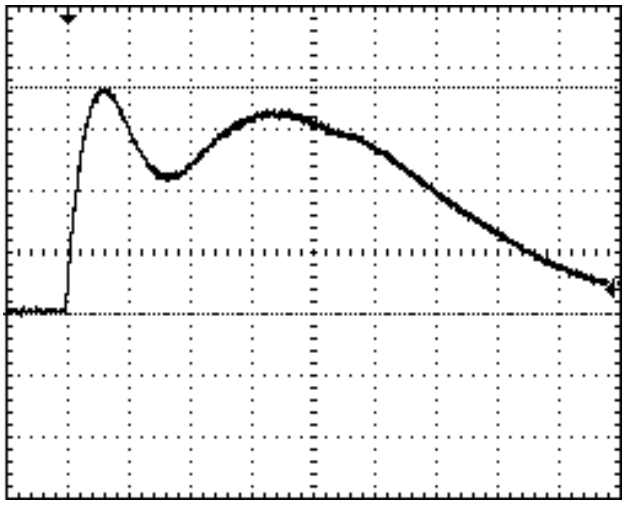

Fig. 7. Oscillogram of the aperiodic artificial lightning current pulse in the circuit of the generator ГИТМ-10/350in the discharge of its PCG-1 – PCG-4 to the electrically exploding digested a round copper conductor of the cross-section of S_1≈3.2 mm^2 of the RF coaxial cable РК 50-7-11 with a solid PET insulation of the length of 0.5 m without the use of tests at its copper-braided screen (I_{mL}≈82.9 кА; δ_{m1}≈I_{mL}/S_1≈ ≈25.9 кА/mm^2; τ_f≈17 μs; t_m≈28 μs; τ_p≈310 μs; J_L≈1.76·10^6 A^2·s; q_L≈37.9 C; $U_{31\text{-}3}$≈16.5 kV; U_{34}≈4.2 kV; vertical scale – 22.52 kA / cell; the horizontal scale – 50 ms / cell)

Fig. 8. View of the working table of the generator ГИТМ-10/350 with rigidly fixed on its massive steel electrodes with solid round copper conductors of the total section of S_1≈5 mm^2 of the TS of the wire ПНП 2×2,5 with a PVC insulation of the length of 0.5 m to the impact on them aperiodic current pulse 15/335 μs of the artificial lightning of amplitude of about I_{mL}≈85.6 кА ($U_{31\text{-}3}$≈16.5 kV; U_{34}≈4.2 kV)

Oscillogram acting on the TS of solid round copper wire conductors ПНП 2×2,5 with PVC insulation by the aperiodic pulse current artificial lightning in this case, virtually the same waveform shown in Fig. 3. Copper wire strands of weathered rendered them strong electro and electrodynamic effects, and its PVC insulation – no. In this case, there has been a local destruction of its PVC insulation because of its heat from flowing through the veins of copper wire considered aperiodic pulse 17/335 μs of the artificial lightning current amplitude I_{mL}≈83.8 кА.

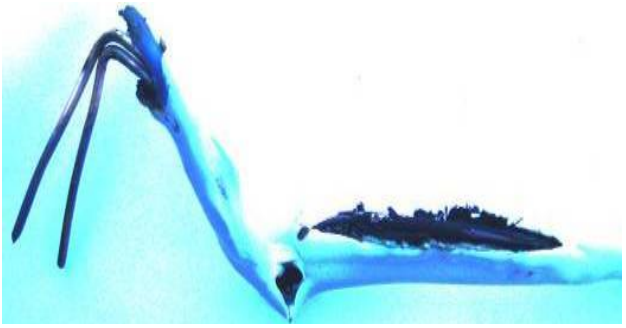

Fig. 9. View of the fragment of the TS of the wire ПНП 2×2,5 with PVC insulation with two parallel-connected in the discharge circuit of the generator ГИТМ-10/350 with round copper conductors of the total section of S_1≈5 mm^2 after flowing over them aperiodic pulse test current 17/335 μs of the artificial line lightning (I_{mL}≈83.8 кА; δ_{m1}≈I_{mL}/S_1≈16.8 кА/mm^2; τ_f≈17 μs; t_m≈28 μs; τ_p≈335 μs; J_L≈1.91·10^6 A^2·s; q_L≈41.2 C; $U_{31\text{-}3}$≈16.5 kV; U_{34}≈4.2 kV)

At considerable heating of the PVC insulation in this type of testing also indicates that the average maximum density pulse current δ_{m1}≈16.8 кА/mm^{2}copper wire ПНП 2×2,5 about 1.8 times the estimated maximum amplitude value allowable density used therein pulse current equal δ_{m1d}≈1.506·10^8·$I_{mL}/(J_L)^{1/2}$≈9.1 кА/mm^2 [15]. In addition, the estimation of the temperature θ_1 of the pulse Joule heating by flowing 17/335 μs pulse current copper wires of said wire on the settlement ratio (2) from [15] shows that she was about θ_1≈912 °C. Of course, what is the value of θ_1 is much higher than the maximum permissible short term temperature θ1k heating wires (cables) with PVC insulation, is about 150 °C [15, 16]. These data indirectly confirm the accuracy of the experiment we found the maximum allowable maximum density of 15/335 μs pulse current linear artificial lightning current carrying parts of copper wires (cables) with PET and PVC insulation, strength totaled about δ_{m1d}≈9 кА/mm^2.

Fig. 10 shows view of electrodes attached to the working table of the generator ГИТМ-10/350 of the TS of the continuous circular aluminum АППВнг2×6 conductor of the cross section S_1≈6 mm^2 of the wire with PVC insulation length of 0.5 m (second aluminum conductor wire was tested by us «muffled»).

Fig. 10. View of the working table of the generator ГИТМ-10/350 with rigidly fixed to its massive steel electrodes solid circular core section of the TS of the continuous circular aluminum АППВнг2×6 conductor of the cross section S_1≈6 mm^2 of the wire with PVC insulation length of 0.5 m before exposure by the aperiodic current pulse 15 / 335 μs of the artificial lightning of amplitude of about I_{mL}≈85.6 кА ($U_{31\text{-}3}$≈16.5 kV; U_{34}≈4.2 kV)

Fig. 11 oscillogram of the test pulse 17/265 μs of the artificial lightning current of amplitude I_{mL}≈83.8 кА flowing through electrically exploding in high-current discharge circuit of the generator ГИТМ-10/350 aluminum conductor with cross-section of S_1≈6 mm^2 of the АППВнг2×6 wire with PVC insulation δ_{m1}≈I_{mL}/S_1≈14 кА/mm^2) is presented.

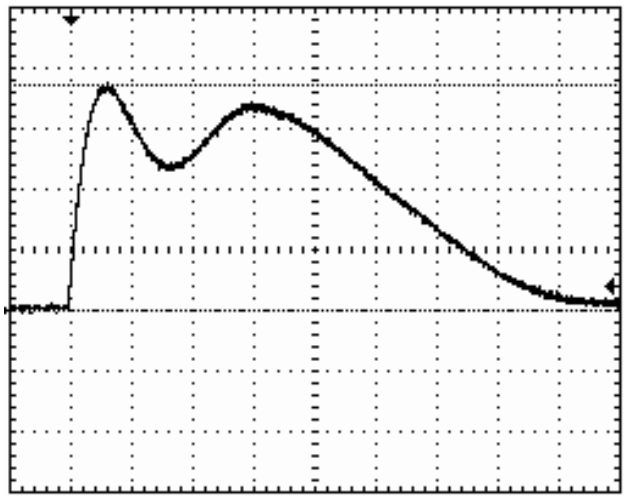

Fig. 11. Oscillogram of the aperiodic artificial lightning current pulse in the circuit of the generator ГИТМ-10/350 at the discharge of its PCG-1 – PCG-4 to electrically exploding solid circular aluminum conductor of the of cross-section S_1≈6 mm^2 of the АППВнг2×6 wire with PVC insulation of the length of 0.5 m (I_{mL}≈83.8 кА; δ_{m1}≈I_{mL}/S_1≈14 кА/mm^2; τ_f≈17 μs; t_m≈28 μs; τ_p≈265 μs; J_L≈1.58·10^6 A^2·s; q_L≈33.3 C; $U_{31\text{-}3}$≈16.5 kV; U_{34}≈4.2 kV; vertical scale – 22.52 kA / cell; the horizontal scale – 50 ms / cell)

Fig. 12 shows an intermediate stage of the EE of the tested in the generator ГИТМ-10/350 discharge circuit [7] of the aluminum cord of the cross-section of S_1≈6 mm^2 of the TS of the wire АППВнг2×6 with PVC insulation of the length of 0.5 m (I_{mL}≈83.8 кА; δ_{m1k}≈14 кА/mm^2).

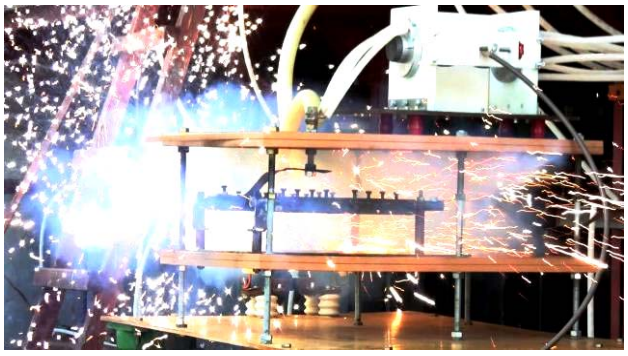

Fig. 12. An intermediate stage of EE of the continuous circular aluminum conductor of the cross-section of S_1≈6 mm^2 of the TS of АППВнг2×6 wire with PVC insulation of the length of 0.5 m in the high discharge circuit of the generator ГИТМ-10/350

The estimated maximum value of the critical density of the current pulse 17/265 μs of the artificial lightning for the aluminum core of the wire АППВнг2×6 with PVC insulation by the approximation ratio δ_{m1k}≈2.863·10^8·$I_{mL}/(J_L)^{1/2}$ [15] indicates that in this electrothermal case it is about 19 kA / mm^2. Obtained empirically for the aluminum core value δ_{m1k}≈14 кА/mm^2 is different from the calculated value δ_{m1k}≈19 кА/mm^2 approximately 26%. Made in further experiments on the generator ГИТМ-10/350 of the TS of АППВнг2×6 wire with PVC insulation length of 0.5 m and its two parallel electrodes are connected to the discharge circuit of said high-current pulse current generator artificial lightning aluminum conductors general section S_1≈12 mm^2 (Fig. 13) showed that the test was carried out at virtually survived have had a strong electro and electrodynamic effects.

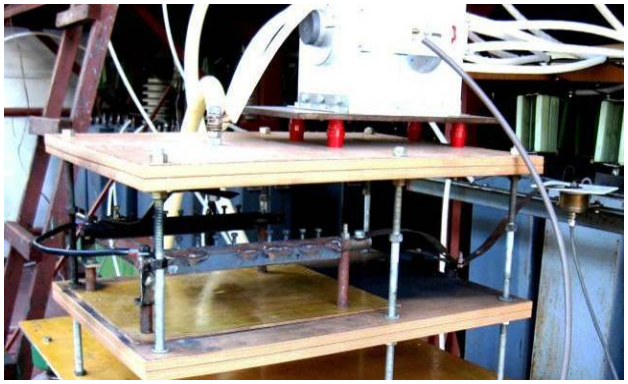

Fig. 13. View of the wire АППВнг2×6 with PVC insulation of the length of 0.5 m with its parallel electrodes connected to working table of the generator ГИТМ-10/350 with two aluminum cords of total section of S_1≈12 mm^2 to exposure by the pulse current 15/335 μs of the artificial lightning of amplitude I_{mL}≈83.8 кА (on the right the measurement shunt ШК-300 [7, 10] included in the high-current discharge circuit of the generator is clearly shown)

Oscillogram of the test pulse 15/335 μs of the simulated lightning current with amplitude I_{mL}≈83.8 кА in this case, virtually the same as the waveform shown earlier in Fig. 3. The peak pulse current density in the mentioned aluminum wire cord of the TS was about δ_{m1}≈I_{mL}/S_1≈6.9 кА/mm^2. Assessment of the maximum allowable limit of the current density in the TS of the aluminum wire of with PVC insulation at 15/335 μs pulse current on the settlement ratio δ_{m1d}≈0,975·10^8·$I_{mL}/(J_L)^{1/2}$ [15] leads us to the fact that in this case δ_{m1d} ≈5.9 кА/mm^2. We can see that obtained with electrothermal tests experienced the peak value of the maximum permissible density δ_{m1d}≈6.9 кА/mm^2 of the used pulse 15/335 μs pulse of current of the artificial lightning in the aluminum cord of the wire АППВнг2×6 with PVC insulation from the corresponding calculated value δ_{m1d} ≈5.9 кА/mm^2 is different by about 14%.

Conclusions.

1. For the first time experimentally it was found that when dealing with actual applications of lightning protection of electrical circuits of industrial electric power to a short stroke of lightning discharges in accordance with the requirements of a number of currently valid international and national standards must be assumed that the maximum allowable pulse density of 15/335 μs lightning current in the current-carrying parts of copper wires (cables) with PET and PVC insulation equals about δ_{m1d}≈9 кА/mm^2, and in the current-carrying parts of their aluminum wires (cables) with PVC insulation – δ_{m1d}≈6 кА/mm^2.

2. From the results experimental studies, carried out in the Institute «Molniya» of the NTU «KhPI» for lightning resistance of samples of cables and wires of the PF on a unique high-voltage current pulse generators of artificial lightning type ГИТМ-10/350 it is follow that the critical density of its impulse 15/335 μs of the current in the copper current-carrying parts of wires (cables) with PET and PVC insulation is about δ_{m1k}≈26 кА/mm^2 and for aluminum current-carrying parts of wires (cables) with PVC insulation – about δ_{m1k}≈14 кА/mm^2 . When reaching in copper (aluminum) cords (screens) of the wires and cables of the electrical circuits of the PF of such a density of the current pulse of lightning they will be subject to EE and failure.

3. Found experimental values of densities δ_{m1d} and δ_{m1k} of normalized according to the requirements of existing International and national Standards of 15/335 μs pulse current artificial lightning in the aluminum and copper live parts of cables and wires of electric circuits of thePF are the appropriate choice and reasonable installation with their view of similar products in electrical power circuits of the PF will help to improve their operational and fire safety in the active thunderstorm activity in a constantly environmental aspects of industrial electric power air atmosphere.

REFERENCES

1. IEC 62305-1: 2010 «Protection against lightning. Part 1: General principles». Geneva, IEC Publ., 2010.

2. IEC 62305-2: 2010 «Protection against lightning.− Part 2: Risk management». Geneva, IEC Publ., 2010.

3. IEC 62305-3: 2010 «Protection against lightning.− Part 3: Physical damage to structures and life hazard». Geneva, IEC Publ., 2010.

4. IEC 62305-4: 2010 «Protection against lightning.− Part 4: Electrical and electronic systems within structures». Geneva, IEC Publ., 2010.

5. *GOST R MEK 62305-1-2010. Nacional'nyj standart Rossijskoj Federacii «Menedzhment riska. Zashhita ot molnii. Chast' 1: Obshhie principy»* [GOST R IEC 62305-1-2010. National Standard of the Russian Federation. Risk management. Protection from lightning. Part 1: General principles]. Moscow, Standartinform Publ., 2011, 46 p. (Rus).

6. Deutsche Norm DIN EN 50164-1: 2008 (VDE 0185-2001). Blitzschutzbauteile. − Teil 1: Anforderungen an Verbindungsbauteile [German Norms DIN EN 50164-1: 2008 (VDE 0185-2001). Protecting from Lightning of Buildings and their Parts. Part 1: Requirements on Parts Buildings and of Connection]. Berlin, Publ. DS, 2008. 16 p. (Ger).

7. Baranov M.I., Koliushko G.M., Kravchenko V.I., Rudakov S.V. A powerful high-voltage generator of aperiodic impulses of current of artificial lightning with the peak-temporal parameters rated on an International Standard IEC 62305-1-2010. *Elektrotekhnika i elektromekhanika – Electrical engineering & electromechanics*, 2015, no.1, pp. 51-56. (Rus).

8. Berzan V.P., Gelikman B.Yu., Guraevsky M.N., Ermuratsky V.V., Kuchinsky G.S., Mezenin O.L., Nazarov N.I., Peregudova E.N., Rud' V.I., Sadovnikov A.I., Smirnov B.K., Stepina K.I. *Elektricheskie kondensatory i kondensatornye ustanovki. Spravochnik* [The electrical capacitors and condenser options. Directory]. Moscow, Energoatomizdat Publ., 1987, 656 p. (Rus).

9. Dashuk P.N., Zayents S.L., Komel'kov V.S., Kuchinskiy G.S., Nikolaevskaya N.N., Shkuropat P.I., Shneerson G.A. *Tehnika bol'shih impul'snyh tokov i magnitnyh polej* [Technique large pulsed currents and magnetic fields]. Moscow, Atomizdat Publ., 1970. 472 p. (Rus).

10. Baranov M.I., Koliushko G.M., Kravchenko V.I., Nedzelskyi O.S., Dnyschenko V.N. A current generator of the artificial lightning for full-scale tests of technical objects. *Pribory i tekhnika eksperimenta – Instruments and experimental techniques*, 2008, no.3, pp. 81-85. (Rus).

11. Baranov M.I. Selection and installation of high-voltage ceramic protective resistors in the charge-discharge circuit powerful capacitive energy storage. *Visnyk NTU «KhPI» – Bulletin of NTU «KhPI»*, 2014, no.50(1092), pp. 13-20. (Rus).

12. Baranov M.I., Koliushko G.M., Nedzel'skiy O.S., Plichko A.V., Ponuzhdaeva E.G. High voltage-controlled high-current spark gap with graphite electrodes RVGU-50. *Visnyk NTU «KhPI» – Bulletin of NTU «KhPI»*, 2014, no.50(1092), pp. 28-37. (Rus).

13. Baranov M.I., Koliushko G.M., Kravchenko V.I., Nedzel'skiy O.S. High-voltage high-current generator air gaps of the current artificial lightning. *Pribory i tekhnika eksperimenta – Instruments and experimental techniques*, 2008, no.6, pp. 58-62 (Rus).

14. Belorussov N.I., Saakjan A.E., Jakovleva A.I. *Elektricheskie kabeli, provoda i shnury. Spravochnik* [Electrical cables, wires

and cords. Directory]. Moscow, Energoatomizdat Publ., 1988. 536 p. (Rus).
15. Baranov M.I., Kravchenko V.I. Electrothermal resistance wire and cable to the aircraft to the striking action pulsed current lightning. *Elektrichestvo − Electricity*, 2013, no.10, pp. 7-15. (Rus).
16. Orlov I.N. *Elektrotehnicheskij spravochnik. Proizvodstvo i raspredelenie elektricheskoj energii. Tom 3, kn. 1* [Electrical Engineering Handbook. Production and distribution of electric energy. Vol. 3, book 1]. Moscow, Energoatomizdat Publ., 1988, 880 p. (Rus).

M.I. Baranov[1], *Doctor of Technical Science, Chief Researcher,*
S.V. Rudakov[2], *Candidate of Technical Science, Associate Professor,*
[1] Scientific-&-Research Planning-&-Design Institute «Molniya», National Technical University «Kharkiv Polytechnic Institute», 47, Shevchenko Str., Kharkiv, 61013, Ukraine.
phone +38 057 7076841, e-mail: eft@kpi.kharkov.ua
[2] National University of Civil Protection of Ukraine, 94, Chernyshevska Str., Kharkiv, 61023, Ukraine.
phone +38 057 7073438, e-mail: serg_73@i.ua

Received 11.09.2015

How to cite this article:
Baranov M.I., Rudakov S.V. Experimental investigations of electro-thermal resistibility of conductors and cables to action of rationed on the International Standard IEC 62305-1-2010 aperiodic impulse of current of artificial lightning. *Electrical engineering & electromechanics*, 2016, no.1, pp. 48-55. doi: 10.20998/2074-272X.2016.1.09.

UDC 621.311 **doi: 10.20998/2074-272X.2016.1.10**

D.A. Gapon, Ya.S. Bederak

GUARANTEEING THE TROUBLE-FREE OPERATION OF CAPACITOR BANKS IN POWER-SUPPLY SYSTEMS OF INDUSTRIAL ENTERPRISES

Purpose. ***The problem of resonance phenomena in power systems of industrial enterprises using capacitor banks for reactive power compensation was detected. Circuit of the capacitor banks tier to downshift main substation tires is present. But there is no common algorithm to calculate and avoid such trouble. The main goal of this article is to introduce some basics for power supply systems with possible resonant circuits engineering.*** ***Methodology.*** ***At the first step the data on the change of the current in the chemical company network when changing capacitor banks value are received. For these purposes the oscilloscope function of digital protection relay was used. Current data samples were analyzed by spectrum detection software. Most significant levels of the 3rd and 5th harmonics were achieved. Comparison of harmonic distortion levels with and without capacitor bank is given.*** ***Results.*** ***Achieved data allow making conclusion about overloading reasons of capacitor banks while higher harmonics currents presence. A voltage and current harmonious composition measuring in the absence of power quality analyzers using digital protection relay terminals or emergencies registers are proposed. The necessity of power quality monitoring near capacitor banks connections to avoid resonance phenomena (current and voltage resonance) in industrial power supply systems is proven. The control algorithm of capacitor banks to provide electromagnetic compatibility, while various modes of nonlinear load operation is given.*** ***Originality.*** ***Using of digital protection relay oscilloscoping for current resonant detection can allow to significally reduce time and cost of solution. Replacement parallel circuit comprising a branch and one active-inductive load to another branch network in the presence of higher harmonics source are proposed.*** ***Practical value.*** ***A sequence for measuring the levels of harmonic components at the connections of capacitor banks in the absence of specialized instruments is proposed. The algorithm to avoid possible resonance currents in the presence of condensing units is proposed.*** References 9, tables 2, figures 2.

Key words: **power supply system, resonance, capacitor bank, power quality, electromagnetic compatibility.**

В статье рассматривается проблема резонансных явлений в системах электроснабжения промышленных предприятий, использующих конденсаторные установки для компенсации реактивной мощности. Приведены данные по изменению токов 3-й и 5-й гармонических составляющих в сети химического предприятия при изменении мощности присоединенных конденсаторных установок. Предложен способ измерения качества электроэнергии при отсутствии анализаторов. Разработан алгоритм обеспечения электромагнитной совместимости на присоединениях конденсаторных установок. Библ. 9, табл. 2, рис. 2.

Ключевые слова: **система электроснабжения, резонанс, конденсаторные установки, качество электрической энергии, электромагнитная совместимость.**

Problem definition. In some cases in power-supply systems of industrial enterprises dangerous resonant phenomena can arise. For example, at simultaneous utilization of the smooth soft start device which includes a semiconductor converter and a capacitor bank, the failure resonant currents able to destroy the capacitor bank as well as the whole power supply-system were fixed [1]. Generally, we can speak that the phenomenon of the current resonance is inherent for power-supply systems to which nonlinear customers and devices of reactive power compensation are connected simultaneously. Trends of the modern electrical customers' development permit to speak that power and number of used semiconductor converters increase permanently. Devices of reactive power compensation including capacitor banks become more and more widely used. So, a task of the capacitor banks and, in general, power supply systems of industrial enterprises protection from resonant phenomena is actual. There is necessity to develop methods and techniques to improve electromagnetic compatibility of power supply systems of industrial enterprises.

Analysis of last investigations and publications. In [2] it is noted that resonance arising on the substation's buses results in sharp increase of the current, mainly by sharp increase of its harmonic components in the resonance circuit. In [3] it is determined that in the circuit including capacitor bank in one loop and active-inductive load in another one, voltage resonance in addition to current one can arise. A technique of the calculation of the resonant frequency in such a circuit is proposed in [4]. Ya.E. Shklyarskiy and A.N. Skamin have determined the dependence of the capacitor bank's overload factor on compensating devices' power, power of linear and nonlinear loads, spectra of current and voltage. Besides, assessment of the power grid's parameters at various conditions of arising of higher harmonics which guarantees the capacitor bank operation without overload is presented [5].

The goal of the paper: to develop a methodology of measurement of harmonic components on capacitor banks' connections and propose measures to prevent current resonance in power supply systems of industrial enterprises which include capacitor banks.

Main research material. Operational regulations for exploitation of consumers' electrical installations [6] recommend that on the medium voltage capacitor installations' connections on-line monitoring of the electrical energy quality parameters should be carried out, and on the low voltage capacitor installations' connections such measurements should be carried out periodically. To do it, it is necessary to use specialized analyzers of the electrical energy quality. A lot of world-wide manufacturers develop and produce such devices. However, they are very expensive, so utilization of such devices in power supply systems of industrial enterprises requires huge expenses. High price of electrical energy quality analyzers is determined mainly by utilization of high-technological elementary base that is necessary to guarantee high requirements for the measurement's

precision. However, the presence of the high accuracy is not principal to determine and analyze the resonance. So, in the case of the absence of specialized measurement devices it is possible to measure the voltage and current harmonic compositions by using microprocessor terminals of the relay protection or fault recorders which have the accuracy class 0.5 for current and voltage measurement. Mainly they have a function of the registration of current and voltage oscillograms at arbitrary time. However, it is necessary to note that some terminals of relay protection (for example, by Siemens) use preliminary signal processing by using an analog band filter to extract first harmonic. It is obvious that in this case information about presence and parameters of higher harmonics losses. Therefore, before the oscillograms registration it is necessary to be sure that the device is able to save necessary spectral components. Obtained data are converted in the COMTRADE format which is open and described in the free Standard permits to proceed information by using a wide spectra of computer codes. There are developments by Siemens, Aniger, Hartron, Uniti and other Companies. Most of codes permits to carry out computations of higher harmonic components of current and voltage.

One-line diagrams of the capacitor bank 6 kV No. 1, 2 are presented in Fig. 1, 2 respectively.

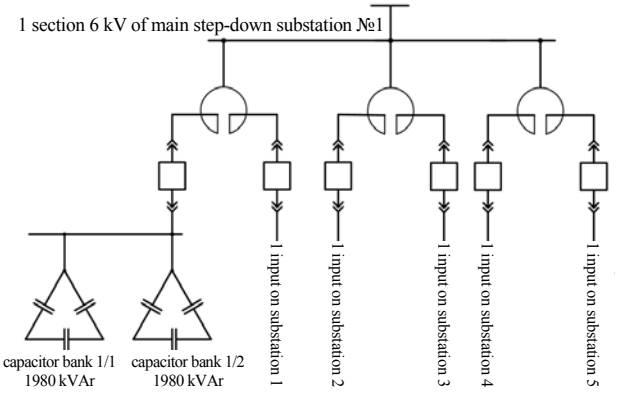

Fig. 1. One-line diagram of the capacitor bank No. 1 connection to buses 6 kV of the main step-down substation of the industrial enterprise

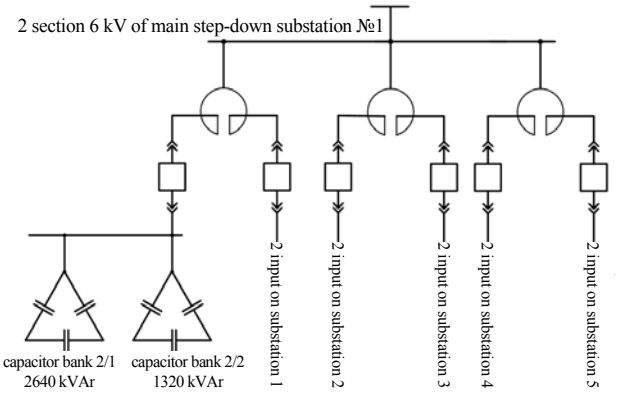

Fig. 2. One-line diagram of the capacitor bank No. 2 connection to buses 6 kV of the main step-down substation of the industrial enterprise

Measurement was carried out on the capacitor bank's connections of 6 kV which are used for the reactive power compensation on the bus section of the step-down substation at the chemical enterprise. In Tables 1, 2 values on *n*-th harmonic components on buses of the capacitor banks No. 1, 2 are respectively presented. It is necessary to note that in both case amplitude of the 3rd voltage harmonic does not exceed 4%, and amplitude of the 5th harmonic component isles than 5% that is permissible in the correspondence with the Sate Standard GOST 13109 – 97 [7].

Table 1

Values of coefficients of the *n*-th current harmonic component in percent before and after the capacitor bank No. 1 connection

Harmonic No.	After the capacitor unity connection (partial connection)		After the capacitor unity connection (full)	
	Current of the phase A	Current of the phase C	Current of the phase A	Current of the phase C
3	0.7	0.41	0.74	0.44
5	8.95	6.63	26.00	18.78

Results of measurements prove that at the change of the connected capacitor bank's power (see Table 1, 2) currents of higher harmonic components can arise essentially exceeding permissible normative values [8] resulting in the capacitor bank's overload. In the same time load on connections can vary widely. Depending on the value of the inductive load the current resonance at the frequency of one or another current harmonic can arise. To prevent such situations it is necessary to change the capacitor bank's connected capacity in such a way that the quiescent frequency of the oscillation circuit do not coincide with the frequency of one of any present higher harmonics. It is necessary to note that realization of such a adjustment requires huge investigations at the first stage of which it is necessary to collect a lot of information about resonant phenomena in power-supply systems of industrial enterprises. Therefore, there is an actual necessity to organize monitoring of the electrical energy quality on the capacitor bank's connections. Proceeding of data collected in such a way will permit to guarantee in the future electromagnetic compatibility of capacitor banks independently on the composition and character of the network loading [9].

Table 2

Values of coefficients of the *n*-th current harmonic component in percent before and after the capacitor bank No. 2 connection

Harmonic No.	After the capacitor unity connection (partial connection)		After the capacitor unity connection (full)	
	Current of the phase A	Current of the phase C		Current of the phase A
3	1.06	0.76	0.59	0.48
5	13.7	10.65	8.9	2.29

So, to prevent resonant phenomena on the capacitor banks' connections the following sequence of actions is proposed:

1. Measurement of parameters of electrical energy quality on the capacitor banks' connections.

1.1. Measurement of parameters of electrical energy quality on the capacitor banks' disconnected connections (determination of the voltage harmonic set).

1.2. Measurement of parameters of electrical energy quality on each stage of the capacitor bank from minimal power to full power of the capacitor bank.

2. Proceeding of the measurement results. Determination of the capacitor bank's power at which there is essential increase of the coefficient of the *n*-th current harmonic component.

3. Determination of sources of nonlinear distortions influencing on the electrical energy quality.

4. Building an equivalent circuit of the parallel one which includes the capacitor unit in one loop and active-inductive load in another one at presence a higher harmonics source in the network.

5. Calculation of the resonance frequency and the pass band in the circuit.

6. Decrease of the capacitor bank's power at the coincide of the resonance frequency in the circuit with the frequency of odd higher harmonics divisible by 50 Hz.

7. Check of the possibility of resonance phenomena arising in the mode of the nonlinear load start at presence of the higher harmonics source in the network that is connected for short time [1].

Conclusions.

1. It is propose to measure the voltage and current harmonics set струму at the absence of electrical energy quality analyzers by using microprocessor relay protection terminals or by fault recorders.

2. Necessity of organization of the electrical energy quality monitoring on the capacitor banks' connections to prevent resonance phenomena (current and voltage resonance) in power-supply systems of industrial enterprises is proved.

3. An algorithm to guarantee the electromagnetic compatibility on the capacitor banks' connections which can work in the mode of the nonlinear load start as well as in the mode of steady operation of electrical load.

REFERENCES

1. Gapon D.A., Bederak Ya.S. Features of the operation regime of the mains during soft start of powerful synchronous motors. *Promyshlennaia energetika – Industrial Power Engineering*, 2014, no.2, pp.27-30 (Rus).

2. Beliy V.B. Electromagnetic compatibility of power-supply systems' elements comprising reactive power compensation devices. *Vestnik Altaiskogo Gosudarstvennogo Agrarnogo Universiteta – Bulletin of the Altai State Agrarian University*, 2009, no.6, pp. 62-65 (Rus).

3. Bederak Y.S., Oleynik S.V., Shuliak A.A. Research of capacitors mode 6 (10) kV connected to branches of dual limiting current reactor. *Elektromekhanichni i enerhozberihaiuchi systemy – Electromechanical and energy saving systems*, 2013, vol.2, part 2, pp. 290-294. (Ukr).

4. Bederak Y.S. Electromagnetic compatibility of complex industrial power supply systems *Visnyk NTU «KhPI» – Bulletin of NTU «KhPI»*, 2014, no.60, pp. 37-45. (Ukr).

5. Shklyarskiy Ya.E., Skamin A.N. Industrial research into high harmonic influence on compensation devices. *Elektrotekhnika i elektromekhanika – Electrical engineering & electromechanics*, 2013, no.1, pp. 69-71 (Rus).

6. *Rules of technical operation of electrical consumers, approved by the Ministry of Fuel and Energy of Ukraine* 25.07.2006, no.258 (as amended by Order of the Ministry of Energy and Coal Industry of 13.02.2012 no.91) with amendments, approved by the Ministry of Energy and Coal Industry of Ukraine 11.16.2012 no.905. (Ukr).

7. *State Standard 13109-97. Electric Energy. Compatibility of technical equipment. Standards of quality of electric energy in power systems for general use. Interstate standard*. Moscow, IPC Standards Publ., 1998. 31 p. (Rus).

8. *IEEE Standard 519-1992. IEEE recommended practices and requirements for harmonic control in electrical power systems*. – 100 p.

9. Bederak Y.S. Current and voltage monitoring implementation with varying load character in the branches of twin reactor in the presence of higher harmonics sources. *Enerhetyka ta elektryfikatsiia – Energetic and electrification*, 2013, no.8, pp. 48-51 (Ukr).

Received 09.10.2015

D.A. Gapon[1]*, Candidate of Technical Science, Associate Professor,*
Ya.S. Bederak[2]*, Engineer,*
[1] National Technical University «Kharkiv Polytechnic Institute», 21, Frunze Str., Kharkiv, 61002, Ukraine.
phone +38 057 7076551, e-mail: dima12345ml@mail.ru
[2] PJSC «AZOT»,
72, Pervomayskaya Str., Cherkassy, 18014, Ukraine.
phone +38 047 2392979, e-mail: ei@uch.net

How to cite this article:
Gapon D.A., Bederak Ya.S. Guaranteeing the trouble-free operation of capacitor banks in power-supply systems of industrial enterprises. *Electrical engineering & electromechanics*, 2016, no.1, pp. 56-58. doi: 10.20998/2074-272X.2016.1.10.

UDC 621.331:621.311.4 **doi: 10.20998/2074-272X.2016.1.11**

O.O. Matusevych

METHODOLOGY OF DETERMINATION OF QUALITY INDEX OF MAINTENANCE SERVICE SYSTEM OF POWER EQUIPMENT OF TRACTION SUBSTATIONS

Purpose. *The purpose of this paper is development of methodology for definition of a quality system of maintenance and repair (M and P) power equipment of traction substations (TS) of electrified railways operating under conditions of uncertainty based on expert information.* ***Methodology.*** *The basic tenets of the theory of fuzzy sets and marks, linguistic and interval estimates of experts were applied to solve this problem.* ***Results.*** *Analysis of the existing diversity of approaches to development of modern methods of improvement of M and P allows us to conclude that the improvement in the quality of the system is achieved by solving individual problems increase the operational reliability of power equipment of traction substations in the following main interrelated areas. There are technical, economic and organizational. The basis of the quality evaluation system is initial data and expertise developed version of the document formalized quality evaluation of electrical equipment of traction substations by experts. The choice of determining the level of Quality service system based on the marks, linguistic and interval estimates of experts, which are reflected in quantitative and / or qualitative form was done. The possible options for expert data presentation and their corresponding quantitative methods of calculating the integral index of quality improvement system maintenance and P of traction substations were described. The methodology and the method of assessing the quality of system maintenance and P of TS allows quickly respond to changing operating conditions of power equipment of traction substations, and to determine the most effective strategies for maintenance of electrical and P TS under conditions of uncertainty functioning distance electricity.* ***Originality.*** *The method of a systematic approach to improve the quality of the system maintenance and P of power equipment of traction substation under conditions of uncertainty based on expert information was further developed. The author offers a number of options at first time. There are version of the document formalized quality evaluation of power equipment of traction substations by experts; expression to define the integral Quality systems maintenance and electrical power P TS, which is absent in the standard system maintenance and P; matrix of quality system with regard to steps (methods) and ways of increasing service quality electrical power control systems. This method makes it possible to conduct an expert assessment of the maintenance system and to predict and select the option rational system of quality improvement and maintenance of power equipment of traction substations considering not only technical but also organizational, legal, financial and economic measures.* ***Practical value.*** *Improvement on electrified railways of Ukraine quality management system maintenance and P TS will improve the efficiency and quality of maintenance of power equipment and provide TA prevent or reduce the severity of possible equipment failures. Based on the relationships matrix components as systems maintenance and electrical power P TP were formed expressions calculating quality indices of integrated systems with directions and stages for specific equipment and systems in general. It was determined that an increase in the quality and maintenance of electrical PR, the rate of change of the measured value at step k during operation is reduced while the standard deviation parameter is also reduced, and the probability of electrical TA increases.* References 8, tables 3.

Key words: **traction substation, technical condition of equipment, quality system of maintenance and repair, expert information, fuzzy sets, integral indicator of quality.**

Целью статьи является разработка методологии определения качества системы технического обслуживания и ремонта (ТО и Р) силового электрооборудования тяговых подстанций (ТП) электрифицированных железных дорог в условиях неопределенности эксплуатации на основе экспертной информации. ***Методика.*** *Для решения поставленной задачи применены основные положения теории нечетких множеств, а также бальных, лингвистических и интервальных оценок экспертов.* ***Результаты.*** *Анализ существующего многообразия подходов к разработке современных методов совершенствования системы ТО и Р позволяет сделать вывод, что решение проблемы повышения качества системы достигается путем решения индивидуальных задач повышения эксплуатационной надежности силового электрооборудования ТП в следующих основных взаимосвязанных направлениях: техническом, экономическом и организационном. В основу оценки качества системы положены начальные экспертные данные и разработан вариант формализированного документа оценки качества обслуживания электрооборудования ТП экспертами. Проведен выбор определения уровня показателя качества системы обслуживания на основе бальных, лингвистических и интервальных оценок экспертов, которые отображаются в количественной и/или качественной форме. Рассмотрены возможные варианты представления экспертных данных и соответствующие им методики расчета количественного интегрального показателя уровня повышения качества системы ТО и Р силового электрооборудования ТП. Разработанная методика и метод оценки качества системы ТО и Р ТП позволяет оперативно реагировать на изменения условий функционирования силового электрооборудования ТП, а также определять наиболее эффективные стратегии ТО и Р электрооборудования ТП в условиях неопределенности функционирования дистанции электроснабжения.* ***Научная новизна.*** *В статье получил дальнейшее развитие метод системного подхода по повышению качества функционирования системы ТО и Р силового электрооборудования ТП в условиях неопределенности на основе экспертной информации. В этом направлении автор впервые предлагает: вариант формализированного документа оценки качества обслуживания силового электрооборудования ТП экспертами; выражение для определения интегрального показателя качества системы ТО и Р силового электрооборудования ТП, которое отсутствует в стандартах системы ТО и Р; матрицу качества системы с учетом этапов (методов) и направлений повышения качества обслуживания силового электрооборудования ТП. Данный метод дает возможность проводить экспертную оценку состояния системы обслуживания, прогнозировать и выбирать рациональный вариант повышения качества системы ТО и Р силового электрооборудования ТП с учетом технических, организационно-правовых и финансово-экономических мероприятий.* ***Практическая значимость.***

Усовершенствование на электрифицированных железных дорогах Украины системы управления качеством ТО и Р ТП позволит повысить эффективность и качество системы технического обслуживания силового электрооборудования ТП, а также предупредить возникновение или снизить тяжесть возможных отказов оборудования. На основе взаимосвязей составляющих матрицы качества системы ТО и Р сформированы выражения для расчета интегральных показателей качества системы по направлениям и этапам для конкретного оборудования и системы в целом. Установлено, что при повышении качества ТО и Р электрооборудования скорость изменения измеряемого значения параметра x_i на i-м шаге во время эксплуатации уменьшается, при этом среднеквадратичное отклонение параметра σ также уменьшается, а вероятность P(t) безотказной работы электрооборудования ТП увеличивается. Библ. 8, табл. 3.

Ключевые слова: **тяговая подстанция, техническое состояние оборудования, качество системы технического обслуживания и ремонта, экспертная информация, нечеткие множества, интегральный показатель качества.**

State of the problems. Topicality. The quality of the system of the maintenance and repair (SMR) of power electrical equipment of traction substations (TS) of electrified railways can be evaluated by the set of different parameters (individual, group, integrated), each of which has a quantitative or qualitative character. Relations between indicators, by which the process of organizing and carrying out SMR of TS is described, have a complex structure. In general, some indicators can be expressed in terms of others who are on the same or different levels of service and model of the process of the equipment service and diagnostics. As the theory and practice of diagnosis show [1, 2], a very common approach to data analysis of the equipment diagnostics is the transition from a certain set of parameters (often single) which values can be easily measured (calculated) in their great quantity, to a small number of integrated indicators which are functionally related to the output ones. The main purpose of the transition from the single set of indicators to group ones, and the last ones to integral is getting the indicators characterizing the integral characteristics of the achieved quality of the SMR and/or its individual components. Evaluation of the SMR of the TS equipment is determined by the degree (fullness) of meeting requirements that apply to the SMR. To perform such an assessment it is necessary to make a formal definition of the task of transformation of quality indicators of the maintenance system components to integral ones.

Analysis of investigations. In the basis of the quality system evaluation we put initial expert data of definition of integrated indicator of the system quality. For the examination an expert group is established and recommendations for the examination are presented [3]. For the purpose of the examination for different types of equipment «the map of the object of examination» is prepared. For example, the author suggests a formalized version of a document of assessment by experts the quality of electrical maintenance of the TS electrical equipment (see Table. 1).

In expert investigations typically they use three types of questions – closed, open and semi-open. In answering closed questions it is possible to select answers only from options pre-defined by questionnaire compilers. In response to an open question the expert opinion in a free manner is presented. Semi-open questions occupy an intermediate position: in addition to the selection from options listed in the map of options estimation, it is possible to add own views and opinions.

Definition of the quality indicator's level of the SMR of the TS may be based on ballroom, linguistic and interval estimates of experts, which are expressed in quantitative and/or qualitative form [3-5]. Scale of the assessments conformity is given in Table. 2.

The task of the expert committee is to choose the optimal strategy of the SMR. There are two fundamentally different approaches to its solution [3].

The first approach is based on a comparison of existing SMR. For example, each of the experts selects the system according to their reasoning. Obtained from experts ordering (ranking) are processed by various mathematical methods to calculate the final opinion of an expert panel.

The second approach aims to compare the importance of various SMR quality parameters and build integrated quality indicator (rating assessment) by the help of which it is possible to order the considered SMR by quality (to calculate the system's rating).

In this case, for the processing the results of expert assessments and determining the resulting indicators of the improvement of the RMS quality it is possible to use additive, multiplicative or maximin resulting indicators [3, 6].

Additive indicator is the sum of weighted normalized partial indicators of the SMR quality improvement indicators (Π_q) and has the form

$$\Pi_q = \sum_{i=1}^{m} \alpha_i q_i , \qquad (1)$$

where α_i is the factor of the relative importance of the direction of the quality improvement of the SMR of the TS electrical equipment; q_i is the actual value of the requirements realization of improving the quality of the SMR of the TS electrical equipment; $0 \le \Pi_q \le 1$, $0 \le \alpha_i \le 1$, $\sum_{i=1}^{m} \alpha_i = 1$.

The higher Π_q, the more it affects the quality improvement of the system operation; $\sum_{i=1}^{m} \alpha_i q_i = 1$; $\alpha_i > 0$; $i = 1, m$.

Multiplicative indicator is produced by multiplying partial indicators taking into account their weight factors and has the form

$$\Pi_q = \prod_{i}^{m} q_i^{a_i} , \qquad (2)$$

where q_i and α_i have the same sense as in the additive indicator.

Table 1

Map of the quality assessment of the SMR of the TS electrical equipment

Components of steps (methods) of examination	Assessment variants	Assessment directions
1. The scientific significance of the adopted strategy of the SMR of the TS electrical equipment	1. Extremely high 2. Much 3. Not high 4. Uncertain (now) 5. Absent	Technical Economic Organizational
2. The practical significance of the adopted service strategy	1. Extremely high 2. Much 3. Not high 4. Uncertain (now) 5. Absent	
3. The scientific novelty, originality of the adopted service strategy	1. No analogues 2. There are no analogues in the country, there are abroad 3. There are no analogues abroad, there are in the country 4. There is evidence of some domestic and foreign analogues 5. Scientific novelty missing	
4. The methods and ways to achieve the goal of improving the quality of the SMR	1. New 2. Modern 3. Traditional 4. Obsolete 5. Inadequate	
5. The potential of executors of the SMR of the TS electrical equipment	1. Sufficient 2. The lack in the part of scientific support (experience) 3. Insufficient in terms of material and technical base 4. Lack of in terms of experience of working team personnel 5. Insufficient data to assess	
6. The term of the carrying out works of the SMR of the TS electrical equipment	1. Real 2. Overvalued 3. Reduced 4. The data sufficient to assess	
7. The cost of work (funding) of the SMR of the TS electrical equipment	1. Acceptable 2. Overstated 3. Dropped 4. The data sufficient to assess	
8. Recommendation on priority measures and works to improve the quality of the SMR of the TS electrical equipment	1. Events (work) of primary importance 2. Measures (work) of high importance 3. Measures (work) are of interest 4. Measures (work) are of negligible interest but deserve support if there are sufficient assets 5. Measures (work) do not deserve support	
9. Operation reliability increase of the TS power equipment	1. Very high 2. Significant 3. Low 4. Undefined (now) 5. Missing	
10. Check of the efficiency and quality of the SMR	1. Very high 2. Significant 3. Low 4. Undefined (now) 5. Missing	
Other……	……..	

Table 2

Scale of correspondence of scoring, linguistic and interval estimations

Scoring estimation	Linguistic estimation	Interval estimation
5 – Excellent	(B) Fully satisfies the requirements	0.9–1
4 – Good	(BC) Almost satisfies	0.7–0.9
3 – Satisfactory	(C) Satisfies mostly	0.5–0.7
2 – Poor	(HC) Not satisfying	0.3–0.5
1 – Completely unsatisfactory	(H) Fully not satisfying	0–0.3

Maximin indicator. In some cases it is quite difficult to substantiate or to apply the type of the resulting target function. In such cases, a possible simple way of solving the problem is to use the maximin indicator. In this case, the rule of choosing the optimal SMR of the TS has the form

$$\max(S \in M)\min(1 \le i \le m)\begin{Bmatrix} q_1^{a_1}(S),...,q_i^{a_i}(S), \\ ...,q_m^{a_m}(S) \end{Bmatrix}. \quad (3)$$

The maximin indicator of the SMR quality improvement guarantees the best (maximal) value of the worst (lowest) from partial quality indicators.

The material of the research. Scientific results obtaining. However, a large number of indicators of the requirements of improving the quality of the SMR of the Ts electrical equipment may cause loss of objectivity of determining the importance factors α_i. So, a promising way to solve this problem is to define the *integral indicator of quality* (I_q) of the SMR taking into account factors indicators importance by directions, methods and stages of the quality improvement of the SMR of the TS electrical equipment.

To determine the integral indicator of quality of the SMR of the TS electrical equipment taking into account the considered conditions and (1) the author firstly proposed the following expression:

$$I_q = \sum_{i=1}^{n}\alpha_i \cdot \sum_{k=1}^{m}\alpha_k \cdot \sum_{j=1}^{h}\alpha_j q_{ikj} = \sum_{i=1}^{n}\alpha_i \cdot q_i + \sum_{k=1}^{m}\alpha_k \cdot q_k + \sum_{j=1}^{h}\alpha_j \cdot q_j \quad (4)$$

where $\sum_{i=1}^{n}\alpha_i = 1$, $\sum_{k=1}^{m}\alpha_k = 1$, $\sum_{j=1}^{h}\alpha_j = 1$ are the factors of relatively importance of directions, methods and stages of the service system quality, respectively; q_{ikj} is the actual value of indicators of the SMR quality improvement level requirements realization for the TS electrical equipment by directions, methods and stages. Such a indicator of the SMR quality estimation is absent in the Standard [7].

Under the proposed elements of the definition of the integrated indicator of the SMR of the TS electrical equipment (4), we build a matrix of a system quality (see Table 3) taking into account steps (methods), directions to increase the service quality of the TS electrical equipment (see Table 1).

Based on the relationships of quality matrix components of the SMR given in Table 2 we form expressions for integrated system of system quality indicators by directions and stages for equipment (1, 2…*N*) and the system as a whole, according to the formulas (1) and (4):

1. $I_{q111} = q_{111}\cdot\alpha_{111}$ is the integral indicator of the SMR quality at the service of the *equipment 1* of the TS at the condition of the realization of the quality improvement requirements level by the stages 1 and technical direction

2. $I_{q22} = q_{221}\cdot\alpha_{221} + q_{222}\cdot\alpha_{222} + q_{223}\cdot\alpha_{223}$ is the integral indicator of the SMR quality at the service of the *equipment 2* of the TS at the condition of the realization of the quality improvement requirements level by the stage 2 and technical, economic and organization directions.

3. $I_{qN} = q_{1n1}\cdot\alpha_{1n1} + \ldots + q_{mn3}\cdot\alpha_{mn3}$ is the integral indicator of the SMR quality at the service of the *equipment N* of the TS at the condition of the realization of the quality improvement requirements level by the stages 1÷*M* and technical, economic and organization directions.

4. $I_{q.SMR} = I_{q1}\cdot\alpha_{eq.1} + I_{q2}\cdot\alpha_{eq.2} + \ldots + I_{яN} \times \alpha_{eq.N}$ is the integral indicator of the SMR quality at the service of the *equipment* 1÷*N* of the TS at the condition of the realization of the quality improvement requirements level by the stages 1÷*M* and technical, economic and organization directions.

Table 3

Quality matrix of the SMR of the TS electrical equipment

Stages of the quality improvement of the SMR of the TS	Equipment 1			Equipment 2			……	Equipment *N*		
	Directions of the quality improvement of the SMR of equipment 1			Directions of the quality improvement of the SMR of equipment 2			……	Directions of the quality improvement of the SMR of equipment *N*		
	010			*020*			……	*0n0*		
	Technical	Economic	Organizational	Technical	Economic	Organizational		Technical	Economic	Organizational
1. ***(100)***	I_q (111)	I_q (112)	I_q (113)	I_q (121)	I_q (122)	I_q (123)	……	I_q (1n1)	I_q (1n2)	I_q (1n3)
2. ***(200)***	I_q (211)	I_q (212)	I_q (213)	I_q (221)	I_q (222)	I_q (223)	……	I_q (2n1)	I_q (2n2)	I_q (2n3)
……	……	……	……	……	……	……	……	……	……	……
M. ***(M00)***	I_q (m11)	I_q (m12)	I_q (m13)	I_q (m21)	I_q (m22)	I_q (m23)	……	I_q (mn1)	I_q (mn2)	I_q (mn3)

It can be seen that in the correspondence with formed expressions it is possible to calculate integral quality indicators of the SMR at service:

- equipment $1 \div N$ of the TS by any direction and selected stage;
- equipment $1 \div N$ of the TS by all directions and selected stage;
- equipment $1 \div N$ of the TS by all directions and stages;
- SMR of the TS electrical equipment by all stages and directions – $111 \div mn3$ (see Table 1).

Let's consider possible variants of the expert data representation and corresponding techniques of the calculation of the quantitative integral indicator of the quality improvement level of the SMR of the TS power electrical equipment [3, 8]:

1. The degree of implementation of each requirement of the quality improvement of the SMR is defined as: the requirement fulfilled $q_i = 1$; the requirement is not fulfilled $q_i = 0$, $i = 1, m$. When the degree of fulfillment is determined by the importance of each requirement, integral index of quality assessment is estimated by expressions (1) and (4).

2. The degree of evaluation in assessing the requirements by point scale (see Table 2). For example, by the most popular five-point scale: $b_i = 5$ – excellent; $b_i = 4$ – good; $b_i = 3$ – satisfactory; $b_i = 2$ – unsatisfactory; $b_i = 1$ – completely unsatisfactory.

For estimation (prediction) of the quality of the SMR the scoring system is written as follows: excellent – the quality system fully meets the requirements; good – almost satisfying; satisfactorily – mainly satisfies; unsatisfactory – not pleased; completely unsatisfactory – is not fully satisfying.

When the degree of fulfillment of requirements for assessment under point scale is determined by the importance of each requirement a_j, then the index of the assessment the level of quality improvement of the SMR is determined by the formula

$$B_q = \sum_{j=1}^{m} a_j b_j , \qquad (5)$$

where $1 \le B_q \le 5$, $0 \le a_j \le 1$, $\sum_{j=1}^{m} a_j = 1$.

Very often at the point scale assessment of the level of requirements execution it is convenient to have the final assessment in a scale from 0 to 1 ($0 < I_q < 1$). In this connection, we will form the scale of matching: $B_q = I_q$, $b_j = q_j, j = 1, \overline{m}$.

The calculation of the integral indicator of the assessment the level of quality improvement of the SMR is performed in accordance with (1) and (4).

3. Calculation of the indicator of the SMR quality improvement by using the linguistic variable.

For example, linguistic variable «Quality indicator of the SMR» is defined on a universal set of options u_j; $i = 1, \overline{n}$. The level of the indicator will be assessed by term B, BC, C, NA, H presented in Table 2.

Let by the expert way the membership function of belonging of requirements for the SMR to a given level of quality $\mu(u_{ij})$ are obtained. Then, using the expressions (4), (5), the integral indicator of the quality of the SMR of electrical railways power supply can be obtained

$$B_q = \sum_{j=1}^{m} a_j \sum_{b_j=1}^{5} b_j \mu(u_i b_i) . \qquad (6)$$

Consider the problem of dependence of operational reliability of electrical power equipment of the TS on the SMR quality. The long experience of operating of the equipment of the TS confirms that the quality of the SMR influences on the reliability of the equipment as at the sudden failure and at a gradual accumulation of failures. In this regard, the overall probability of failure of equipment can be expressed as

$$P(t) = P_k(t) \cdot P_m(t) , \qquad (7)$$

where $P_k(t)$ is the probability of failure of electrical equipment of the TS, which is conditioned by the presence of elements of equipment failure which are sudden and can be removed to improve the quality of the SMR; $P_m(t)$ is the probability of failure of electrical equipment of the TS with the gradual accumulation of failures of equipment that can be prevented to improve the quality of the SMR by reducing the speed of the parameter that determines the operation ability of electrical equipment.

To calculate $P(t)$ in the first approximation it is possible to take the normal distribution law for the uptime operation assessment [2]

$$P(t) = \frac{1}{\sigma\sqrt{2\pi}} \int_0^{\infty} e^{-\frac{(x-\bar{x})^2}{2\sigma^2 dx}} , \qquad (8)$$

where σ is the root-mean-square deviation of the parameter; x is the measured value of the parameter; $\bar{x}$ is the average value of the parameter (mathematical expectation).

$$\bar{x} = \frac{\sum_{i=1}^{n} x_i}{n} , \qquad (9)$$

$$\sigma = \sqrt{\frac{\sum_{i=1}^{n} (x - \bar{x})^2}{n-1}} , \qquad (10)$$

where x_i is the measured value of the parameter at the i-th step; n is the number of measurements of the parameter.

Analysis of the obtained calculation expressions permits to suggest that at the decrease in the speed of change of the measured value x_i on the i-th step during operation by improving the quality of of the SMR of the TS electrical equipment the root-mean-square deviation of the parameter σ will also be reduced, and the probability $P(t)$ of failure-free operation f the TS electrical equipment will increase.

Conclusions. The developed technique and the method of assessing the quality of the SMR of the TS electrical equipment allow: to respond quickly to changes in operating conditions of electrical power equipment of the TS; to determine the most effective strategies of the SMR of the TS electrical equipment under uncertainty functioning of power supply distance; to set (simulate) the

various operating conditions of the equipment of the TS to select the optimal variant of service and achieve the required level of quality of the SMR; to check state of the improvement of the system; to determine the level of actual integrated indicator of the system quality.

In the paper the author firstly proposes: a formalized version of a document of the assessment of the quality of the electrical power equipment of the TS service by experts; an expression to determine the integral indicator of quality of the SMR of the power electrical equipment of the TS, which is absent in the Standard of the SMR; a matrix of the quality of the system based on stages (methods) and ways to increase service quality of electrical power control systems. This method allows you to perform expert assessment of the service system and predict and choose a rational option of the quality improvement of the SMR of the power electrical equipment of the TS taking into account not only technical but also organizational, legal, financial and economic measures.

REFERENCES

1. Rassalsky A.N., Sakhno A.A., Konogray S.P., Spitsa A.G., Guk A.A. The basic principles of continuous monitoring of high-voltage oil-filled electrical isolation condenser type under operating voltage. *Elektromekhanichni i enerhozberihaiuchi systemy – Electromechanical and energy saving systems,* 2009, no.2, pp. 53-55. (Rus).

2. Matusevych O.O. *Udoskonalennia metodolohii systemy tekhnichnoho obsluhovuvannia i remontu tiahovykh pidstantsii : monohrafiia* [Improving the system of maintenance and repair of traction substations: Monograph]. Dnipropetrovsk, Dnipropetrovsk National University of Railway Transport named after Academician V. Lazaryan Publ., 2015. 295 p. (Ukr).

3. Pankow L.A., Petrovsky A.M., Schneiderman N.V. *Organizatsiia ekspertizy i analiz ekspertnoi informatsii* [Organization of examination and analysis of expert information]. Moscow, Nauka Publ., 1984. 214 p. (Rus).

4. Kruglov V.V. *Nechetkaia logika i iskusstvennye seti* [Fuzzy logic and artificial networks]. Moscow, Fizmatlit Publ., 2001. 221 p. (Rus).

5. Borisov A.N., Krumberg O.A., Fedorov I.P. *Priniatie resheniia na osnove nechetkikh modelei: primery ispol'zovaniia* [Making a decision based on fuzzy models usage examples]. Riga, Znanie Publ., 1990. 184 p. (Rus).

6. Matusevych O.O. The method of reliability estimation of the automated control system functioning of traction power supply of electric transport. *Nauka ta prohres transportu. Visnyk Dnipropetrovskoho natsionalnoho universytetu zaliznychnoho transportu – Science and Transport Progress. Bulletin of Dnipropetrovsk National University of Railway Transport*, 2009, no.28, pp. 42-44. (Ukr).

7. *GOST 18322-78. Sistema tekhnicheskogo obsluzhivaniia i remonta tekhniki. Terminy i opredeleniia* [State Standart 18322-78. System maintenance and repair of equipment. Terms and definitions]. Moscow, Standartinform, 2007. 12 p. (Rus).

8. Matusevych O.O. Methods of improving the reliability of the control system traction power supply of electric transport based on an expert information. *Nauka ta prohres transportu. Visnyk Dnipropetrovskoho natsionalnoho universytetu zaliznychnoho transportu – Science and Transport Progress. Bulletin of Dnipropetrovsk National University of Railway Transport*, 2009, no.26, pp. 63-66. (Ukr).

Received 30.11.2015

O.O. Matusevych, Candidate of Technical Science, Associate Professor,
Dnipropetrovsk National University of Railway Transport named after academician V. Lazaryan,
2, Lazaryana Str., Dnipropetrovsk, 49069, Ukraine.
phone +38 067 6367851, e-mail: al_m0452@meta.ua

How to cite this article:
Matusevych O.O. Methodology of determination of quality index of maintenance service system of power equipment of traction substations. *Electrical engineering & electromechanics*, 2016, no.1, pp. 59-64. doi: 10.20998/2074-272X.2016.1.11.

UDC 621.315 **doi: 10.20998/2074-272X.2016.1.12**

A.N. Moroz, N.M. Cheremisin, V.V. Cherkashina, A.V. Kholod

NEURAL NETWORK MODELING IN PROBLEMS OF ELECTRICAL GRIDS MODES PREDICTION

Purpose. Forming a neuro-fuzzy network based on temperature monitoring of overhead transmission line for the prediction modes of the electrical network. Methodology. To predict the load capacity of the overhead line architecture provides the use of neuro-fuzzy network based on temperature monitoring of overhead line. The proposed neuro-fuzzy network has a four-layer architecture with direct transmission of information. To create a full mesh network architecture based on hybrid neural elements with power estimation accuracy of the following two stages of the procedure: - in the first stage a core network (without power estimation accuracy) is generated; - in the second stage architecture and network parameters are fixed obtained during the first stage, and it is added to the block estimation accuracy, the input signals which are all input, internal and output signals of the core network, as well as additional input signals. Results. Formed neuro-fuzzy network based on temperature monitoring of overhead line. Originality. A distinctive feature of the proposed network is the ability to process information specified in the different scales of measurement, and high performance for prediction modes mains. Practical value. The monitoring system will become a tool parameter is measuring the temperature of the wire, which will, based on a retrospective analysis of the accumulated information on the parameters to predict the thermal resistance of the HV line and as a result carry out the calculation of load capacity in real time. References 10, figures 1.

Key words: **electric grid, neural grid, neuro-fuzzy grid, temperature monitoring of overhead transmission line, electric grid modes prediction.**

В статье сформирована нейро-фаззи сеть с учетом температурного мониторинга воздушной линии. Отличительной особенностью, предложенной сети, являются возможность обработки информации, заданной в разных шкалах измерения, и высокое быстродействие для прогнозирования режимов работы электрической сети. Библ. 10, рис. 1.

Ключевые слова: **электрическая сеть, нейросеть, нейро-фаззи сеть, температурный мониторинг воздушной линии, прогнозирование режимов работы электрической сети.**

Introduction. An important factor in the operation of electrical networks (EN), is an increase in load and the aging power grid equipment, which is typical for most industrialized countries. The capacity of the EN is reduced over time due to branching and complexity of network configuration. This fact increases the burden of overhead transmission lines (OL) as the backbone and distribution ones. The lack of information about the real parameters of the OL forces to use close to reality calculations of allowable power network modes. In most cases, they do not correspond to the actual operating conditions of networks, which leads to a significant reduction in transit overflows of power and overload of EN elements.

To eliminate unacceptable overload of EN elements measures of emergency control are provided. Devices of OL automatic overload limiting are designed for emergency control, which includes: EN configuration change, off of parts of the electricity consumers which reliability category allows a break of power supply, disconnect the OL.

The main requirement for such devices is the selectivity of action, i.e. automatic should only act at inadmissible modes of operation, without limiting the EN capacity. Prediction of the EN capacity is possible on the basis of real and stored information on its parameters.

Analysis of recent publications. As the analysis of the scientific information sources shown, the problems of predicting energy consumption are solved almost by all the institutions associated with the production and its distribution. To solve these problems traditional forecasting methods (regression, correlation, spectral analysis Box-Jenkins approach, exponential smoothing, adaptive predictors, etc.), as well as more advanced approaches based on data mining – Data Mining [1] are used.

The advantage of the traditional approaches is to ease the use of predictive models and the availability of affordable software. However, due to the fact that the link between energy consumption and its underlying causes are often complex and non-linear, in the framework of these approaches to achieve acceptable accuracy predictions is not always possible [2].

Significant difficulties in using computational intelligence systems occur when a part of the processed information is not given in the quantitative but ordinal or nominal scales. Already traditional neuro- and neuro-fuzzy networks are ill-suited to the kind of information processing «bad, normal, good weather», «strong or weak wind», «cloudy – foggy – frosty», etc. [3].

In connection with this the synthesis of a predictive neuro-fuzzy network able to perceive the data in different scales and its training algorithm, which has a high rate of convergence and the ability to process information as it becomes available in real time are proposed [4].

As an effective alternative an approach based on the application of the methods of computational intelligence and, above all, artificial neural networks and fuzzy inference systems can serve. The effectiveness of these systems is linked with their universal approximating capabilities and ability to learn directly in the prediction process.

Today, these techniques have proven their effectiveness in solving a wide range of problems associated with forecasting in the power industry [5-7].

Methods for forecasting the EN electricity load, whose architecture is based on a hybrid of neural elements with estimation accuracy block is largely allows to obtain results as close to the real data. However, taking into account the significant impact of environmental conditions (wind speed and direction, ambient temperature, etc.) on the OL capacity, there is a need in saturation of quantitative and ordinal variables of the hidden layer for a more reliable forecast of the EN permissible mode [7-9].

The OL parameters monitoring system will become a tool for measuring the temperature of the wire, which will, based on a retrospective analysis of the stored information on the OL parameters to predict the thermal resistance of the OL and as a result to carry out the calculation of the permissible load capacity in real time.

The goal of the paper is to form a neuro-fuzzy network based on temperature monitoring of overhead transmission line for the prediction of the electrical network modes.

Main materials of investigation. To predict the OL permissible load capacity the use of the architecture of neuro-fuzzy network taking into account the temperature monitoring of the OL is proposed.

The proposed neuro-fuzzy network has a four-layer architecture with direct transmission of information. To create a fully connected mesh network architecture based on hybrid neural elements with estimation accuracy block the following two stages of the procedure are carried out:

- at the first stage by the main network (without estimation accuracy block) is generated;
- at the second stage architecture and network parameters obtained during the first stage are fixed, and to it the estimation accuracy block is added, the inputs of which are all input, internal and output signals of the main network, and additional input signals (if necessary).

From the zero-th layer the information is supplied to the first hidden layer delay and fuzzification of the input signals. In this layer the history of the predicted signal is formed, as well as the membership function of factors that are given in different scales of measurement. From the output of this layer information in digital form is supplied to the second and third hidden layers, which are formed from the same type of elementary Rosenblatt neurons. The output layer is formed by a single neuron with non-linear activation function, on the output of which the predicted signal is formed [9, 10].

Adding the accuracy estimation block significantly expands the operational capabilities of the network through the addition to point approximations estimations of their expected accuracy, which reduces the level of uncertainty in the process of further decision-making.

On the input of the first hidden layer the following information is fed:

- quantitative variables:

– the current value of the predicted signal $y(k)$ (here k = 0, 1, 2, ..., N have the meaning of the current discrete time, N is the length of the sample);

– air temperature;

- ordinal variables:

– relative humidity in the form of «low – medium – high»;

– the wind speed in the form of «calm – weak – strong – Hurricane»;

– cloudiness in the form of «clear – variable – dense»;

– the number of hour of the day: 0, 1, 2, ..., 23;

– day of the week in the form of «Monday – Tuesday – ... – Sunday»;

- nominal variables:

– the type of the day in the form of «working – holiday – a holiday – a regional holiday – ported off – the transferred working»;

– the type of weather in the form of «rain – fog – rain – snow».

Variables are precoded in the interval [0, 1] as follows:

$$\tilde{x}_l = \frac{\hat{x}_l - \hat{x}_{l\min}}{\hat{x}_{l\max} - \hat{x}_{l\min}}, \quad (1)$$

$$\hat{x}_l = \hat{x}_{l\max}\tilde{x}_l - \hat{x}_{l\min}\left(\tilde{x}_l - 1\right), \quad (2)$$

where $\hat{x}_l$ is the value of the i-th input variable in the initial measurement scale: MW·h, °C; $\tilde{x}_l$ is the coded value of the l-th input variable; $\hat{x}_{l\min}$, $\hat{x}_{l\max}$ are the minimal and maximal values of the l-th input variable in the initial scale.

Further, in the first hidden layer by using the delay elements z^{-1} the background predicted signal is formed as $y(k–1)$, $y(k–2)$, $y(k–24)$, $y(k–48)$, $y(k–168)$, $y(k–336)$, which is fed to the second hidden layer as a $x_1(k)$, $x_2(k)$, $x_3(k)$, $x_4(k)$, $x_5(k)$, $x_6(k)$, and depending on the horizon of anticipation and other delay values different from the above can be used [8-10].

Later in the same layer fuzzification of the air temperature signals, number of the hour of a day, relative humidity, wind speed, cloud cover, and day of the week using the triangular membership functions uniformly distributed in the range [0, 1] which have the following form is made:

$$\mu_{l1} = \frac{c_{l2} - \tilde{x}_l}{c_{l2}}, \quad \tilde{x}_l \in \left[0, c_{l2}\right], \quad (3)$$

$$\mu_{li} = \begin{cases} \dfrac{\tilde{x}_l - c_{l,i-1}}{c_{li} - c_{l,i-1}}, & \tilde{x}_l \in \left[c_{l,i-1}, c_{li}\right], \\ \dfrac{c_{l,i+1} - \tilde{x}_l}{c_{l,i+1} - c_{li}}, & \tilde{x}_l \in \left[c_{li}, c_{l,i+1}\right], \\ i = 2,..., p_l - 1, \end{cases} \quad (4)$$

$$\mu_{p_l i} = \frac{\tilde{x}_l - c_{l,p_l-1}}{1 - c_{l,p_l-1}}, \quad \tilde{x}_l \in \left[c_{l,p_l-1}, 1\right], \quad (5)$$

where c_{li} is the placement of the centre of the i-th function of the l-th variable membership, p_l is the number of functions of the l-th variable membership.

The architecture of the predictive neuro-fuzzy network taking into account the parameters of the OL wire is shown in Fig. 1.

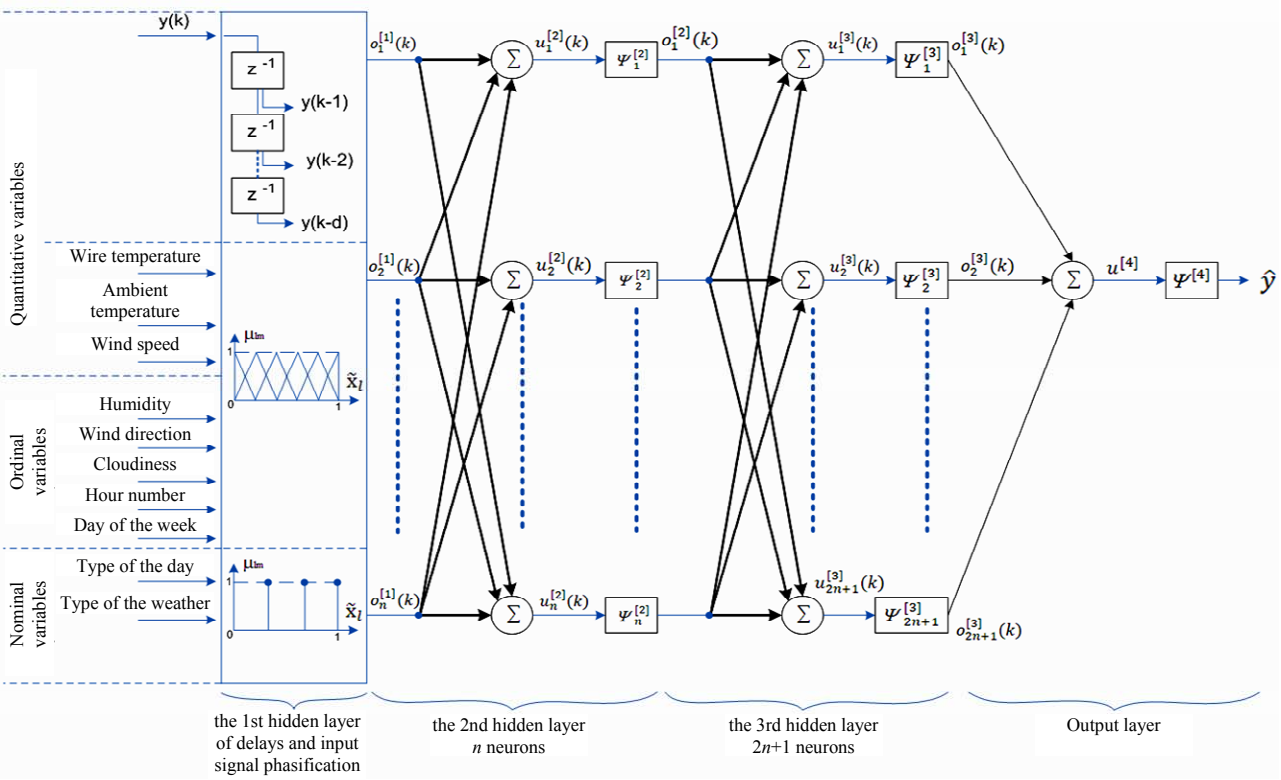

Fig. 1. Architecture of the predictive multilayer neuro-fuzzy network

As a result of processing of the original data in the first hidden layer a set of output signals $o_1^{[1]}$, $o_2^{[1]}$,…, $o_n^{[1]}$ is formed which are then fed to the second hidden layer in the form of the $(n+1)\times 1$-vector

$$x^{[2]} = \left(1, o_1^{[1]}, o_2^{[1]}, ..., o_n^{[1]}\right)^T, \quad (6)$$

where the unit component needed to assess the displacement of each neurons of the subsequent layers.

The second hidden layer of the proposed neuro-fuzzy network has n neurons of the same type with nonlinear sigmoidal activation functions $\psi_j^{[2]}$, $j = 1, 2, \ldots, n$ and contains $n(n+1)$ adjustable synaptic weights $w_{ji}^{[2]}$. The output of the j-th neuron of the second hidden layer has the form

$$o_j^{[2]} = \psi_j^{[2]}\left(u_j^{[2]}\right) = \psi_j^{[2]}\left(\sum_{i=0}^{n} w_{ji}^{[2]} x_i^{[2]}\right), \quad (7)$$

where $w_{j0}^{[2]} \equiv \theta_j^{[2]}$ is the level of the j-th neuron displacement, and the output signal of the layer:

$$o^{[2]} = \Psi^{[2]}\left(W^{[2]} x^{[2]}\right), \quad (8)$$

where $o^{[2]}$–$(n\times 1)$ is the vector signal transmitted to the third hidden layer in the form $x^{[3]} = (1, o^{[2]T})^T$, $\Psi^{[2]} = \mathrm{diag}\{\psi_j^{[2]}\}$ – $(n\times n)$ is the matrix activation function, $W^{[2]}$ – $n\times(n+1)$ is the adjustable matrix of synaptic weights.

The third hidden layer contains $2n+1$ neurons and generates signals in the form

$$o_j^{[3]} = \psi_j^{[3]}\left(u_j^{[3]}\right) = \psi_j^{[3]}\left(\sum_{i=0}^{n} w_{ji}^{[3]} x_i^{[3]}\right), \quad (9)$$

$$o^{[3]} = \Psi^{[3]}\left(W^{[3]} x^{[3]}\right), \quad (10)$$

where $\Psi^{[3]} = \mathrm{diag}\{\psi_j^{[3]}\}$ – $((2n+1)\times(2n+1))$ is the matrix activation function, $W^{[3]}$ – $((2n+1)\times(n+1))$ is the matrix of adjustable synaptic weights, $o^{[3]}$–$((2n+1)\times 1)$ is the vector signal transmitted to the output layer in the form

$$x^{[4]} = \left(1, o^{[3]T}\right)^T.$$

The output layer of the network is formed by a single neuron, forming a scalar signal of the forecast

$$\hat{y} = \psi^{[4]}\left(u^{[4]}\right) = \psi^{[4]}\left(\sum_{i=0}^{2n+1} w_i^{[4]} x_i^{[4]}\right) = \psi^{[4]}\left(w^{[4]T} x^{[4]}\right), \quad (11)$$

where $w^{[4]}$–((2n+2)×1) is the vector of adjustable synaptic weights.

Combining expressions (9-11), the transfer function of the whole network has the form:

$$\hat{y} = \psi^{[4]}\left(w^{[4]T} \Psi^{[3]}\left(W^{[3]} \Psi^{[2]}\left(W^{[2]} x^{[2]}\right)\right)\right). \quad (12)$$

The proposed in the paper approach provides high accuracy in forecasting at the conditions of the climate variability and stochastic input data for the prediction of the set of interrelated time series describing the consumption of electric energy within the several regions of the same territory which are included to the unified energy system.

Conclusions. The neuro-fuzzy network based on temperature monitoring of the overhead line is formed. A distinctive feature of the proposed network is the ability to process information specified in the different scales of measurement, and high performance for prediction modes of an electrical network.

REFERENCES

1. Naumov A.N., Vendrov A.M., Ivanov V.K. *Sistemy upravleniia bazami dannykh i znanii* [Database management systems and knowledge]. Moscow, Finansy i statistika Publ., 1991. 352 p. (Rus).

2. Kenneth C. Sevcik. Priority scheduling disciplines in queueing network models of computer systems. *In Proceedings of IFIP Congress'77*. August 8-12, 1977, Toronto, Canada, pp. 565-570.

3. V. Mainkar, K.S. Trivedi. Approximate analysis of priority scheduling systems using stochastic reward nets. *In Proceedings of the 13th International Conference on Distributed Computing Systems ICDCS'93*. May 1993, Pittsburgh, PA, USA, pp. 466-473. doi:10.1109/icdcs.1993.287678.

4. Leonard Kleinrock. *Queueing Systems. Volume 8: Computer Applications*. John Wiley and Sons, New York, USA, 1976.

5. Popov S.V., Cheremisin M.M., Parkhomenko O.V., Shkuro K.A. Neural network method for predicting accidents due to formation of ice on power lines overhead. *Visnyk Vinnytskoho politekhnichnoho instytutu – Visnyk of Vinnytsia Politechnical Institute*, 2012, no.1, pp.161-163. (Ukr).

6. Popov S.V., Shkuro K.A., Cheremisin N.M., Parkhomenko O.V. A hybrid method of predicting ice load on power lines overhead. *Enerhetyka ta elektryfikatsiia – Energetic and electrification*, 2013, no.5, pp. 33-38. (Rus).

7. Kruglov V.V. Methods of forecasting multivariate time series. *Pribory i sistemy. Upravlenie, kontrol', diagnostika – Devices and systems. Management, monitoring, diagnostics*, 2005, no.2, pp. 62-66. (Rus).

8. Popov S.V., Shkuro K.A. Evolutionary neuro-fuzzy network based on hybrid neural elements. *17 mizhn. konf. z avtomatychnoho upravlinnia «Avtomatyka-2010». Tezy dopovidei* [Proceedings of 17th Int. Conf. of Automatic Control «Automation 2010»]. Kharkiv (Ukraine), 2010, vol.2, pp. 193-194. (Rus).

9. Popov S.V. Specialized architecture of artificial neural networks based on hybrid neural elements. *Zbirnyk naukovykh prats Natsionalnoho hirnychoho universytetu – The collection of scientific works of National Mining University*, 2009, vol.2, no.33, pp. 76-82.

10. Titov N.N. *Povyshenie nadezhnosti i kachestva funktsionirovaniia avtomatizirovannykh sistem dispetcherskogo upravleniia elektroenergeticheskimi sistemami* [Improving the reliability and quality of the functioning of the automated systems of dispatching management of power systems]. Kharkov, Fakt Publ., 2013. 200 p. (Rus).

Received 20.10.2015

A.N. Moroz[1]*, Doctor of Technical Science, Professor,*
N.M. Cheremisin[1]*, Candidate of Technical Science, Professor,*
V.V. Cherkashina[2]*, Candidate of Technical Science, Associate Professor,*
A.V. Kholod [3]*, Engineer,*
[1] Kharkiv Petro Vasylenko National Technical University of Agriculture,
19, Engelsa Str., Kharkiv, 61052, Ukraine.
e-mail: moroz-fekt@inbox.ru, cheremisin.energy@rambler.ru
[2] National Technical University «Kharkiv Polytechnic Institute»,
21, Frunze Str., Kharkiv, 61002, Ukraine.
e-mail: cherk34@rambler.ru
[3] Company «ELAKS»,
1, build. 12, Ac. Proskura Str., Kharkiv, 61085, Ukraine.
e-mail: underholod@mail.ru

How to cite this article:
Moroz A.N., Cheremisin N.M., Cherkashina V.V., Kholod A.V. Neural network modeling in problems of electrical grids modes prediction. *Electrical engineering & electromechanics*, 2016, no.1, pp. 65-68. doi: 10.20998/2074-272X.2016.1.12.

UDC 621.31 **doi: 10.20998/2074-272X.2016.1.13**

Iu.A. Sirotin, T.S. Ierusalimova

INSTANTANEOUS AND INTEGRAL POWER EQUATIONS OF NONSINUSOIDAL 3-PHASE PROCESSES

Purpose. *To identify the mathematical relationship between the instantaneous powers (classical and vectorial) and integral powers in non-sinusoidal mode and to get complex form of instantaneous powers in 3-phase 4-wire power supply in terms of the spectral approach.* ***Methodology.*** *We have applied the vector approach with one voice allows you to analyze the energy characteristics of 3-phase power supply circuits (for 4-wire and 3-wire circuits) in sinusoidal and non–sinusoidal mode, both the time domain and frequency domain. We have used 3-dimensional representation of the energy waveforms with the complex multi-dimensional Fourier series.* ***Results.*** *For 4-wire network with a non-sinusoidal (regardless of their symmetry) processes, we have developed the mathematical model one-dimensional representations of the complex form for the active (scalar) instantaneous power (IP) and 3-dimensional form (inactive) vectorial IP. It is possible to obtain two dual integral power equations for complex scalar and vector integrated power of non-sinusoidal modes. The power equations generalize generalizes the equations of sinusoidal modes for 4-wire network.* ***Originality.*** *In addition to the classification of energy local regimes in the time domain for the first time we spent the classification of non-sinusoidal modes in the spectral region and showed the value and importance of the classification of regimes based on the instantaneous powers.* ***Practical value.*** *The practical value the obtained equations is the possibility of their use for improving the quality of electricity supply and the quality electricity consumption.* References 3, figures 3.

Key words: **three-phase circuit, classical instantaneous power, vector instantaneous power, complex 3-dimensional Fourier series, active and reactive power, complex vector power, apparent power, complex pulsation power, power equation, unbalanced mode, non-sinusoidal mode, 3-phasor.**

Для 3– фазной схемы электроснабжения рассмотрены несинусоидальные режимы, классифицируемые скалярной и векторной мгновенными мощностями (ММ). В рамках временного и спектрального подходов теории мощности получены комплексные формы активной (скалярной) ММ и (неактивной) векторной ММ. Для 4– проводной сети получены уравнения мощности комплексных скалярных и комплексных векторных мощностей несинусоидальных режимов. Уравнения мощностей обобщают соответствующие уравнения синусоидальных несимметричных режимов в 4- проводной сети. Библ. 3, рис. 3.

Ключевые слова: **трехфазная цепь, классическая мгновенная мощность, векторная мгновенная мощность, комплексный 3-мерный ряд Фурье, активная и реактивная мощность, комплексная векторная мощность, кажущаяся мощность, комплексная мощность, уравнение мощности, несбалансированный режим, несинусоидальный режим, трехмерный комплексный коэффициент.**

Introduction. Non-ideal (active-reactive, nonsymmetrical and nonlinear) load consumes not only electrical energy (EE) of active power but and EE of non-active components of apparent power (AP). For a number of such loads, consumption of EE of non-active components is caused by technological reasons and guarantees a long-term normal mode of the non-ideal (distorting) load operation. Non-active components of the AP cause additional losses in the power network making worse the power supply quality but they is not accounted and rested of.

An effective solution of the problem of the losses decrease and the EE account precision's increase is joint utilization of compensating devices (CD) and EE accounting tools. Existing accounting tools measure EE caused by the symmetry and linearity of the load's elements. Non-active TP components caused by the non-symmetry and nonlinearity of active-reactive load's element are not measured and accounted. Compensation, measurement and account of AP components are coupled, supplementing each other problems which from different economical points of view solve a problem of the effective EE consumption and should be solved in the frame of the general power theory (PT) at real conditions of failure of the symmetry and the sinusoidality of the supply and consumption mode.

Problem definition. Increasing theoretical and practical interest for the PT definitions, interpretations of the reactive power conception interpretations, physical sense search, ambiguity of the apparent power determination in multiphase systems, the problem difficulty have been led to the creation of various PT «schools» (partial bibliography is presented in [1]). For non-sinusoidal multiphase processes two alternative approaches of investigation and analysis of the PT concepts are used: spectral (Budeanu, Quade, Pukhov, Emanuel, Czarnecki, Shidlovsky, Kuznetsov, Lev-Ari and Stanković, etc.) and temporar (Buchholz, Fryze, Depenbrock, Demirchan, Maevsky, Nabae and Akagi, Willems, Watanabe and Aredes, Tolber, Tonkal and Novoseltsev, etc.).

The temporal method of the analysis is based on a special expansion of the 3-phase current on orthogonal components. One of components of such a special expansion determines the active current which after the compensation remains in the source's network and guarantees supply of EE of active power. Temporal method used two approaches to the 3-phase processes investigation. The first approach considers 3-phase processes as 3D curves on the averaging interval, is connected with generalization on the multiphase processes of the Fryze method and uses integral powers (IntP). The second one is based on instantaneous energetic characteristics: classical (scalar) instantaneous power (IP) and new vectorial IP (a cross-vector theory). This approach has a practical value and resulted in the development of so-called active filters. However, even for the sinusoidal mode mathematical connections between new IP and classical integral powers of the spectral approach did not finally determine [1].

The aim of the work is determination of the connection between the IP and integral powers and obtaining the

complex form of the scalar and vectorial IP for non-sinusoidal modes classification in the 3-phase 4-wire electric power supply circuit in the terms of the spectral approach.

The used methodology is based on the vector approach with from the common point of view permits to analyze energetic characteristics both for 4-wire and for 3-wire circuits, both at sinusoidal and at non-sinusoidal mode, and both in time and in frequency domain.

Scalar (classical) IP. At the consideration of a 3-phase 4-wire network we assume that voltage in phase are measured relatively the neutral terminal (Fig. 1). In every time moment t voltage instantaneous values (IV) (regarding «neutral terminal's» wire) and current IV in phases are considered as 3D vectors of an arithmetic 3D space $R^{(3)}$

$$\boldsymbol{u}(t)=\left[u_a(t)\ \ u_b(t)\ \ u_c(t)\right]^{\tau},\ \boldsymbol{i}(t)=\left[i_a(t)\ \ i_b(t)\ \ i_c(t)\right]^{\tau}, \quad (1)$$

here in after τ is the sign of transposition.

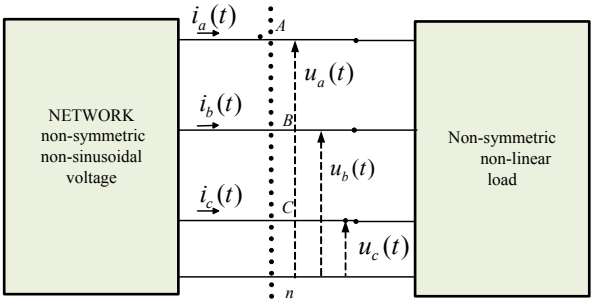

Fig. 1. Energetic processes in 4-wire electric power supply circuit

Determination of the norm in the 3D arithmetic space $R^{(3)}$ in each moment of time determines the norm of the vector of the current and voltage IV

$$|\boldsymbol{u}|=|\boldsymbol{u}(t)|=\sqrt{\boldsymbol{u}^{\tau}\boldsymbol{u}}=\sqrt{u_a(t)^2+u_b(t)^2+u_b(t)^2}\ , \quad (2)$$

$$|\boldsymbol{i}|=|\boldsymbol{i}(t)|=\sqrt{\boldsymbol{i}^{\tau}\boldsymbol{i}}=\sqrt{i_a(t)^2+i_b(t)^2+i_b(t)^2}\ . \quad (3)$$

A local state of the energetic mode in the 3D section <*A*, *B*, *C*> is characterized by the (classical) IP

$$p(t)=u_a(t)i_a(t)+u_b(t)i_b(t)\ +u_c(t)i_c(t)=\frac{dW}{dt}. \quad (4)$$

IP is determined as a sum of pair-wise products of current and voltage IV of three phases and determines the velocity of the energy transfer $W=W(t)$ in the section <*A*, *B*, *C*>. As appears from (4), at each moment of time the IP equals to the scalar product (SP) of vectors (1) in the space $R^{(3)}$

$$p(t)=(\boldsymbol{i},\boldsymbol{u})=\boldsymbol{i}^{\tau}\boldsymbol{u}=\left[i_a(t)\ \ i_b(t)\ \ \ i_c(t)\right]\cdot\begin{bmatrix}u_a(t)\\ u_b(t)\\ u_c(t)\end{bmatrix}. \quad (5)$$

Vectorial IP and an equation of IP. Product of norms of the vectors (2), (3) determines the apparent (total) IP of the energetic mode

$$s(t)=|\boldsymbol{i}(t)|\cdot|\boldsymbol{u}(t)|=i(t)\cdot u(t). \quad (6)$$

In the 3D space $R^{(3)}$ for any couple vectors the Cauchy-Schwarz inequality is true that for the vectors (1) inequality gives an implication

$$|\boldsymbol{i}^{\tau}(t)\boldsymbol{u}(t)|\ \le\ |\boldsymbol{i}(t)|\cdot|\boldsymbol{u}(t)|\ \Rightarrow\ \ p(t)\le s(t). \quad (7)$$

The vector IP is a vector of the space $R^{(3)}$ which is introduces as the vector product (VP) of IV of vectors (1) of currents and voltages [1]

$$\boldsymbol{q}(t)=\boldsymbol{i}\times\boldsymbol{u}=[\underbrace{i_bu_c-i_cu_b}_{q_a}\ \ \underbrace{i_cu_a-i_au_c}_{q_b}\ \ \underbrace{i_au_b-i_bu_a}_{q_c}]^{\tau}. \quad (8)$$

The Gram determinant [2] (composed from pair-wise scalar products of the current and voltage IV vectors) equals to square of the vectorial IP (8)

$$\begin{bmatrix}\boldsymbol{i}^{\tau}\boldsymbol{i} & \boldsymbol{i}^{\tau}\boldsymbol{u}\\ \boldsymbol{i}^{\tau}\boldsymbol{u} & \boldsymbol{u}^{\tau}\boldsymbol{u}\end{bmatrix}=[\underbrace{\boldsymbol{i}\times\boldsymbol{u}}_{\boldsymbol{q}(t)}]^{\tau}[\underbrace{\boldsymbol{i}\times\boldsymbol{u}}_{\boldsymbol{q}(t)}]=|\boldsymbol{q}(t)|^2. \quad (9)$$

The geometrical sense of the Gram determinant – the «square of the area of the parallelogram built by current and voltage vectors» is shown in Fig. 2.

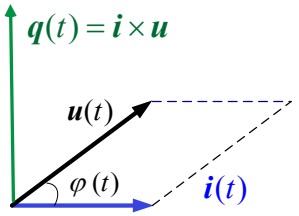

Fig. 2. Current vector, voltage vector, and the vector IP

Area of such an «instantaneous» parallelogram equals to

$$q(t)=|\boldsymbol{i}(t)|\cdot|\boldsymbol{u}(t)|\cdot|\sin\varphi(t)|=s(t)\cdot|\sin\varphi(t)|, \quad (10)$$

here $\varphi(t)$ is the instantaneous angle between vectors (1) in the space $R^{(3)}$ at the moment of time t.

The area of the parallelogram is equal to zero if vectors generating it are parallel (collinear, $\boldsymbol{i}\,\|\,\boldsymbol{u}$) when the apparent IP equals to the scalar (classical) IP. Therefore, norm of the VP of the current and voltage is interpreted as *non-active* IP. To underline this interpretation, the scalar (classical) IP (5) is named as *active* IP. Expansion (9) is invariant regarding the exchange of the vectors $\boldsymbol{i}$ and $\boldsymbol{u}$, but $\boldsymbol{i}\times\boldsymbol{u}=-\boldsymbol{u}\times\boldsymbol{i}$. In this paper (as in [1]) *vectorial (non-active)* IP is determined in the correspondence with (8). Vectors $\boldsymbol{i}$, $\boldsymbol{u}$, $\boldsymbol{i}\times\boldsymbol{u}$ create a right-hand system.

The Gram determinant at each moment of time quadratically complements the scalar IP to the total (*apparent*) IP (6)

$$\underbrace{(\boldsymbol{i}^{\tau}\boldsymbol{i})}_{i^2(t)}\underbrace{(\boldsymbol{u}^{\tau}\boldsymbol{u})}_{u^2(t)}=\underbrace{(\boldsymbol{i}^{\tau}\boldsymbol{u})}_{p(t)}^{2}+[\underbrace{\boldsymbol{i}\times\boldsymbol{u}}_{\boldsymbol{q}(t)}]^{\tau}[\boldsymbol{i}\times\boldsymbol{u}] \quad (11)$$

and gives an equation for instantaneous powers

$$s^2(t)=p^2(t)+q^2(t), \quad (12)$$

which is illustrated by Fig. 3.

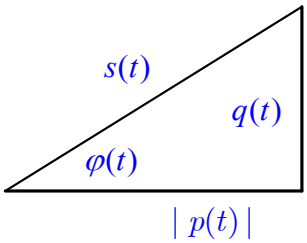

Fig. 3. A triangle of instantaneous powers

In the triangle of the IP two cathetus correspond to active and non-active instantaneous powers. If the non-active IP is determined by $\sin\varphi(t)$, than the active IP is determined by $\cos\varphi(t)$

$$p(t) = (\boldsymbol{i}^{\tau}\boldsymbol{u}) = \underbrace{|\boldsymbol{i}|\,|\boldsymbol{u}|}_{s(t)} \cdot \underbrace{\frac{(\boldsymbol{i}^{\tau}\boldsymbol{u})}{|\boldsymbol{i}|\,|\boldsymbol{u}|}}_{\cos\varphi(t)} = s(t)\cdot\cos\varphi(t)\,. \quad (13)$$

The angle $\varphi(t)$ in the triangle of the IP equals to the angle between current and voltage vectors introduced earlier. If the active IP (4) characterizes the effectiveness of the energetic mode, than the vector IP (13) characterizes the losses of the energetic mode.

Steady-state pulsed and unbalanced energetic mode. A steady-state energetic mode in a 3-phase section <*A*, *B*, *C*> is determined by 3D *T*-periodic curves of the current and voltage processes (waveforms):

$$\boldsymbol{u}(t) = \boldsymbol{u}(t+T)\,,\ \boldsymbol{i}(t) = \boldsymbol{i}(t+T)\,. \quad (14)$$

For *T*-periodic processes the (integral) average IP is correctly determined, and the variable component is inambiguously extracted

$$P = \overline{p} = \frac{1}{T}\int_{v}^{v+T} p(t)dt\,,\quad p(t) = \overline{p} + \widetilde{p}(t)\,. \quad (15)$$

If IP has no variable (pulsed) component $\widetilde{p}(t) \equiv 0$, the mode is non-pulsed. In the general case $\widetilde{p}(t) = p(t) - \overline{p} \neq 0$ and the steady mode is pulsed.

Like (15) in the vector IP it is possible to extract vector components: constant and variable ones

$$\overline{\boldsymbol{q}} = \frac{1}{T}\int_{v}^{v+T} \boldsymbol{q}(t)dt\,;\quad \boldsymbol{q}(t) = \overline{\boldsymbol{q}} + \widetilde{\boldsymbol{q}}(t)\,. \quad (16)$$

A mode at which the *vectorial* IP has no variable component $\widetilde{\boldsymbol{q}} = \widetilde{\boldsymbol{q}}(t) \equiv 0$ is named as a *balanced* mode [1].

The mode is <u>*really*</u> *balanced* if the vectorial IP (*non-active* IP) identically equal to zero

$$\boldsymbol{q}(t) \equiv 0 \ \Leftrightarrow\ (\overline{\boldsymbol{q}} = 0)\,\&\,(\widetilde{\boldsymbol{q}}(t) \equiv 0)\,. \quad (17)$$

As a result, the mode is <u>*really balanced*</u> ($q(t) \equiv |\boldsymbol{q}(t)| \equiv 0$) if at each moment (identically) current and voltage vectors (1) are parallel in the arithmetic 3D space $R^{(3)}$

$$q(t) \equiv 0 \ \Leftrightarrow\ \boldsymbol{i} \,\|\, \boldsymbol{u} \ \Leftrightarrow\ \boldsymbol{i}(t) = y(t)\boldsymbol{u}(t)\,. \quad (18)$$

The scalar quantity $y(t)$ (it has dimensionality of the conductivity) is not obligatory a constant.

So, a couple of instantaneous characteristics – scalar (5) and vectorial (8) ones – characterize the local energetic mode in the section <*A*, *B*, *C*>.

Spectral analysis of the periodic processes of the finite energy. A set of 3D (3-phase) *T*-periodic vector curves

$$\boldsymbol{x}(t) = [x_a(t)\ \ x_b(t)\ \ x_c(t)]^{\tau}, \quad (19)$$

with finite-average quadratic value

$$\|\boldsymbol{x}\|^2 = \overline{\boldsymbol{x}}^2 = \frac{1}{T}\int_{v}^{v+T} \boldsymbol{x}(t)^{\tau}\boldsymbol{x}(t)dt < \infty \quad (20)$$

creates a Gilbert infinite-dimensional space of 3D curves of the «finite energy»

$$L_2^{(3)}(T) = \{\boldsymbol{x}(t),\quad t \in (v, v+T) : \|\boldsymbol{x}\| < \infty\}\,. \quad (21)$$

For 3-phase vector curves $\boldsymbol{x}(t), \boldsymbol{y}(t) \in L_2^{(3)}(T)$ a scalar product is determined

$$<\boldsymbol{x},\boldsymbol{y}> = \frac{1}{T}\int_{v}^{v+T} \boldsymbol{x}(t)^{\tau}\boldsymbol{y}(t)dt = \frac{1}{T}\int_{v}^{v+T} (\boldsymbol{x}(t),\boldsymbol{y}(t))dt \quad (22)$$

as integral average scalar product of IV in 3D space $R^{(3)}$. The Cauchy-Schwarz inequality is true [2]

$$<\boldsymbol{x},\boldsymbol{y}> \ \leq\ \|\boldsymbol{x}\|\cdot\|\boldsymbol{y}\|\,. \quad (23)$$

The *T*-periodic curve $\boldsymbol{x}(t) = \boldsymbol{x}(t+T)$ is expanded into the functional Fourier series of 3D harmonic components (sinusoidal, cosinusoidal, complex, etc.)

$$\boldsymbol{x}(t) = \boldsymbol{x}_0(t) + \boldsymbol{x}_1(t) + \boldsymbol{x}_2(t) + ... + \boldsymbol{x}_k(t) + ... \quad (24)$$

For the complex Fourier series a 3D vector harmonic $\boldsymbol{x}_k(t) \in L_2^{(3)}(T)$ of the *k*-th order

$$\boldsymbol{x}_k(t) = \sqrt{2}\Re e[\boldsymbol{X}_k e^{jk\omega t}]\,,\ (T\omega = 2\pi)\,, \quad (25)$$

is calculated by using a 3D complex coefficient (3-phasor)

$$\boldsymbol{X}_k = \frac{\sqrt{2}}{T}\int_{v}^{v+T} \boldsymbol{x}(t)e^{-jk\omega t}\,,\ (k = 0, 1, 2, ...)\,, \quad (26)$$

$\boldsymbol{X}_k = [\dot{X}_{a,k}\ \ \dot{X}_{b,k}\ \ \dot{X}_{c,k}]^{\tau}$ is the 3D vector with complex coordinates, $\Re e(\dot{z})$ is the real part of the complex number $\dot{z}$.

A set of 3-phasors composes a 3D complex space $C^{(3)}$ with complex scalar product [1]

$$(\boldsymbol{X},\boldsymbol{Y}) = \boldsymbol{X}^{\tau}\boldsymbol{Y}^{*}\,, \quad (27)$$

* is the symbol of complex conjugation (CC). Further let's suppose that the constant component in the complex Fourier series is absent ($\boldsymbol{X}_0 = 0$)

$$\boldsymbol{x}(t) = \sum_{k=1}^{\infty} \boldsymbol{x}_k(t) = \sum_{k=1}^{\infty} \underbrace{\sqrt{2}\Re e[\boldsymbol{X}_k e^{jk\omega t}]}_{\boldsymbol{x}_k(t)}\,. \quad (28)$$

The complex form of the scalar IP. The spectral analysis of the *T*-periodical energetic processes of the current and voltage is used their representation by the complex Fourier series

$$\boldsymbol{u}(t) = \sqrt{2}\Re e\sum\nolimits_{k\geq 1} \boldsymbol{U}_k e^{jk\omega t}\,, \quad (29)$$

$$\boldsymbol{i}(t) = \sqrt{2}\Re e\sum\nolimits_{k\geq 1} \boldsymbol{I}_k e^{jk\omega t}\,. \quad (30)$$

The Euler formula [2] represents components of the 3-curves of voltage (29) and current (30) expansion by using the CC of the 3-phasor

$$\boldsymbol{i}_k(t) = \frac{1}{2}[\boldsymbol{I}_k e^{jk\omega t} + \boldsymbol{I}_k^{*} e^{-jk\omega t}]\,, \quad (31)$$

$$\boldsymbol{u}_k(t) = \frac{1}{2}[\boldsymbol{U}_k e^{jk\omega t} + \boldsymbol{U}_k^{*} e^{-jk\omega t}]\,. \quad (32)$$

In view of the scalar product's linearity, the IP equals to the sum of partial scalar IP's of the vector harmonics of the current of the *k*-th order and of the voltage of the *m*-th order

$$p(t) = (\boldsymbol{i},\boldsymbol{u}) = \boldsymbol{i}^{\tau}\boldsymbol{u} = \sum_{k,m} \underbrace{\boldsymbol{i}_k(t)^{\tau}\boldsymbol{u}_m(t)}_{p_{k,m}(t)} = \sum_{k,m} p_{k,m}(t)\,. \quad (33)$$

Representations (31), (32) of the vector harmonics by using the 3-phasor and its CC for the IV of the product of the vector harmonics of the current of the *k*-th order and of the voltage of the *m*-th order give an identity

$$p_{k,m}(t) = \Re e[\underbrace{\boldsymbol{I}_k^{\tau}\boldsymbol{U}_m^{*}}_{\dot{N}_{k-m}} e^{j(k-m)\omega t} + \underbrace{\boldsymbol{I}_k^{\tau}\boldsymbol{U}_m}_{\dot{N}_{k+m}} e^{j(k+m)\omega t}]\,. \quad (34)$$

If the current and voltage harmonics have the same order ($m = k$) their scalar IP has both constant and variable components

$$p_k(t) = \Re e[\underbrace{\boldsymbol{U}_k^{\tau}\boldsymbol{I}_k^{*}}_{\dot{S}_{G_k}} + \underbrace{\boldsymbol{I}_k^{\tau}\boldsymbol{U}_k}_{\dot{N}_k} e^{j2k\omega t}]. \qquad (35)$$

The scalar IP (4) is represented by the current and voltage 3-phasors as

$$\begin{aligned} p(t) &= \Re e\{\sum_{k\ge 1}[\dot{S}_{G_k} + \dot{N}_k e^{j2k\omega t}]\} + \\ &+ \Re e\{\sum_{k\ne m}[\dot{N}_{k-m} e^{j(k-m)\omega t} + \dot{N}_{k+m} e^{j(k+m)\omega t}]\} \end{aligned} \qquad (36)$$

and has constant and variable (pulsed) components.

The constant component

$$\overline{p} = \sum_{k\ge 1} \Re e[\dot{S}_{G_k}] = \sum_{k\ge 1} P_k = P \qquad (37)$$

equals to active (average) power of the non-sinusoidal mode and is represented as the real part of the complex (geometrical) power of all harmonics

$$\dot{S}_G = \sum_{k\ge 1} \underbrace{\boldsymbol{U}_k^{\tau}\boldsymbol{I}_k^{*}}_{\dot{S}_{G_k}} = \sum_{k\ge 1} \dot{S}_{G_k} = P + jQ\,. \qquad (38)$$

The complex (geometrical) power (38) equals to the sum of harmonic components' complex powers

$$\dot{S}_{G_k} = \boldsymbol{U}_k^{\tau}\boldsymbol{I}_k^{*} = (\boldsymbol{U}_k, \boldsymbol{I}_k) = P_k + jQ_k, = S_{G_k} \cdot e^{j\varphi_k}\,. \qquad (39)$$

The complex power (39) of the vector harmonics of the current and voltage of the k-th order equals to the complex scalar product (27) of the 3-phasor of the voltage and the 3-phasor of the current of the k-th order in the complex 3D space $C^{(3)}$.

The imaginary part of the complex power (38)

$$Q = \Im m \sum_{k\ge 1} \underbrace{\boldsymbol{U}_k^{\tau}\boldsymbol{I}_k^{*}}_{\dot{S}_{G_k}} = \sum_{k\ge 1} \underbrace{\Im m[\boldsymbol{U}_k^{\tau}\boldsymbol{I}_k^{*}]}_{Q_k} = \sum_{k\ge 1} Q_k$$

determines the non-sinusoidal mode's reactive power of the 3-phase section <*A*, *B*, *C*> and gives the generalization of the reactive power by Budeanu to 3-phase processes

$$Q = \sum_{k\ge 1} \underbrace{\Im m[\boldsymbol{U}_k^{\tau}\boldsymbol{I}_k^{*}]}_{Q_k} = \sum_{k\ge 1} Q_k = \sum_{k\ge 1} S_{Q_k} \sin\varphi_k\,. \qquad (40)$$

Complex *pulsation powers* of the scalar IP:

- of the harmonics of the k-th order of the even frequency $2k\omega$

$$\dot{N}_k = \boldsymbol{I}_k^{\tau}\boldsymbol{U}_k\,; \qquad (41)$$

- of the harmonics of the k-th order and m-th order of the sum and difference frequency

$$\dot{N}_{k+m} = \boldsymbol{I}_k^{\tau}\boldsymbol{U}_m\,,\ \dot{N}_{k-m} = \boldsymbol{U}_k^{\tau}\boldsymbol{I}_m^{*} \qquad (42)$$

determined the transient (pulsed) component of the scalar IP

$$\begin{aligned} \widetilde{p}(t) &= \Re e\{\sum_{k\ge 1} \dot{N}_k e^{j2k\omega t}\} + \\ &+ \Re e\{\sum_{k\ne m}[\dot{N}_{k-m} e^{j(k-m)\omega t} + \dot{N}_{k+m} e^{j(k+m)\omega t}]\}. \end{aligned} \qquad (43)$$

If three types of the complex powers equal to zero

$$\dot{N}_k = \dot{N}_{k+m} = \dot{N}_{k-m} = 0\,,\ (k, m = 1, 2, ..),$$

then the mode is non-pulsed.

The complex form of the scalar IP of the non-sinusoidal mode (36) expands the complex form of the scalar IP of the non-symmetric sinusoidal mode [1]

$$p(t) = \Re e\{\dot{S}_{G_1} + \dot{N}_1 e^{j2k\omega t}\}\,,$$

where $\dot{S}_{G_1} = \boldsymbol{U}_1^{\tau}\boldsymbol{I}_1^{*}$, $\dot{N}_1 = \boldsymbol{I}_1^{\tau}\boldsymbol{U}_1$ – complex (*geometrical*) power and complex *pulsation power* of current and voltage fundamental harmonics.

Vectorial instantaneous power of the non-sinusoidal mode. Because of the linearity of the vector product, the vector IP

$$\boldsymbol{q}(t) = \boldsymbol{i} \times \boldsymbol{u} = \sum_{k,m} \underbrace{\boldsymbol{i}_k \times \boldsymbol{u}_m}_{\boldsymbol{q}_{k,m}(t)} = \sum_{k,m} \boldsymbol{q}_{k,m}(t) \qquad (44)$$

equals to the sum of vector products of the current harmonics of the k-th order and voltage harmonics of the m-th order

$$\boldsymbol{q}_{k,m}(t) = \Re e[\underbrace{\boldsymbol{I}_k \times \boldsymbol{U}_m^{*}}_{\boldsymbol{D}_{k-m}} e^{j(k-m)\omega t} + \underbrace{\boldsymbol{I}_k \times \boldsymbol{U}_m}_{\boldsymbol{D}_{k+m}} e^{j(k+m)\omega t}]\,. \qquad (45)$$

If the current and voltage harmonics have the same order $m = k$, then their VP has both constant and variable components

$$\boldsymbol{q}_k(t) = \Re e[\underbrace{\boldsymbol{I}_k \times \boldsymbol{U}_k^{*}}_{\boldsymbol{K}_k} + \underbrace{\boldsymbol{I}_k \times \boldsymbol{U}_k}_{\boldsymbol{D}_k} e^{j2k\omega t}]\,. \qquad (46)$$

The complex form of the vector IP is represented by the 3-phasors of the harmonics as

$$\begin{aligned} \boldsymbol{q}(t) &= \Re e\{\sum_{k\ge 1}[\boldsymbol{K}_k + \boldsymbol{D}_k e^{j2k\omega t}]\} + \\ &+ \Re e\{\sum_{k\ne m}[\boldsymbol{D}_{k-m} e^{j(k-m)\omega t} + \boldsymbol{D}_{k+m} e^{j(k+m)\omega t}]\}. \end{aligned} \qquad (47)$$

The 3-phasors of the current and voltage harmonics' *balanced* power of the k-th order

$$\boldsymbol{K}_k = \boldsymbol{I}_k \times \boldsymbol{U}_k^{*}\ \ (k = 1, 2, ...) \qquad (48)$$

determine the constant component of the vector IP.

The variable (pulsed) component of the vector IP is determined by 3-phasors of the power of the *unbalance*:

- of the current and voltage harmonics of the k-th order of the twice frequency $2k\omega$

$$\boldsymbol{D}_k = \boldsymbol{I}_k \times \boldsymbol{U}_k\ \ (k = 1, 2, ...); \qquad (49.a)$$

- of the current harmonics of the k-th order and the voltage harmonics of the m-th order of the sum and difference frequency ($k, m = 1, 2, \ldots$)

$$\boldsymbol{D}_{k+m} = \boldsymbol{I}_k \times \boldsymbol{U}_m\,,\ \boldsymbol{D}_{k-m} = \boldsymbol{I}_k \times \boldsymbol{U}_m^{*}\,. \qquad (49.b)$$

If 3-phasors (49) equal to zero

$$\boldsymbol{D}_k = \boldsymbol{D}_{k+m} = \boldsymbol{D}_{k-m} = 0\,, \qquad (50)$$

than the mode is balanced.

If in addition to the conditions (50) the following condition is fulfilled

$$\Re e\boldsymbol{K}_k = \Re e[\boldsymbol{I}_k \times \boldsymbol{U}_k^{*}] = 0\ \ (k = 1, 2 ...), \qquad (51)$$

then the mode is *really balanced*.

The complex form of the vector instantaneous power of the non-sinusoidal mode (47) expands the complex form of the vector IP of the sinusoidal non-symmetrical mode [1]

$$\boldsymbol{q}(t) = \Re e\{\boldsymbol{K}_1 + \boldsymbol{D}_1 e^{j2\omega t}\}\,,$$

where $\boldsymbol{K}_1 = \boldsymbol{I}_1 \times \boldsymbol{U}_1^*$, $\boldsymbol{D}_1 = \boldsymbol{I}_1 \times \boldsymbol{U}_1$ are 3-phasors of the *balanced* power and the power of the *unbalance* of the current and voltage fundamental harmonic.

Equations of the non-sinusoidal mode's complex powers. For the square of the (apparent) total power the following equality is true

$$S^2 = (\sum_{k=1}^{\infty} U_k^2) \cdot (\sum_{m=1}^{\infty} I_m^2) = \sum_{m=k}^{\infty} I_m^2 \cdot U_m^2 + \sum_{m \neq k}^{\infty} I_m^2 U_k^2 . \quad (52)$$

The connection between the scalar and vector products of 3-phasors $\boldsymbol{X}, \boldsymbol{Y} \in C^{(3)}$ is determined by the identity [1]

$$|\boldsymbol{X}|^2 |\boldsymbol{Y}|^2 = |\boldsymbol{X}^{\tau} \boldsymbol{Y}^*|^2 + |\boldsymbol{X} \times \boldsymbol{Y}|^2 , \quad (53)$$

which expands the corresponding identity of vector algebra of real vectors [2].

At $\boldsymbol{X} = \boldsymbol{U}_k$, $\boldsymbol{Y} = \boldsymbol{I}_m$ from the identity (53) the following equalities follow

$$I_m^2 U_k^2 = |\boldsymbol{U}_k|^2 |\boldsymbol{I}_m|^2 = |\underbrace{\boldsymbol{U}_k^{\tau} \boldsymbol{I}_m^*}_{\dot{N}_{k-m}}|^2 + |\underbrace{\boldsymbol{U}_k \times \boldsymbol{I}_m}_{\boldsymbol{D}_{k+m}}|^2 , \quad (54)$$

which at $m = k$ give

$$I_k^2 U_k^2 = |\boldsymbol{U}_k|^2 |\boldsymbol{I}_k|^2 = |\underbrace{\boldsymbol{U}_k^{\tau} \boldsymbol{I}_k^*}_{\dot{S}_{G_k}}|^2 + |\underbrace{\boldsymbol{U}_k \times \boldsymbol{I}_k}_{\boldsymbol{D}_k}|^2 . \quad (55)$$

Expansion of the square of the apparent power (52) taking into account (54), (55) gives an equation for the complex scalar and vector powers including active (37) and reactive (40) powers of the sinusoidal mode

$$S^2 = \sum_{k=1}^{\infty} (P_k^2 + Q_k^2 + D_k^2) + \sum_{m \neq k}^{\infty} (N_{k-m}^2 + D_{k+m}^2) . \quad (56)$$

The power equation (56) generalizes the power equation for the sinusoidal non-symmetrical mode [1]

$$S^2 = P_1^2 + Q_1^2 + D_1^2 . \quad (57)$$

The equation (56) includes not all complex scalar and vector powers of the complex form of the scalar (36) and vector (47) IP.

If to use a couple of sequences $\{\boldsymbol{U}_k\}_{k \geq 1}$, $\{\boldsymbol{I}_m^*\}_{m \geq 1}$ then an additional equation for the complex scalar and vector powers which are not included in (56) is true. At $\boldsymbol{X} = \boldsymbol{U}_k$, $\boldsymbol{Y} = \boldsymbol{I}_m^*$ from the identity (53) the following equalities follow

$$|\boldsymbol{U}_k|^2 |\boldsymbol{I}_m|^2 = |\underbrace{\boldsymbol{U}_k^{\tau} \boldsymbol{I}_m}_{\dot{N}_{k+m}}|^2 + |\underbrace{\boldsymbol{U}_k \times \boldsymbol{I}_m^*}_{\boldsymbol{D}_{k-m}}|^2 . \quad (58)$$

At $m = k$ equalities (58) give

$$|\boldsymbol{U}_m|^2 |\boldsymbol{I}_m|^2 = |\underbrace{\boldsymbol{U}_m^{\tau} \boldsymbol{I}_m}_{\dot{N}_m}|^2 + |\underbrace{\boldsymbol{U}_m \times \boldsymbol{I}_m^*}_{\boldsymbol{K}_m}|^2 . \quad (59)$$

Expansion of the square of the apparent power (52) taking into account (58), (59) gives an additional equation for the complex scalar and vector powers

$$S^2 = \sum_{k=1}^{\infty} (K_m^2 + N_m^2) + \sum_{m \neq k}^{\infty} (N_{k+m}^2 + D_{k-m}^2) . \quad (60)$$

It is possible to show that for each harmonic the following implication is true

$$\boldsymbol{D}_m = 0 \Rightarrow K_m^2 + N_m^2 = P_m^2 + Q_m^2 \ (k = 1, 2 \ldots).$$

The obtained power equation (60) generalizes the additional equation for the sinusoidal non-symmetrical mode [1]

$$S^2 = K_1^2 + N_1^2 . \quad (61)$$

As shown in [1] at the sinusoidal mode equations (57), (61) are determined by two different orthogonal expansions of the 3-phase current. The problem of building the current's orthogonal expansion at the sinusoidal mode is used for the solution of the problem of the apparent power's non-active components compensation [3]. Building the orthogonal expansion which is associated with power equations (56), (60) is not considered in this paper and required additional investigations.

The practical value of the obtained equations is a possibility of their utilization for the increase both quality of delivery and quality of consumption of electrical energy.

Conclusion. For the 3-phase 4-wire network with non-sinusoidal (independently on their symmetry) processes the complex forms of the active (scalar) and (non-active) vector IP are obtained. The power equations for complex scalar and complex vector powers of non-sinusoidal modes are obtained. The power equations generalize the power equations for sinusoidal modes in the 4-wire network.

REFERENCES

1. Sirotin Iu.A. Vectorial instantaneous power and energy modes in three-phase circuits. *Tekhnichna elektrodynamika – Technical electrodynamics*, 2013, no.6, pp. 57-65. (Rus).

2. Korn G., Korn T. *Spravochnik po matematike dlia nauchnykh rabotnikov i inzhenerov* [Mathematical handbook for scientists and engineers]. Moscow, Nauka Publ., 1973. 832 p. (Rus).

3. Sirotin Iu.A. Non-pulsed mode of supply in a three-phase system at asymmetrical voltage. *Przeglad Elektrotechniczny*, 2013, no.7, pp. 54 -58.

Received 16.10.2015

Iu.A. Sirotin[1], *Doctor of Technical Science, Professor,*
T.S. Ierusalimova[1], *Assistant Lecturer,*
[1] National Technical University «Kharkiv Polytechnic Institute», 21, Frunze Str., Kharkiv, 61002, Ukraine.
e-mail: yuri_sirotin@ukr.net, Ierusalimovat@mail.ru

How to cite this article:
Sirotin Iu.A., Ierusalimova T.S. Instantaneous and integral power equations of nonsinusoidal 3-phase processes. *Electrical engineering & electromechanics*, 2016, no.1, pp. 69-73. doi: 10.20998/2074-272X.2016.1.13.